# Degradation and Failure Characteristics of NPP Containment Protective Coating Systems

by

R. L. Sindelar

Westinghouse Savannah River Company
Savannah River Site
Aiken, South Carolina 29808

M. E. Dupont                                            P.  E.  Zapp

N. C. Iyer

P. S. Lam

T. E. Skidmore

F. R. Utsch

WSRC-TR-2001-00067

# Degradation and Failure Characteristics of NPP Containment Protective Coating Systems (U)
## Interim Report No. 3

## SRTC Coating System No. 1
(Phenoline® 305 epoxy-phenolic topcoat, Carbozinc® 11 primer, carbon steel substrate)

Prepared by

### M. E. Dupont, N. C. Iyer, P. S. Lam, R. L. Sindelar, T. E. Skidmore, F. R. Utsch and P. E. Zapp

Savannah River Technology Center
Westinghouse Savannah River Company
Aiken, SC 29808

For

Division of Engineering Technology
Office of Nuclear Regulatory Research
U.S. Nuclear Regulatory Commission
Washington, DC 20555
NRC Job Code W6959

### NRC Project Managers: A. W. Serkiz
### M. L. Marshall, Jr.

Publication Date: February 2001

**DOES NOT CONTAIN
UNCLASSIFIED CONTROLLED
NUCLEAR INFORMATION**

ADC &
Reviewing
Official:
K. A. Dunn 773-41A
Date: 2-8-01
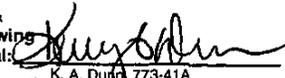
## Westinghouse Savannah River Company
## Savannah River Site
## Aiken, SC 29808

## DISCLAIMER

This report was prepared as an account of work sponsored by an agency of the United States Government. Neither the United States Government nor any agency thereof, nor any of their employees, makes any warranty, express or implied, or assumes any legal liability or responsibility for the accuracy, completeness, or usefulness of any information, apparatus, product or process disclosed, or represents that its use would not infringe privately owned rights. Reference herein to any specific commercial product, process or service by trade name, trademark, manufacturer, or otherwise does not necessarily constitute or imply its endorsement, recommendation, or favoring by the United States Government or any agency thereof. The views and opinions of authors expressed herein do not necessarily state or reflect those of the United States Government or any agency thereof.

This report has been reproduced directly from the best available copy.

Available for sale to the public, in paper, from: U.S. Department of Commerce, National Technical Information Service, 5285 Port Royal Road, Springfield, VA 22161, phone: (800) 553-6847
fax: (703) 605-6900
email: orders@ntis.fedworld.gov
online ordering: http://www.ntis.gov/ordering.htm

Available electronically at http://www.doe.gov/bridge
Available for a processing fee to U.S. Department of Energy and its contractors, in paper, from: U.S. Department of Energy, Office of Scientific and Technical Information, P.O. Box 62, Oak Ridge, TN 37831-0062, phone: (865) 576-8401
fax: (865) 576-5728
email: reports@adonis.osti.gov

**DOCUMENT:**   WSRC-TR-2001-00067

**TITLE:**   Degradation and Failure Characteristics of
NPP Containment Protective Coating Systems (U)

**APPROVALS**
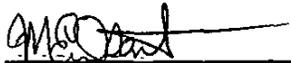
Date: 2/8/01

Mark E. Dupont, Author
Materials Applications & Process Technology Group
Materials Technology Section
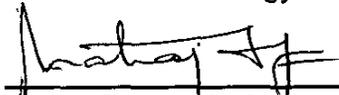
Date: 2/8/01

Natraj C. Iyer, Author and Manager
Materials Technology Section
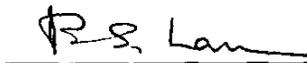
Date: 2/8/2001

Poh-Sang Lam, Author
Materials Applications & Process Technology Group
Engineering Development Section
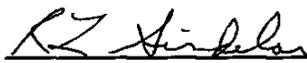
Date: 2/8/01

Robert L. Sindelar, Author and Manager
Materials Applications & Process Technology Group
Materials Technology Section

Date: 2/8/01

T. Eric Skidmore, Author
Materials Consultation Group
Materials Technology Section

Date: 2/8/01

Philip E. Zapp, Author
Materials Performance & Corrosion Technology Group
Materials Technology Section

This page left blank intentionally.

## Abstract

A research program to investigate the performance and potential for debris formation of Service Level I coating systems[1] used in nuclear power plant containment is being performed at the Savannah River Technology Center. The research activities are aligned to address phenomena important to cause coating disbondment as identified by the Industry Coatings Expert Panel. The period of interest for performance covers the time from application of the coating through 40 years of service, followed by a medium-to-large break loss-of-coolant accident scenario, which is a design basis accident (DBA) scenario.

The SRTC program consists of three major interactive elements: Materials Properties Development, Deformation Modeling of Coating Performance, and Coating Performance Testing. These elements are directed at evaluating Service Level I coatings performance under simulated DBA-LOCA conditions. The coating materials properties data (not previously available) are input to coatings deformation models which are then compared against coating behavior under simulated DBA-LOCA conditions, including the PWR profile in ASTM D3911-95, to evaluate the coating performance. The response of the coating is characterized in terms of blistering, cracking, and debris formation. The results are used as input to the NRC's GSI-191, "PWR Sump Blockage" research program. The effects of aging on coating materials properties and performance are addressed by applying an aging treatment (irradiation to $10^9$ rads, per ASTM D4082-95) to the test specimens.

The interactive program elements are described in this report and the application of these elements to evaluate the performance of the specific coating system of Phenoline® 305 epoxy-phenolic topcoat over Carbozinc® 11 primer on a steel substrate. This system is one of the predominant coating systems present on steel substrates in NPP containment. The original formulations of Phenoline® 305 and Carbozinc® 11 were obtained to prepare to coating specimens use in the DBA-LOCA performance testing to best represent the existing systems in NPP containment service.

---

[1] The Service Level designation of coatings in nuclear power plants is described in ASTM Standard D5144-00

**Table of Contents**

To Be Developed in final formatting

# List of Figures

# List of Tables

# List of Abbreviations

| | | | |
|---|---|---|---|
| AE | Acoustic Emission | NACE | National Association of Corrosion Engineers |
| ASTM | American Society for Testing and Materials | NMRS | Nuclear Magnetic Resonance Spectroscopy |
| BWR | Boiling Water Reactor | NPP | Nuclear Power Plant |
| CSS | Containment Spray System | NRC | (U.S.) Nuclear Regulatory Commission |
| DBA | Design Basis Accident | PIRT | Phenomena Identification and Ranking Table |
| DFT | Dry Film Thickness | PTFE | Polytetrafluorethylene |
| DSC | Differential Scanning Calorimetry | PWR | Pressurized Water Reactor |
| ECCS | Emergency Core Cooling System | SEM | Scanning Electron Microscopy |
| EDS | Energy Dispersive Spectroscopy | SIMS | Secondary Ion Mass Spectroscopy |
| EIS | Electrochemical Impedance Spectroscopy | SRTC | Savannah River Technology Center |
| EPRI | Electric Power Research Institute | SSC | Structure, System, and Component |
| ETC | Environmental Test Chamber | SSPC | Steel Structures Painting Council |
| FT-IR | Fourier Transform-Infrared Spectroscopy | TEM | Transmission Electron Microscopy |
| IOZ | Inorganic Zinc | TGA | Thermogravimetric Analysis |
| LOCA | Loss of Coolant Accident | XRD | X-ray Diffraction |

# Executive Summary

The U. S. Nuclear Regulatory Commission (NRC) has identified the potential for degradation and failure[1] of "qualified" protective coatings within nuclear power plant primary containment during the design life of such plants, and has communicated such concerns to license holders in NRC Generic Letter 98-04 dated July 14, 1990. As a consequence of this letter, the NRC commissioned the Savannah River Technology Center (SRTC) to investigate the potential for degradation and failure of such coating systems when subjected to DBA-LOCA conditions, and to characterize coating debris. The formation and transport of coating debris to a PWR ECCS sump debris screen may have an undesirable safety impact during the post-LOCA period. The results of the SRTC coatings research program will be integrated into the NRC's GSI-191, "PWR Sump Blockage" research program.

An investigative approach was previously established in the SRTC program and applied to a reference coating system (ref. WSRC-TR-2000-00079; USNRC Public Electronic Reading Room, ADAMS Accession No. ML003703890), and to a predominant Service Level I protective coating system used for concrete substrates (ref. WSRC-TR-2000-00340; USNRC Public Electronic Reading Room, ADAMS Accession No. ML003772811). This approach was next applied to investigate a predominant Service Level I protective coating system used for steel substrates and the approach and results are contained in this report. The coating system, SRTC System 1, is an epoxy-phenolic (or phenolic-modified epoxy) topcoat over an inorganic zinc primer that was applied to steel substrates within PWR containment in the early to mid-1970s.

Original formulations of the specific topcoat, Phenoline® 305, and primer, Carbozinc® 11, were obtained from the vendors, and steel panels were prepared in accordance with ASTM D5139-90. The effects of an accumulated gamma dose of a 40-year service plus DBA-LOCA on the coating performance were simulated by irradiating the coating to $10^9$ rads at $1 \times 10^6$ rads/hour at 120°F within the specifications of ASTM D4082-95. Laboratory specimens were exposed to simulated DBA-LOCA conditions specified in the ASTM D3911-95 steam temperature profile for PWR containment, and also to other simulated DBA-LOCA conditions, including a "pulse" steam temperature profile and a high temperature (up to 200°F) water immersion.

The major findings are:

1. Properly applied coatings that have not been subjected to irradiation of $10^9$ rads, can be expected to remain fully adhered and intact on a steel substrate, following exposure to all simulated DBA-LOCA conditions. In addition, no minor cracking in defect-free regions of the coating and regions near embedded defects was observed. This is in contrast to previous test results on a concrete system (ref. WSRC-TR-2000-00340) and is predicted by the deformation modeling.

2. Properly applied coatings that have been subjected to irradiation of $10^9$ rads exhibited profound blistering, leading to disbondment of a near-surface coating layer (1-2 mils of the 10 mils thickness) when exposed to elevated temperatures and moisture conditions within the range of DBA conditions. This phenomenon produced a coating debris source term.

---

[1] "Coating failure" is defined as disbondment of portions of the coating system that constitute coating debris.

# Acknowledgments

# 1.0 Background

Nuclear power plants (NPPs) must ensure that the emergency core cooling system (ECCS) or safety-related containment spray system (CSS) remains capable of performing its design safety function throughout the life of the plant. This requires ensuring that long-term core cooling can be maintained following a postulated loss-of-coolant accident (LOCA). Adequate safety operation can be impaired if the protective coatings which have been applied to the concrete and steel structures within the primary containment fail, producing transportable debris which could then accumulate on BWR ECCS suction strainers or PWR ECCS sump debris screens located within the containment.

Service Level I coatings were used on the interior containment steel shells, concrete walls and floors, and other structures, thereby providing environmental protection to these substrates and facilitating decontamination, as necessary. The coatings, which were applied during plant construction, were expected to last throughout the 40-year license period or design life of the plant, except for minor local damage due to mechanical impact or cleaning chemicals. These coatings were selected based on demonstrated adequate survivability under simulated DBA-LOCA conditions as described in ASTM Standard D3911-95, or earlier ANSI standards. The assumption was that qualified coatings that were properly selected and applied at time-of-construction would not fail during normal plant operation or during a LOCA.

There is clear evidence for failure of qualified coatings during plant design life. Such failures are described in attachments to NRC GL 98-04, "Potential for Degradation of Emergency Core Cooling System and Containment Spray System after a Loss-of-Coolant Accident Because of Construction and Protective Coating Deficiencies and Foreign Material in Containment," July 14, 1998. This evidence resulted in NRC's Office of Nuclear Reactor Regulation requesting that research (Reference 1) be directed at debris generation testing of protective coatings that are likely to fail during an accident. The research would determine the timing of the coating failure during an accident (e.g., minutes, hours, days) and the characteristics of the failed coating debris (e.g., chips, large strips, particulate materials). This research need was the basis for NRC's Office of Nuclear Regulatory Research, Division of Engineering Technology, initiating a program through the Savannah River Technology Center to research the performance of aged containment coatings under simulated LOCA conditions.

SRTC's program is designed to investigate NPP containment coatings through a better understanding of coating material properties (e.g., property changes introduced by elevated temperature and irradiation effects), development of a predictive coating failure model, and DBA performance testing of coating samples representative of coatings applied in NPPs. The ultimate goal is to establish a coating debris database that characterizes and quantifies the failed material. The SRTC program elements and interactive approach are described in Sections 2 and 3, and the results for a specific steel coating system (steel substrate, inorganic zinc primer, and epoxy-phenolic topcoat) are described in Section 3.

This Interim Report highlights research findings that have been reported in monthly letter status reports to the NRC since project initiation in July 1998. Research results on various other coating systems have been reported also in public meetings, held on November 5, 1998, April 15, 1999, November 22, 1999, and September 26, 2000 at NRC Headquarters. A topical report on SRTC's coating System 5, epoxy polyamide topcoat over epoxy polyamide primer on steel, was issued in March 2000 (Reference 2), and a topical report on SRTC's coating System 2, epoxy-phenolic topcoat over epoxy surfacer on concrete, was issued in October 2000 (Reference 3). Those reports established the experimental and analytical approach used in this Interim Report. Licensees, industry NPP coatings groups, and individual NPP coatings specialists have shown considerable interest and offered assistance to the program. Similar public interaction will be continued throughout the research project. The data obtained are to be integrated into NRC's Generic Safety Issue (GSI) 191, PWR Sump Blockage project. In addition, the research findings from this study will be used in evaluating a potential need for review and revision of ASTM Standards D3911-95, "Standard Test Method for Evaluating Coatings Used in Light-Water Nuclear Power Plants at Simulated Design Basis Accident (DBA) Conditions, and D4082-95, "Standard Method for Effects of

Gamma Radiation on Coatings for Use in Light-Water Nuclear Power Plants", which are presently used by licensees in the qualification of Service Level I coatings.

References:

1. "Supplemental User Need Request Regarding Potential For Loss of Emergency Core Cooling For a Pressurized Water Reactor Due to LOCA Generated Coating Debris Clogging the Containment Sump Screens," Collins, S., Memorandum to Morrison, D., U.S. Nuclear Regulatory Commission, Washington, DC, June 2, 1997.
2. "Degradation and Failure Characteristics of NPP Containment Protective Coating Systems (U) Interim Report", WSRC-TR-2000-00079, March 2000, (USNRC Public Electronic Reading Room, ADAMS Accession No. ML003703890).
3. "Degradation and Failure Characteristics of NPP Containment Protective Coating Systems (U) SRTC Coating System No. 2", WSRC-TR-2000-00340, October 2000, (USNRC Public Electronic Reading Room, ADAMS Accession No. ML003772811).

# 2.0 SRTC Program Elements and Structure

The Savannah River Technology Center coatings research program is designed to investigate the potential degradation and failure of Service Level I protective coatings under postulated LOCA conditions. The key program elements and interactive paths are shown in Figure 2-1. The program goal is to evaluate the performance of "qualified" coating systems exposed to DBA-LOCA conditions. Coating response could range from "no failure," to minor blistering and/or cracking, to production of debris through disbonded chips or particles that could degrade the performance of PWR ECCS sumps. The assumption has been that properly selected and applied "qualified" coatings will not fail during the normal plant design life (i.e., 40 years) plus exposure to a DBA-LOCA. Minor blistering and cracking are not considered to be failures, whereas coating disbondment and the accompanying "free" material that constitutes a debris source term is considered a failure.

**Material Properties**
- Mechanical
  -Non-aged
  -Aged
- Physical
  -Non-aged
  -Aged

**LOCA Conditions**

-ASTM D3911 (PWR)
-Plant-Specific LOCA

**Service Level I Coatings**

- Selected by Coatings Industry PIRT Panel

**Coating Specimens**

- Laboratory w/ & w/o defects
- From NPP Containments

**Deformation Modeling of Coating Performance**

- Postulate Defects (i.e., from PIRT)
- Calculate Loading (FE Model)
- Evaluate Deformation and Potential for Blistering and Cracking (FE Model)

**Measured Performance Under DBA-LOCA Conditions**

- ASTM D3911 for PWR
- Plant-Specific Pressure and Temp Profile
- Water Immersion

**Experimental Insights**

**Insights from Predictive Modeling of Coating Performance**

**Model Verification**

**Coating Performance**
- No Failure
- Blistering and/or Cracking
- Debris (Disbonded chips or particulates)

**Figure 2-1. Task Logic Diagram for SRTC Project**

The four principal program elements are to:
a) measure key coating materials' properties,
b) develop predictive coatings models to evaluate deformation and potential for failure,
c) subject selected coatings to design basis accident conditions, or simulated LOCA conditions, and measure performance, and
d) evaluate the performance of Service Level I coatings and, if failures occur, identify debris source characteristics which include size, shape, and amount (per unit exposed area).

Protective coating materials applied in NPPs were identified from the EPRI "Coatings Handbook for Nuclear Power Plants," EPRI TR-106160, June 1996 [2.1], from plant specific responses, from surveys performed by several industry groups, and from the industry PIRT panel. Although EPRI TR-106160 lists data collected from 29 nuclear industry respondents and represents over 200 unique coating products in over 1000 different plant-specific applications, the data set does not lend itself to identification of a limited set of generic coating systems on which to focus the research effort. This identification of generic coating systems that represent widespread use in NPPs was facilitated by formation of an industry Phenomena Identification and Ranking Table panel. A detailed description of a generic PIRT process is described in reference 2.2. The specific PIRT process, panel members and the PIRT relevant to this Interim Report [2.3] are discussed in Appendix G. Table 2.1 identifies the available coating products reviewed in this project, and also cross-references such materials with the PIRT panel's generic descriptions.

**Table 2-1. Cross-Reference Table for Coating Systems Presently Investigated by the SRTC Project and Those Evaluated by the Industry Coatings PIRT Panel**

| Substrate | Generic Description | Coating Products Tested at SRTC | SRTC System No. | PIRT System Letter |
|-----------|--------------------|--------------------------------|-----------------|---------------------|
| Steel | **Epoxy-phenolic over inorganic zinc** | **Phenoline® 305 over Carbozinc® 11** | 1 | a (1) |
| Concrete | **Epoxy-phenolic over surfacer** | **Phenoline® 305 over Starglaze® 2011S surfacer** | 2 | e (5) |
| Steel | Phenolic-modified epoxy over inorganic zinc | Amercoat® 90HS over Dimetcote® 9 | 3 | |
| Steel | Phenolic-modified epoxy over epoxy-polyamide | Amercoat® 90HS over Amercoat® 370 | 4 | |
| Steel | **Epoxy-polyamide over epoxy-polyamide** | **Amercoat® 370 over Amercoat® 370** | 5 | d (4) |
| Steel | Inorganic zinc | Dimetcote® 9 | 6 | (9) |
| Steel | Epoxy-phenolic over epoxy-phenolic | | | b (2) |
| Steel | Epoxy over inorganic zinc | | | c (3) |
| Concrete | Epoxy over surfacer | | | f (6) |
| Concrete | Epoxy-phenolic over epoxy-phenolic | | | g (7) |
| Concrete | Epoxy over epoxy | | | h (8) |

These generic coating systems encompass NPP Service Level I protective coatings that date back to the early 1970s. Coating systems applied to PWR containment internal steel surfaces and to concrete walls and floors are to be investigated in this project. PIRT System "a" was identified to be of primary interest due to an instance of significant "area of detachment" of the topcoat from the IOZ primer in a NPP and also based on insights from the PIRT completed for that system. The PIRT system "f" was identified as the primary concrete coating system since this is the most widely used system. A previous Interim Report addressed the PIRT panel coating system d (SRTC designation System 5). System 5 was used to benchmark the adequacy and success of the technical approach of the project. The present Interim Report discusses the investigation of the steel coating system "a". System "a" will hereafter be referred to as System 1, in accordance with the project's nomenclature.

The ASTM standards accepted by the nuclear industry for preparation of coating test samples (ASTM D5139-90)[2.4], irradiation of test samples (ASTM D4082-95)[2.5], and simulation of DBA-LOCA testing (ASTM D3911-95)[2.6] are an integral part of this research program. Additional irradiation aging treatments and DBA-LOCA exposure conditions relevant to containment service and postulated LOCA conditions were also investigated.

The integration of PIRT panel evaluations (which are derived from identification of phenomena and processes that could lead to coating failure, and the ranking thereof) is illustrated in Table 2.2. The linking of project activities and PIRT phenomena/process elements is represented by the central column identifying physical properties and

phenomena of importance. Project resources were directed at PIRT phenomena/processes ranked high and, to a lesser degree, to the PIRT phenomena/processes of medium rank.

Section 3 of this report details results for material property testing, predictive failure modeling, DBA test findings and coating performance following a DBA test for SRTC System 1. Significant findings are provided in Section 4, and Section 5 discusses conclusions and potential follow-up activities for this project.

**Table 2-2. Project Alignment with Industry PIRT System a(1) (Steel Substrate, Inorganic Zinc Primer, Epoxy Phenolic Topcoat)**

| High-Ranked Industry PIRT Phenomena/Processes | Time Phase | Related Inputs and Physical Properties | Related Project Activities |
|---|---|---|---|
| Coating Anomalies in Primer | 2,5 | Surface Cleanliness | Adhesion and DBA Testing with Defect 1 Coupons |
| Expansion/Contraction at Primer/Topcoat Interface and Topcoat | 2,3 | Coefficient of Thermal Expansion | DBA Testing and Modeling of Stresses |
| Diffusion Rate of Air/Water at Primer/Topcoat Interface | 3,4,5 | Permeation | DBA Testing |
| Contraction of Topcoat | 3 | Coefficient of Thermal Expansion | DBA Testing and Modeling of Stresses |
| Air/Water Intrusion in Primer Through Damage Sites in Topcoat | 5 | Permeation | DBA Testing |
| Environmental Exposure to Topcoat | 1 | Total Radiation Dose, Temperature/Humidity History, Decontamination Chemicals, Corrosion, Erosion, Abrasion | Radiation Aging and Thermal Aging of Laboratory Specimens, Characterization and Testing of Plant Specimens |
| **Medium-Ranked Industry PIRT Phenomena/Processes** | **Time Phase** | **Related Inputs and Physical Properties** | **Related Project Activities** |
| Film Splitting | 1,2,3,4,5 | Cohesive Strength | Testing with Defect 1 Coupons and Modeling of Stresses, DBA Testing |
| Diffusion Rate of Air/Water into Primer | 3 | Permeation | DBA Testing |
| Mechanical Damage in Topcoast | 1 | Permeation | DBA Testing of Type 2 Defect |
| Expansion/Contraction at Primer/Topcoat Interface | 1 | Coefficient of Thermal Expansion | DBA Testing and Modeling of Stresses |
| Diffusion of Air/Water into Topcoat | 5 | Permeation | DBA Testing |
| Chemical Attack in Primer | 4 | Water Chemistry | DBA Testing |
| Air/Water Intrusion in Primer Through Damage Sites in Topcoat | 4 | Permeation | DBA Testing |
| Diffusion of Air/Water into Primer Above Pool Interface | 4 | Permeation | DBA Testing |
| Water Intrusion into Topcoat or Primer Below Pool Surface | 5 | Permeation | DBA Testing |
| Coating Anomalies in Primer and Topcoat | 1,3,4 | Surface Cleanliness | Adhesion and DBA Testing with Defect 1 Coupons |

Phase 1: Normal service to 40 years.  
Phase 2: 0 to 40 seconds into loss-of-coolant accident.  
Phase 3: 40 seconds to 30 minutes after LOCA.  
Phase 4: 30 minutes to 2 hours after LOCA.  
Phase 5: Beyond 2 hours after LOCA.

## 2.1 Material Properties

The coating system material properties being assembled in the coatings research program are a fundamental set of properties that are used to analyze coating performance and potential for coating failure. The properties may be dependent on temperature and wetness, and may be changed by aging mechanisms (e.g., oxidation, irradiation-induced scissioning, and thermal-induced cross-linking or scissioning) active during the service period and/or the design basis accident (DBA) scenario.

Material properties are required input to analytical models of coating deformation and failure (see Figure 2-1). The input property parameters used for coating System 1 are contained in Table 2-3. The property parameters have been categorized as either "properties for loading" or "properties for mechanical response." The properties for loading are those used to calculate the stress distribution in the coating system including those during DBA-LOCA

transients; the properties for mechanical response are those used to calculate deformation of the coating system subjected to stresses. The steps in analytical modeling are outlined in section 2.2. The table also includes several property parameters, not used directly as inputs to modeling, that provide a quantitative measure of the effects of aging and DBA exposure conditions on the potential for coating failure. One such parameter being measured in the research program is the adhesion strength. It is a simple measurement with sensitivity to detect differences in specimens tested at various conditions of temperature, wetness, and irradiation exposure. A reduction in the adhesion strength indicates an increase in potential for failure.

**Table 2-3. Material Property Parameters Used in Analyzing Coating Performance***

| Material Property Parameter | Topcoat | Surfacer | Substrate |
|---|---|---|---|
| **Properties for Mechanical Response** | | | |
| Ultimate Tensile Strength ($\sigma_u$) | Applicable | Applicable | Not Applicable |
| Ductility (Total Strain at Failure, $\varepsilon_f$) | Applicable | Applicable | Not Applicable |
| Young's Modulus (E) | Applicable | Applicable | Applicable |
| Poisson's Ratio (v) | Applicable | Applicable | Applicable |
| Adhesion Strength to Under Layer | Applicable | Applicable | Not Applicable |
| Adhesion Energy to Under Layer ($G_{material}$) | Applicable | Applicable | Not Applicable |
| Cohesion Energy | Applicable | Applicable | Not Applicable |
| **Properties for Loading** | | | |
| Coefficient of Thermal Expansion ($\alpha_T$) | Applicable | Applicable | Applicable |
| Glass Transition Temperature | Applicable | Applicable | Not Applicable |
| Thermal Conductivity | Applicable | Applicable | Applicable |
| Specific Heat | Applicable | Applicable | Applicable |
| Density ($\rho$) | Applicable | Applicable | Applicable |

*Parameters listed as "not applicable" are those that either have no meaning for the coating component or are not significant to coating performance.

Most of these parameters are not available either in the open literature or from the coatings vendors. The properties that are available are either not at specific environmental conditions of interest (e.g., temperature and wetness of a DBA) or may not be accurate for the specific formulation of a coating of interest (e.g., Phenoline® 305). Therefore, the coating-specific properties are being measured at DBA-relevant conditions in the coatings research program. The temperature range (100-300°F) and wetness (dry and wet) at which the properties are being measured span the conditions of the ASTM DBA profile for a PWR [2.6]. Section 3.1 describes the properties that have been measured for Phenoline® 305. These properties are collected in embedded look-up tables as described in section 3.1.

The testing methods to measure the properties for loading are ASTM standard methods. The testing methods for the mechanical response have been developed in the research program. The mechanical test methods are described in detail in Appendix A of this report.

An irradiation exposure to $1 \times 10^9$ Rad at $1 \times 10^6$ Rad/hr at 120°F in a cobalt-60 gamma source, within the specifications of ASTM standard D4082-95 [2.5], has been applied to the mechanical test specimens as an aging treatment. Properties for the parameters in Table 2-3 are collected for coatings in both the "non-aged" condition, to represent a properly formulated, properly cured coating in its initial condition, and the "aged" condition, represented by a coating subjected to treatment according to ASTM D4082-95. Appendix B describes the aging treatment in detail. Section 3.1 contains the properties for the non-aged and aged Phenoline® 305 coating.

## 2.2    Deformation Modeling

Analytical modeling of coating deformation is used to predict coating performance under the environmental conditions of the DBA-LOCA. These conditions include elevated temperatures and pressures from steam, including expected transient and steady-state conditions. Environmental conditions can create stresses in the coating that, if high enough, can cause cracking in the coating, or delamination of the coating, or both. Either cracking or delamination events are precursors in the production of a debris source (e.g., free chip). It is the production of debris that constitutes failure of the coating.

The analytical modeling is capable of predicting cracking and delamination events. The approach is to build finite element analysis models of the topcoat/primer/substrate system and input the conditions of interest to analyze the system response. There are three fundamental categories of inputs to the models:

1. Configuration - includes an initial defect postulate, location of the defect in the coating system, number of coatings and coating thickness, and the type of substrate onto which the coating is applied.
2. Materials Properties – includes mechanical and physical properties of the coating layers and substrate materials.
3. Loading – includes both direct loads (e.g., impingement of water) and environmental conditions that lead to coating stresses.

There are two parts in the analysis of coating performance. The first part is the determination of the stress distribution in a non-defected coating system at a time period of interest in the DBA cycle and a check of the following criterion for cracking:

$$\sigma_{\text{material failure}} \leq \sigma_{\text{applied}} \text{ or } \varepsilon_{\text{material failure}} \leq \varepsilon_{\text{applied}}.$$

The second part is the consideration of a defect postulate in the coating. One type of postulate is a "Type 1 defect," defined as a local delaminated region beneath the surface of the coating, as shown in Figure 2-2. This type of defect may be subject to "Mode 1 deformation" that is the formation of a blister dome, followed by delamination and cracking. As described in Appendix A, the resistance to separation of a coating along an interface may be quantified through the property $G_{\text{material}}$. $G_{\text{material}}$ is the adhesion energy to separate a coating layer from an under layer or substrate at a defect. $G_{\text{applied}}$ is the calculated adhesion energy developed by external forces acting on a coating layer at the defect. The stress-strain and $G_{\text{applied}}$ distributions are determined at a time period of interest in the DBA profile. Separation of a coating layer will proceed if the criterion expressed by the following inequality is satisfied:

$$G_{\text{material}} \leq G_{\text{applied}}.$$

Cracking may also occur near at this defect if the previous criterion is satisfied. That is, the criteria for both delamination and cracking are checked as the coating deforms to determine whether coating conditions significant to lead to formation of a debris source may be present.



**Figure 2-2. Type 1 Defect in Coating System**

The details of analytical modeling are outlined in Appendix C of this report. Section 3.2 provides the results of the analyses of coating System1 for various specific Type 1 defect postulates and DBA profiles using the measured properties for Phenoline® 305 and Carbozinc® 11 as listed in section 3.1.

## 2.3    Measured Performance Under DBA Conditions

Direct measurement of coating system performance is achieved by exposing laboratory specimens, with and without initial design defects, and in as-applied and irradiation-aged conditions, to DBA profiles. The specimens

are characterized with standard metallurgical practices to quantify blistering, cracking, and debris. The performance tests completed on the SRTC System 1 coating system were:

| Test Performed | Test Description | Test Conditions |
| --- | --- | --- |
| ASTM D3911 DBA-LOCA Test | 7 day test per ASTM D3911-95 | Included immersion of a portion of the specimens |
| Plant-Specific Pressure/Temperature Test | Pulse test incorporating rapid heating and rapid cooling of specimen | Included immersion of a portion of the specimens |
| Coating System Immersion Test | Immersion test of complete coating system (concrete substrate, surfacer, topcoat) | Testing performed from room temperature to 200°F and with 200°F initial condition |
| Free-film Immersion Test | Immersion of free-film specimens of surfacer and topcoat, in aged and non-aged conditions | Testing performed at 200°F |

Carbon steel plates were coated and used as laboratory specimens for both the mechanical tests (adhesion strength tests (i.e., pull tests) and adhesion energy tests (i.e., G-value tests)) and for DBA testing. Figure 2.4 shows plate specimens with the System1 coating before and after the irradiation aging treatment.
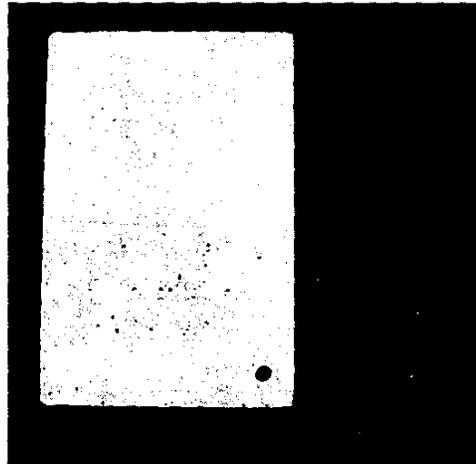


**Figure 2-4. System 1 laboratory specimens before (left) and after (right) exposure to $10^9$ rad per ASTM D4082-95.**

The specimens also were fabricated to contain a Type 1 defect at the IOZ/steel substrate interface. Type 1 defects were created by either attaching 0.472-in.-(12 mm) diameter, 0.005-in.-thick glass discs to the steel, or by applying polytetrafluorethylene (Teflon®) on the steel in well-defined locations, prior to application of the IOZ primer.

There are two DBA profiles investigated in this study: the pressurized water DBA profile specified in ASTM standard D3911-95 [2.6], termed the "full DBA profile" in this report, and a plant-specific rapid pressure/temperature pulse test. Figure 2-5 below shows the ASTM profile, which is run for a total exposure period of approximately one week.
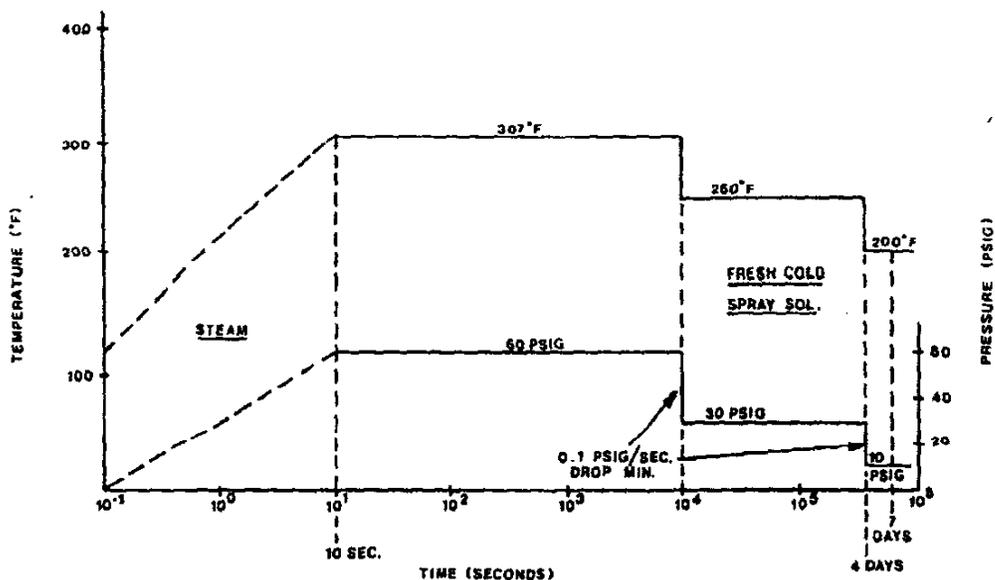
**Figure 2-5. DBA Profile for PWR per ASTM D3911-95**

The SRTC Monitored Environmental Test Chamber has been designed to duplicate, as closely as possible, the conditions specified in the ASTM profile. A description of this unique facility, which is fully equipped for video monitoring and recording and data logging, is provided in Appendix D of this report.

A "plant-specific" DBA was used in the program to investigate the performance of a coating under a rapid heat-up and cool-down pulse. Calculations of plant-specific temperature/pressure profiles typically contain this transient, which is not incorporated in the D3911-95 DBA profile.

The industry PIRT panel ranked as medium-to-high the potential for coating degradation during immersion, following a LOCA event. The significance of this observation was reinforced during the course of testing, when SRTC observed a propensity for blistering of irradiated coatings when subjected to a water soak at elevated temperature. Therefore, SRTC modified the standard ASTM DBA test sequence to include water immersion for a portion of the test specimens. To study this blistering phenomenon in greater detail, SRTC developed an apparatus for videotaping the performance of coating test specimens while immersed in water at a range of temperatures. Descriptions of the DBA and soak testing of coatings are contained in Appendices D and E of this report.

## 2.4    Coating Performance

Measurement of coating performance following combinations of irradiation aging and DBA exposure is performed by a variety of standard metallurgical and analytical techniques. Chemical information is obtained using SEM/EDS (energy dispersive spectroscopy). Optical and scanning electron microscopy are used to provide details on the structure and debris source term geometric characteristics. Appendix F contains a description of the techniques applied to the coating specimens in the coatings research program at SRTC. Section 3.4 of this report provides the results of characterization of System 1 following irradiation, DBA exposure, and irradiation plus DBA exposure. The coatings research program also includes characterization and DBA testing of NPP plant specimens. The intent is to investigate and compare the performance of plant specimens with aged laboratory specimens.

**References for Section 2**

2.1     "Coatings Handbook for Nuclear Power Plants," EPRI TR-106160, June 1996.

2.2     G. E, Wilson and B. E. Boyack, *Nuclear Engineering and Design* 186, 23-37, 1998.

2.3     Industry Coatings PIRT Report No. IC99-02, June 16, 2000, "PWR Containment Coatings Research Program Phenomena Identification and Ranking Tables (PIRTs)," by Jon R. Cavallo, Tim Andreychek, Jan Bostelman, Brent Boyack, Garth Dolderer, and David Long.

2.4    ASTM D5139-96, "Standard Specification for Sample Preparation for Qualification Testing of Coatings to be Used in Nuclear Power Plants."

2.5    ASTM D4082-95, "Standard Test Method for Effects of Gamma Radiation on Coatings for Use in Light-Water Nuclear Power Plants."

2.6    ASTM D3911-95, "Standard Test Method for Evaluating Coatings Used in Light-Water Nuclear Power Plants at Simulated Design Basis Accident (DBA) Conditions."

# 3.0 Coating System 1 Performance

## 3.1 Material Properties

This section reports the values of the physical and mechanical properties used for analyzing the performance of coating System 1, epoxy-phenolic topcoat and inorganic zinc primer on steel. The properties of specific coating products, epoxy-phenolic Phenoline® 305 and inorganic zinc primer Carbozinc® 11 used in coating System 1 tests, are reported.

As discussed in section 2.1, the properties are functions of temperature, aging condition, and wetness or moisture content. The limits of these variables were enumerated in a statistical design developed for the coatings program. The temperature range was 100, 200, and 300°F; the aging condition was non-aged (no irradiation) and aged (irradiation to $10^9$ rad at $10^6$ rad/hr at 120°F); and either wet (by soaking in water for 16 hours at the test temperature of interest) or dry (no soak). The effect of moisture on mechanical properties was evaluated at 100 and 200°F. Physical properties, including thermal conductivity, coefficient of thermal expansion, specific heat, and glass transition temperature, were measured by program subcontractors using standard laboratory techniques. Mechanical properties were measured at SRTC, with techniques developed specifically for this program. Appendix A describes the mechanical property testing techniques. It was not possible to obtain free-films for testing the properties of the inorganic zinc primer Carbozinc® 11. Therefore, the properties reported for Carbozinc® 11 are based on literature values for metallic zinc and on engineering judgement.

The measured data for coating System 1, along with literature data for the inorganic zinc primer and the steel substrate, are organized in Table 3-1 with data from the non-aged condition and, where available, the aged condition. The connections of the data in Table 3-1 to the failure model are emphasized through the grouping of (1) those properties that govern the mechanical response of the coating and (2) those properties that govern the loading on the coating induced by the DBA environment. Entries in these tables either are data values themselves or are references to subsequent tables ("embedded tables") which then list the values of the specific property under all the measurement conditions. The tabulated data for adhesion, $G_{material}$, and free-film tensile strength are supplemented with load/extension or stress/strain curves at selected conditions. The mechanical properties are discussed in the order of their appearance in Table 3-1 in the following sections.

## 3.1.1 Tensile Properties: Tensile Strength, Ductility (strain at failure), and Modulus

Tensile properties were measured on free-film specimens, prepared with methods described in Appendix A. The Phenoline® 305 specimens were from 0.009 to 0.016 inch in thickness with a gage length of 1.4 inches and a gage width of 0.25 inch. It was not possible to prepare free-film specimens of Carbozinc® 11. The tensile specimens were pulled to failure in an Instron universal testing machine. The extension rate was 0.02 to 0.05 inch/minute. Figure 3-1 shows the engineering stress-engineering strain curves for Phenoline® 305 in the dry condition calculated from the load-displacement data, and Figure 3-2 the curves for Phenoline® 305 in the wet condition. The stress-strain curves were subsequently adjusted for toe compensation according to ASTM D882-97 "Standard Test Method for Tensile Properties of Thin Plastic Sheeting." The parameters calculated from the adjusted curves are the elastic modulus and percent strain at failure; ultimate stress was measured from the raw data. Table 3-2 reports these parameters for Phenoline® 305.

The Phenoline® 305 data show that temperature and radiation are significant factors affecting tensile properties. Increasing temperature and irradiation to $1 \times 10^9$ rad markedly reduces the ultimate strength and the modulus. Irradiation to a total dose of $10^9$ rad reduces strength especially at the higher test temperatures of 200 and 300°F. At 300°F in the dry condition, the ultimate strength falls from 460 psi in the non-irradiated specimens to 30 psi in the irradiated one. Strain at failure does not change monotonically with irradiation. It decreases with irradiation at 100°F, increases at 200°F, and is little changed at 300°F, compared with measurements on non-irradiated specimens. Phenoline® 305 was tested at a lower total gamma radiation dose of $1 \times 10^7$ rads in the 200°F dry condition (Figure 3-3). The $10^7$-rad specimens showed a slight strengthening and similar ductility compared with the unirradiated specimen. The wetness condition (dry versus overnight immersion in tap water at the test temperature) affects the coating differently depending on temperature. It has a high impact on the 100°F data, but a low impact on the 200°F data. This may result from the unavoidable drying of the wet 200°F test specimen during equilibration in the oven just before testing.

### 3.1.2 Adhesion (Adhesion Strength to Under Layer)

The adhesion test, also referred to as the adhesion pull test to distinguish it better from the adhesion G-value test below, measures the adhesion strength of the coating to its under layer(s). Adhesion tests were performed on System 1 in the non-irradiated, dry and wet conditions at 100°F and 200°F. The adhesion strengths are listed in Table 3-7.

### 3.1.3 Adhesion G-Value (Adhesion Energy to Under Layer)

The adhesion $G_{material}$ test measures the adhesion energy between layers of a coating, or in other words, the resistance to separation of layers. A comparison of the $G_{material}$ with a calculated $G_{applied}$ that represents the environmental loading on the coating permits one to predict whether a coating defect will grow by delamination. As described in Appendix A, the $G_{material}$ test is an adhesion test with the puller affixed to the coating directly over a zero-adhesion defect. The defect was created on System 1 specimens by either affixing a 12-mm-diameter, 0.13-mm thick glass disk to the steel surface, or by applying polytetrafluorethylene (Teflon®) through a mask onto a designated location on the surface. A valid test requires extension of the defect by delamination. If the test specimen fails intra-layer, then the calculation of $G_{material}$ from the load-displacement record should not be used.

The adhesion G-value test results for System 1 (Phenoline® 305 topcoat over Carbozinc® 11 primer on steel) are shown in Figure 3-4. Separation occurred at the intentional defect in all the 100°F tests and in the 200°F unirradiated dry and wet tests. The 200°F irradiated tests showed separation within the topcoat at very low loads, as in the System 2 tests. The separation appeared to occur deeper within the topcoat rather than in the near-surface layer. A G value cannot be calculated from tests in which separation occurs within the topcoat. As in the System 2 tests, separation, or failure, between the puller and the coupon or block must occur at the designed defect in order to calculate a G value. The trends in the G-value data (shown in Table 3-8) are consistent with tests of System 2, which had the same Phenoline® 305 topcoat, but on Starglaze® 2011S surfacer on concrete. The coating system strength at 100°F greatly exceeds that at 200°F. Water exposure tends to increase the ductility (as expressed by the extension to maximum load) and decrease the modulus. Previous testing has revealed a decrease in maximum load with irradiation, but the 100°F dry irradiated test shows a higher maximum load than does the corresponding wet condition test. These observations are based on single tests at the stated conditions. One duplicate test was run, however, at the 100°F dry irradiated condition. The duplicate was run after the exposure of the coupon to the 200°F dry test condition, and that thermal history substantially reduced the maximum load of the duplicate compared to that of the initial 100°F dry irradiated test. This change is probably related to the mobilization of radiolytic products and other thermal effects at 200°F, such as have been seen in water immersion tests at 200°F.

### 3.1.4 Cohesion Energy

Cohesion energy is a test of tearing resistance in free-film specimens subjected to a tensile test. The test specimen is similar to the 'dog-bone' used to determine tensile strength, but contains a defect in the form of an edge notch in the middle of the gage length. Cohesion tests were run only on Phenoline® 305 at the sole condition of dry, non-irradiated, 200°F.

## Table 3-1. Material Properties for Coating Failure Analysis[a,b]

| Material Property | Non-Aged Condition | | | Aged Condition Representing 40 Years of Service including $10^9$ rad Exposure | | |
|---|---|---|---|---|---|---|
| | Epoxy Phenolic | IOZ Primer | Steel | Epoxy Phenolic | IOZ Primer | Steel |
| Properties for Mechanical Response | | | | | | |
| Tensile Strength (psi) | See Table 3-2 | nd | 43,000 [11] | See Table 3-2 | nd | 43,000 [11] |
| Ductility (Total Strain at Failure) (%) | See Table 3-2 | nd | 30 [11] | See Table 3-2 | nd | 30 [11] |
| Modulus (mPa) | See Table 3-2 | 1700 @ 100° F 3600 @ 200° F | 207,000 [12] | See Table 3-2 | nd | 207,000 [12] |
| Poisson's Ratio | 0.35 [8] | 0.4 | 0.3 [13] | 0.35 [8] | | 0.285 [13] |
| Adhesion Strength (psi) to Under Layer | See Table 3-7 | | | See Table 3-7 | | |
| Adhesion Energy (J/m²) to Under Layer ($G_{material}$) | See Table 3-8 | | | See Table 3-8 | | |
| Cohesion Energy (in-lb/in²) | | | | | | |
| Properties for Loading | | | | | | |
| Coefficient of Thermal Expansion (m/m/°C) | See Table 3-5 | $4 \times 10^{-5}$ | $1.3 \times 10^{-5}$ | See Table 3-5 | See Table 3-5 | $1.8 \times 10^{-5}$ |
| Glass Transition Temperature (°C) | 74.8 | N/A | N/A | 76.6 | N/A | N/A |
| Thermal Conductivity (W/m/K) | See Table 3-4 | 110 | 43 [9] | See Table 3-4 | nd | 49 [9] |
| Specific Heat (J/kg/K) | See Table 3-6 | 400 | 473 [10] | See Table 3-6 | nd | 450 [10] |
| Density (kg/m3) | See Table 3-3 | 7140 | 7801 [14] | See Table 3-3 | nd | 7840 [14] |

[a]Listed properties are a function of moisture content and temperature and are for dry films near room temperature
[b]Table values without [] are measured values
nd – not determined

### Table 3-2. Free-Film Tensile Test Results for Phenoline® 305

| Temp. °F | Aging | Wetness Condition | Ultimate Strength (psi) | Modulus (psi) | % Strain at Failure |
|---|---|---|---|---|---|
| 100 | Non-irradiated | Dry | 1700 | 43000 | 16 |
| 100 | Non-irradiated | Dry | 2000 | 110000 | 10 |
| 200 | Non-irradiated | Dry | 480 | 2000 | 2.3 |
| 300 | Non-irradiated | Dry | 460 | 3100 | 15 |
| 100 | Non-irradiated | Wet | 1200 | 26000 | 16 |
| 200 | Non-irradiated | Wet | 740 | 3200 | 26 |
| 100 | Irradiated | Dry | 300 | 80000 | 0.4 |
| 100 | Irradiated | Dry | 1000 | 51000 | 2.5 |
| 200 | Irradiated | Dry | 180 | 280 | 63 |
| 300 | Irradiated | Dry | 30 | 190 | 11 |
| 100 | Irradiated | Wet | 290 | 35000 | 1.4 |
| 200 | Irradiated | Wet | 220 | 290 | 68 |

### Table 3-3. Densities

| | Non-Irradiated (kg/m³) | Irradiated (kg/m³) |
|---|---|---|
| Phenoline® 305 | 1423 | 1497 |
| Carbozinc ® 11 | 7140 | nd |

nd – not determined

### Table 3-4. Thermal Conductivity

| | Phenoline® 305 | Carbozinc® 11* |
|---|---|---|
| Temperature (°F) | Non-irradiated (W/m•K) | Non-irradiated (W/m•K) |
| 100 | 1.591 | 110 |
| 200 | 1.640 | |
| 300 | 1.717 | |

Note: Insufficient irradiated Phenoline® 305 was available for testing.

* Based on metallic zinc; no temperature dependence assumed.

**Table 3-5. Coefficients of Thermal Expansion[†]**

| Temperature (°C) | Phenoline® 305 | | Carbozinc ® 11* |
|---|---|---|---|
| | Non-irradiated (m/m•K) | Irradiated (m/m•K) | Non-irradiated (m/m•K) |
| -20 | $6.0 \times 10^{-5}$ | $5.9 \times 10^{-5}$ | |
| -10 | $5.6 \times 10^{-5}$ | $6.0 \times 10^{-5}$ | |
| 0 | $5.4 \times 10^{-5}$ | $5.9 \times 10^{-5}$ | |
| 10 | $5.6 \times 10^{-5}$ | $5.8 \times 10^{-5}$ | |
| 20 | $5.9 \times 10^{-5}$ | $5.6 \times 10^{-5}$ | $4 \times 10^{-5}$ |
| 30 | $6.3 \times 10^{-5}$ | $5.6 \times 10^{-5}$ | |
| 40 | $6.8 \times 10^{-5}$ | $5.8 \times 10^{-5}$ | |
| 50 | $7.4 \times 10^{-5}$ | $6.1 \times 10^{-5}$ | |
| 60 | $8.0 \times 10^{-5}$ | $6.4 \times 10^{-5}$ | |
| 70 | $8.5 \times 10^{-5}$ | $6.7 \times 10^{-5}$ | |
| 80 | $9.1 \times 10^{-5}$ | $7.2 \times 10^{-5}$ | |
| 90 | $9.7 \times 10^{-5}$ | $7.9 \times 10^{-5}$ | |
| 100 | $10.1 \times 10^{-5}$ | $8.7 \times 10^{-5}$ | |
| 110 | $10.6 \times 10^{-5}$ | $9.4 \times 10^{-5}$ | |
| 120 | $11.3 \times 10^{-5}$ | $10.2 \times 10^{-5}$ | |
| 130 | $12.2 \times 10^{-5}$ | $11.1 \times 10^{-5}$ | |
| 140 | $13.5 \times 10^{-5}$ | $12.3 \times 10^{-5}$ | |

[†] Total thermal expansion from reference temperature at -30°C.
* Based on metallic zinc; no temperature dependence assumed.

**Table 3-6. Specific Heats**

| Temperature (°C) | Phenoline® 305 | | Carbozinc ® 11* |
|---|---|---|---|
| | Non-irradiated (J/kg•K) | Irradiated (J/kg•K) | Non-irradiated (J/kg•K) |
| -20 | 954.95 | 855.1 | |
| -10 | 1013.95 | 896.05 | |
| 0 | 1051.55 | 926.05 | |
| 10 | 1086 | 957.8 | |
| 20 | 1122.5 | 994.45 | 400 |
| 30 | 1163 | 1033.25 | |
| 40 | 1207 | 1080.4 | |
| 50 | 1271 | 1171 | |
| 60 | 1395 | 1248.5 | |
| 70 | 1450.5 | 1302.5 | |
| 80 | 1525 | 1371 | |
| 90 | 1575 | 1424.5 | |
| 100 | 1594.5 | 1451 | |
| 110 | 1606 | 1467.5 | |
| 120 | 1616.5 | 1482 | |
| 130 | 1627.5 | 1496 | |
| 140 | 1633 | 1505 | |
| 150 | 1636 | 1511 | |
| 160 | 1643.5 | 1519.5 | |
| 170 | 1648.5 | 1528.5 | |

* Based on metallic zinc; no temperature dependence assumed.
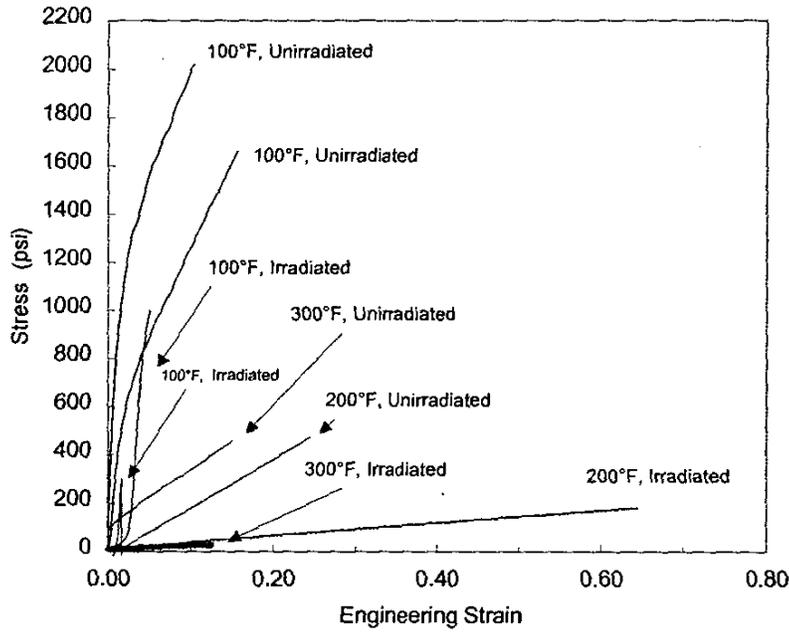
**Figure 3-1. Free-film tensile test results for Phenoline® 305 in the dry condition.**
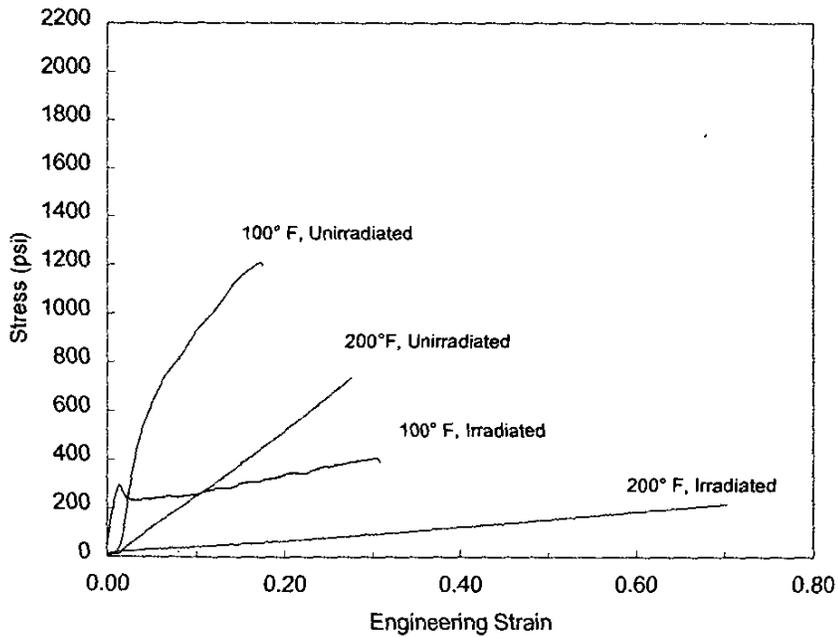


**Figure 3-2. Free-film tensile test results for Phenoline® 305 in the wet condition.**

Phenoline 305 Tensile Data, 200°F Dry Condition
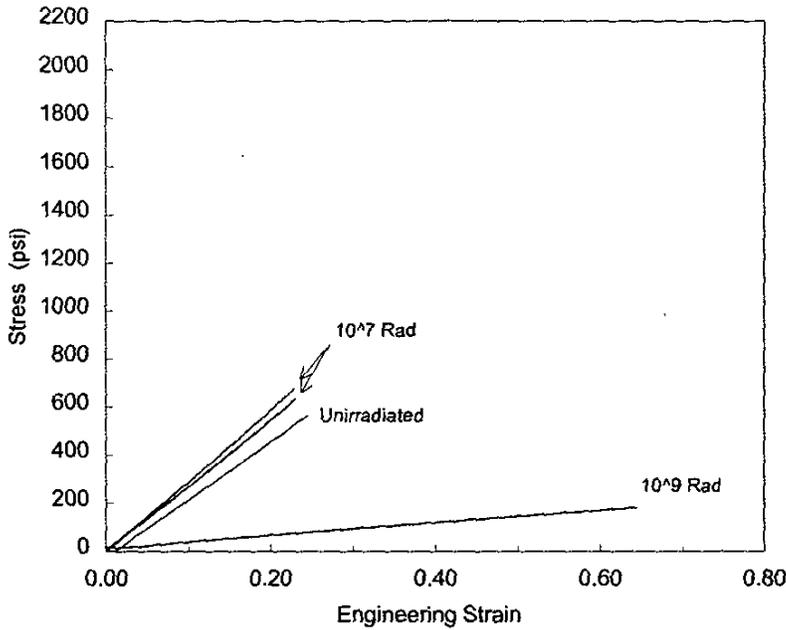


Figure 3-3. Tensile test data for Phenoline® 305 at 200°F obtained in the dry condition.

Table 3-7. Adhesion Pull Test Results for System 2

| Temperature °F | Aging | Wetness Condition | Adhesion Strength (psi) |
|---|---|---|---|
| 100 | Non-irradiated | Dry | 809 |
| 200 | Non-irradiated | Dry | 219 |
| 100 | Non-irradiated | Wet | 863 |
| 200 | Non-irradiated | Wet | 429 |

Table 3-8. Adhesion G-Value Test Results for System 1

| Temperature °F | Aging | Condition | Peak Load (lb) | Material G-Value (J/m$^2$) | Failure Location |
|---|---|---|---|---|---|
| 100 | Non-irradiated | Dry | 51.55 | 77 | At glass defect |
| 100 | Non-irradiated | Wet | 72.98 | 266 | At glass defect |
| 200 | Non-irradiated | Dry | 11.46 | 23 | At glass defect |
| 200 | Non-irradiated | Wet | 26.76 | 98 | At glass defect |
| 100 | Irradiated | Dry | 73.23 | 77 | At glass defect |
| 100 | Irradiated | Wet | 70.51 | 250 | At glass defect |
| 200 | Irradiated | Dry | 1.92 | nd [‡] | At topcoat surface |
| 200 | Irradiated | Wet | 4.96 | nd [‡] | Within topcoat |

nd = not determined

[‡]: Calculations were not performed because the failure locations were not at glass defects.

System 1 G-Value Test
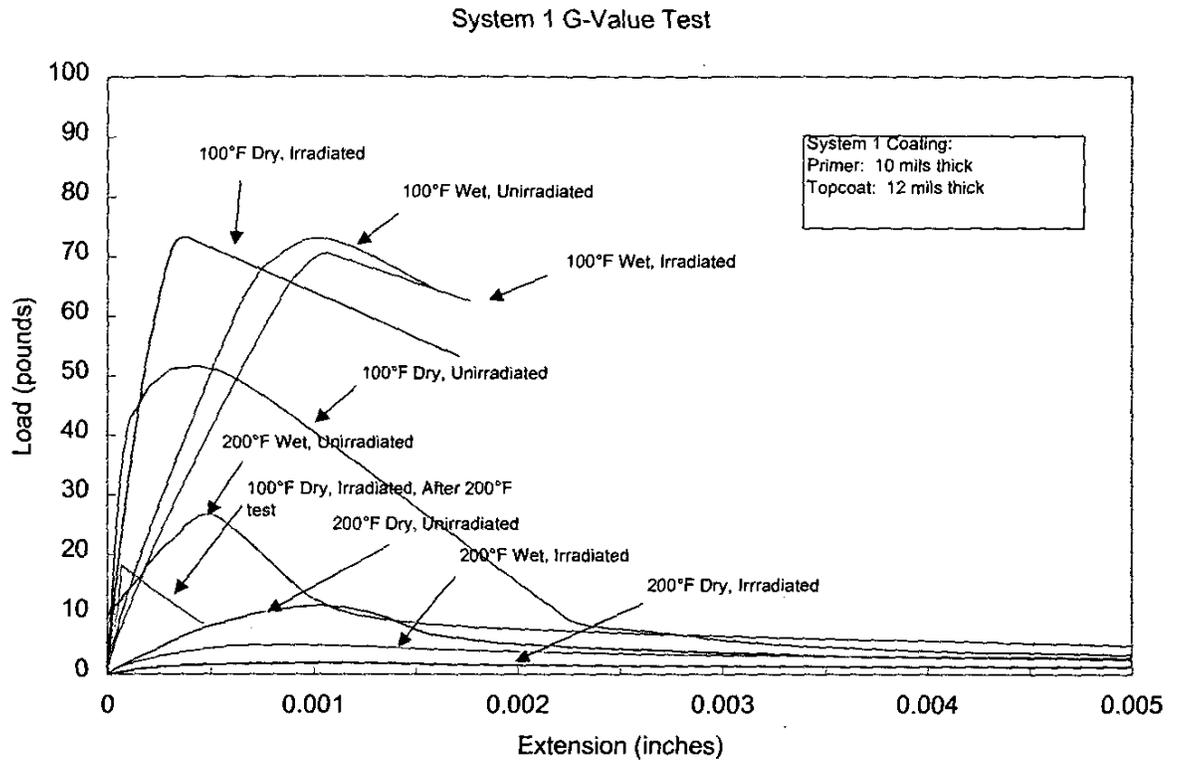


**Figure 3-4. Adhesion G-value test results for System 1.**

## 3.2 Deformation Modeling

Analytical modeling is used to predict the performance of coating System 1 under the temperature and pressure conditions of the DBA. The temperature and pressure conditions include both transient and steady state. Coating stresses and deformations are calculated using finite element analysis. The resulting coating conditions are evaluated with respect to: 1) stress/strain overloads; and 2) fracture instabilities in order to determine the onset of coating failure. The analytical modeling does not extend beyond cracking and blistering of the coating to predict the total disbondment in the creation of chip or particulate debris that would fall from the surface. Appendix C provides the details of the finite element method to calculate temperature profiles and coating deformations to analyze coating performance.

Two separate analytical models for deformation of the coating were established to analyze the coating deformation where either a blister first forms (Mode 1 deformation) or a crack first forms (Mode 2 deformation). Figure 3-5 is a schematic of the Mode 1 deformation model. For Mode 1 analysis, it is assumed that a defect (Type 1 defect) may exist in the coating materials (topcoat or primer) or on the material interfaces (between topcoat and primer or between primer and the substrate). Mode 1 deformation would cause a blister to grow in size or crack or both under DBA conditions. The second type of defect model (Type 2 defect), Figure 3-6, is a coating defect emanating from the end of surface scratch or a through-coating crack. Mode 2 deformation would cause an initial cracked and delaminated region to extend in size or "peel back".

Analytical models are built for the configurations of the non-defected and defected laboratory specimens used in the experimental DBA testing. The material properties used in this analysis are listed in Tables 3-1 to 3-6. The coating thicknesses were measured from a sectioned block. As a result, the topcoat (Phenoline® 305) thickness input to the finite element model is 10 mils and the primer (Carbozinc® 11) thickness input is 12 mils.

The defected laboratory specimens are those with Type 1 internal defects (Figure 2-2). Type 1 specimens were subjected to DBA testing as described in section 3.3.

This section provides the results of the analysis of the coating System 2 for the following general cases under the transient conditions of the DBA:

Non-irradiated, non-defected
Non-irradiated, Type 1 defect, no trapped water
Non-irradiated, Type 1 defect, trapped water

The objective of the analytical modeling is to predict coating performance under the ASTM D3911-95 DBA-LOCA exposure using the temperature-dependent and wetness-dependent material properties. The most severe events of the ASTM DBA-LOCA exposure in terms of thermal excursion are 1) heating during the first 10 seconds and 2) the cool-down after long-term (10,000 seconds) steady state exposure. Therefore, a 10-second rise time from 120°F to 307°F and a 5-second fall from 307°F to 250°F were evaluated as the first two transients in the profile. The predicted performance is summarized in section 3.2.4.
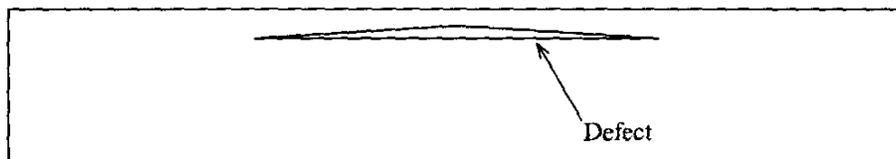


Figure 3-5. Mode 1 Analysis model
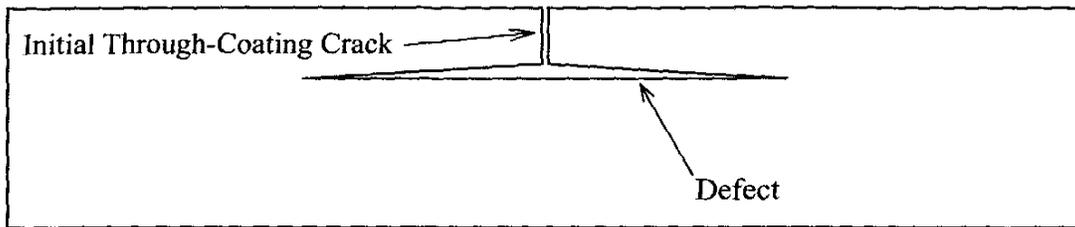
Figure 3-6. Mode 2 Analysis model

### 3.2.1 Thermal-Stress Analysis for Coating System 1

The coating systems with or without defects under DBA temperature were calculated with the temperature dependent Young's moduli (Table 3-2). For this analysis it was assumed that the deformation of the coating system would not affect the heat transfer characteristics of the model. Therefore, the temperature distributions in the coating-substrate system were first calculated with a thermal transient finite element analysis. These temperature distributions were then input to the stress analysis using the same finite element mesh but with continuum type of elements. The Young's modulus determined at 200°F was used for the temperatures above 200°F where the data are not available.

### 3.2.2 Failure Prediction for Coating System 1 – Non-Defected Coating

The stress level in the coatings was calculated for an idealized system in which the topcoat (Phenoline®
305) is uniformly 10 mils and the primer (Carbozinc® 11) is uniformly 12 mils. The stresses in the non-defected topcoat and the primer are always under compression during the DBA exposure. Therefore, no major cracking in either the topcoat or the primer is predicted.

### 3.2.3 Failure Prediction for Coating System 1 – Type 1 Defect in Coating

The following analysis and results reported in this section show that a Type 1 defect in the System 1 coating at the primer/steel interface will not propagate as a large blister or crack during DBA exposure, even when water is trapped within the defect.

Thermo-mechanical analysis was performed to characterize the response of a System 1 coating with a Type 1 defect (12 mm in diameter). The front surface of the specimen was assumed to be subjected to the ASTM D3911-95 DBA temperature-pressure profile: The temperature rises from 122 °F to 307 °F in 10 seconds; remains at 307 °F for 10,000 seconds, and then drops from 307 °F to 250 °F in five seconds. The calculation continued for an additional 10 seconds to show the post-spray effects.

The calculated temperature profile was input to the mechanical analyses. Two cases were considered: 1) The defect is traction free (no moisture), and 2) The defect is loaded by the net pressure defined as the difference between the vapor pressure inside the defect and the ambient pressure of the test chamber.

Both the thermal and mechanical properties of the steel substrate were obtained from the properties compiled in Section 3.1. The Young's modulus is 207,000 MPa, coefficient of thermal expansion is $1.3 \times 10^5$ m/m•K (averaged), thermal conductivity is 43 W/m•K (averaged), specific heat is 473 J/kg•K (averaged), and density is 7801 kg/m³. The physical and thermal properties for the coating materials can be found in Tables 3-2 to 3-6.

The selected tensile data input for the topcoat at 100 and 200 °F under wet conditions are listed in Table 3-2. (The load-deflection curves were converted to the stress-strain curves by procedures suggested in the ASTM D882-97). The Poisson's ratios for the substrate and coating materials are given in Table 3-1.

A Type 1 defect with diameter 12 mm was placed between the primer and the steel substrate. The J-integral option in the finite element code (ABAQUS) was used to evaluate the applied G-values for this

defect with and without vapor pressure due to trapped water in the defect. When there is no vapor pressure present inside the defect, the applied G-value is mainly due to the thermal expansion mismatch. The maximum applied G-value ($0.6 \text{ J/m}^2$) occurs about 0.1 seconds after the initial heating is complete (10 seconds and at 307 °F), as shown in Figure 3-7. It can be seen that the peak value of the applied G-value is insignificant compared to the material G-values in Table 3-8 ($98 \text{ J/m}^2$), and thus no delamination would occur. It can be concluded that this defect will not grow under the condition in which there is no trapped water in the defect.
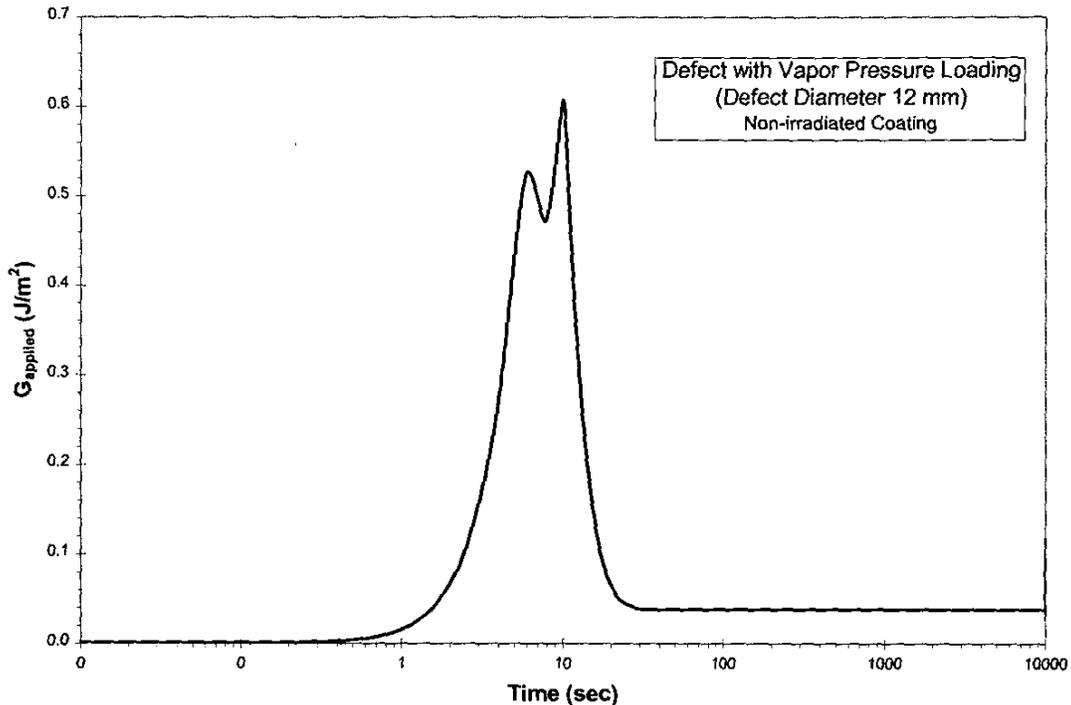


Figure 3-7. Applied G-Values at the Edge of a Dry Defect (Diameter 12 mm) during DBA Test (Logarithmic Time Scale).

During the application of cooling water spray, the DBA temperature and the associated pressure will decrease. However, the defect temperature, dominated by the steel underneath the defect, remains high due to the insulation of the topcoat and the primer. If moisture is present inside the defect, the vapor pressure inside the defect would surpass the ambient pressure in the DBA. The net pressure will cause the defect to form a blister. The applied G-value is thus increased dramatically during the cool-down stage. The highest applied G-value achieved is $59 \text{ J/m}^2$ (Figures 3-8 and 3-9), which is below the material G-value ($98 \text{ J/m}^2$) tested at 200 °F in Table 3-8. Therefore, this defect under vapor pressure loading is predicted to be stable. When the cooling spray is completed, the defect temperature gradually equilibrates with the ambient, and the net pressure eventually returns to zero.

As the defect forms a blister under the pressure loading, the material would be stretched under tensile stress and strain (parallel to the layers). Because the Carbozinc® 11 primer layer is not expected to sustain tensile load, only the stress and strain states at the apex of the blister in the topcoat were examined.

Figure 3-10 shows the maximum tensile stress in the topcoat layer at the apex of the blister during the first 10025 seconds of the DBA testing time. It can be seen that the tensile stress in the cool-down phase in the Phenoline® 305 topcoat is below the ultimate stress (Table 3-2). The failure of the coating is not predicted under the maximum stress criterion. (Figure 3-11).

Similarly, the time history of the maximum tensile strain in the highly stressed area (at the apex of the blister in the topcoat) is plotted in Figures 3-12 and 3-13, along with the evolution of the failure strain which is a function of temperature. Based on the failure strain criterion, the coating would not fail, as shown in Figures 3-13.

The analysis results are consistent with the DBA tests in which no coating failures were observed.
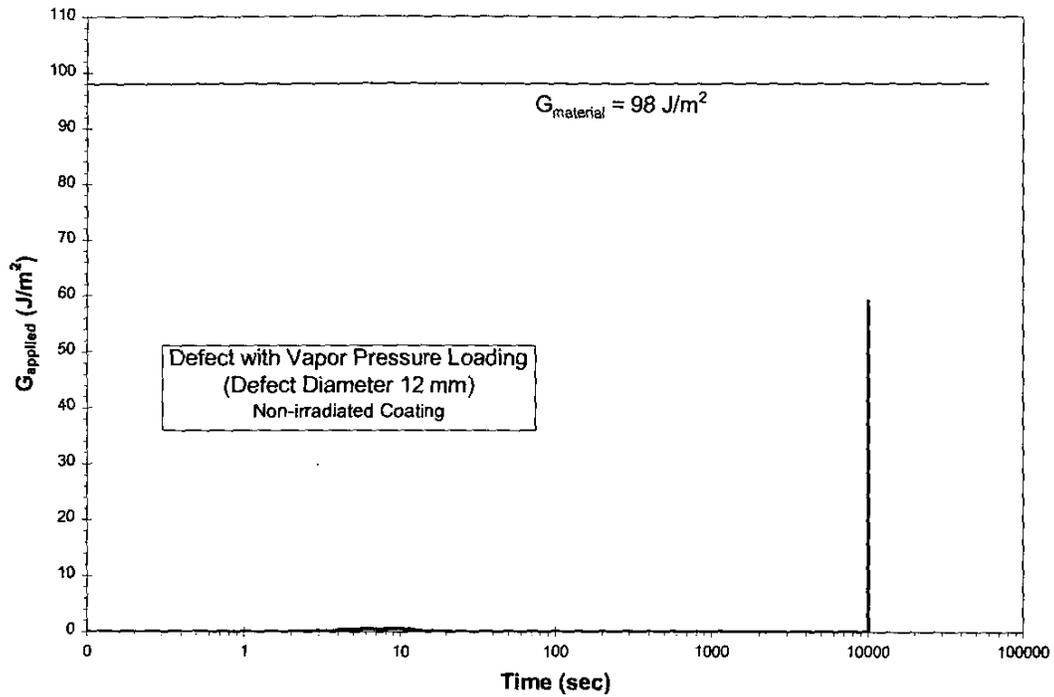


Figure 3-8. Applied G-Values at the Edge of a Vapor Pressurized Defect (Diameter 12 mm) During DBA Test (Logarithmic Time Scale).
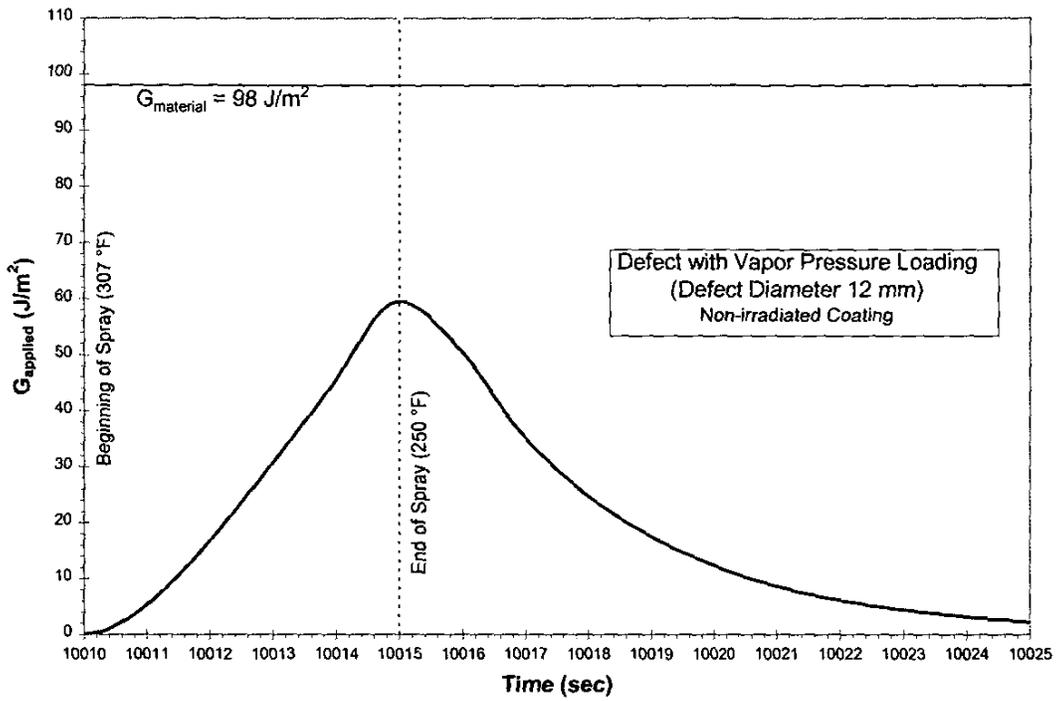
Figure 3-9. Applied G-Values at the Edge of a Vapor-Pressurized Defect (Diameter 12 mm) During Cooling Phase in DBA Test (Linear Time Scale).
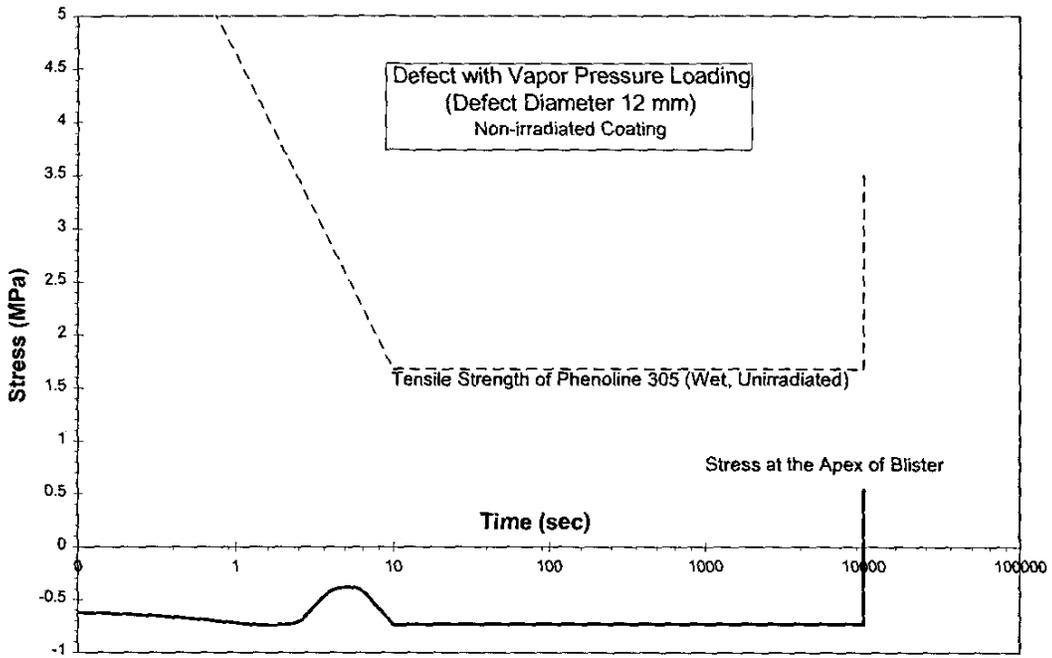
Figure 3-10. Failure Assessment of Type 1 Defects Using the Peak Tensile Stress Criterion
(Entire Time History with Logarithmic Time Scale).
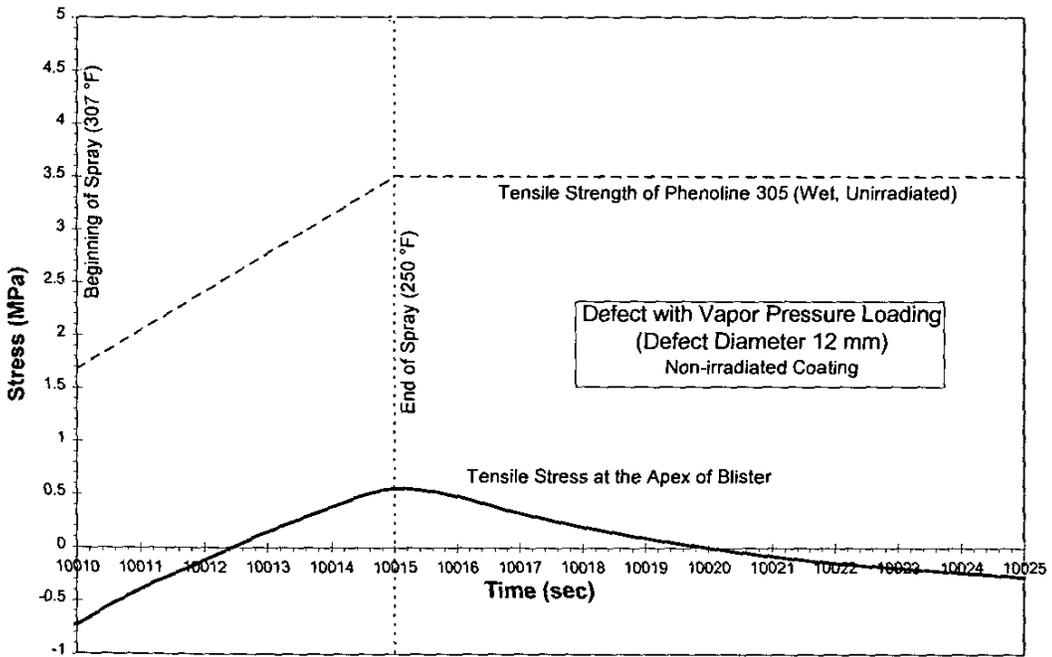


Figure 3-11. Failure Assessment of Type 1 Defects Using the Peak Tensile Stress Criterion
(Cool-down Phase with Linear Time Scale).

3-6
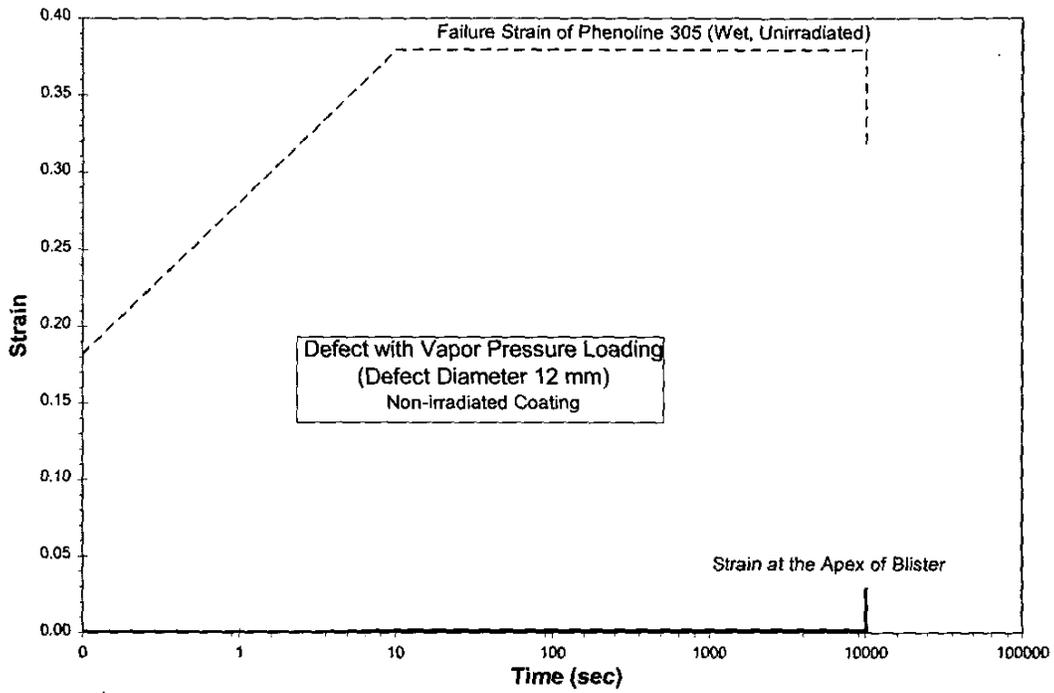
Figure 3-12. Failure Assessment of Type 1 Defects Using the Failure Strain Criterion
(Entire Time History with Logarithmic Time Scale).
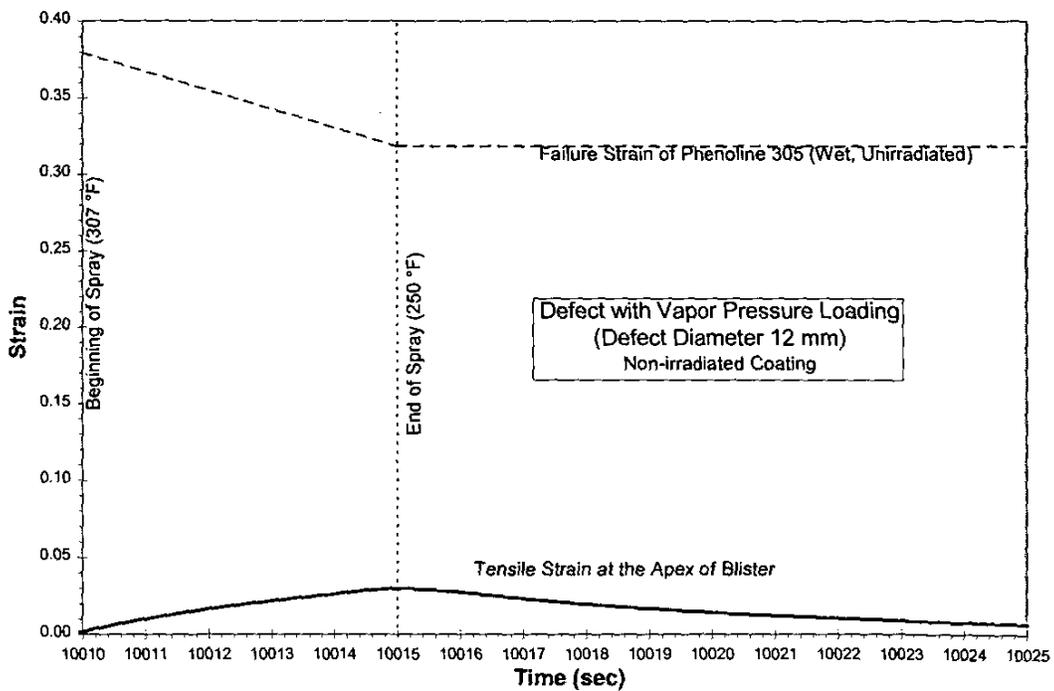


Figure 3-13. Failure Assessment of Type 1 Defects Using the Failure Strain Criterion
(Cool-down Phase with Linear Time Scale).

### 3.2.4 Deformation Modeling Predictions

Analytical modeling of coating deformation using finite element analysis is performed to predict deformations that precede failure. That is, "incipient failure" (blister formation & growth, cracking, peel-back of cracked films) can be predicted.

The results in the preceding sections show that no deformation significant to lead to failure occurs in non-defected or defected System 1 coating. The intact (non-defected), non-irradiated coating System 1 using Phenoline® 305 topcoat and Carbozinc® 11 primer is not predicted to undergo major cracking under DBA conditions because a compressive stress exists in the coating throughout the time period. For the same reason, a coating containing Type 2 defects will not result in peel-back deformations. The Type 1 defects of 12mm diameter will not undergo growth or cracking, even if they contain water vapor pressure loading.

### 3.3 Measured Performance Under DBA and Immersion Test Conditions

Two DBA profiles are used in this study: a full DBA test per ASTM D3911-95, and a rapid transient DBA pressure/temperature pulse test to simulate a "plant-specific" DBA. In addition, immersion tests (in water) were performed at elevated temperatures to simulate submergence of coatings following a DBA.

| Test Performed | Test Description | Test Conditions |
|---|---|---|
| ASTM D3911 DBA-LOCA Test | 7 day test per ASTM D3911-95 | Included immersion of a portion of the specimens |
| Plant-Specific Pressure/Temperature Test | Pulse test incorporating rapid heating and rapid cooling of specimen | Included immersion of a portion of the specimens |
| Coating System Immersion Test | Immersion test of complete coating system (steel substrate, primer, topcoat) | Testing performed from room temperature to 200°F and with 200°F initial condition |
| Free-film Immersion Test | Immersion of free-film specimens of topcoat, in aged and non-aged conditions | Testing performed from room temperature to 200°F |

The standard DBA temperature and pressure profile for qualification of coating systems is given in ASTM standard D3911-95 and is termed the "full DBA profile" in this report. Figure 3-14 shows this profile, which is run for a total exposure period of approximately 1 week. A typical temperature-pressure profile from a DBA test performed in the SRTC Monitored Environmental Test Chamber is shown in Figure 3-15. The temperature/pressure profile is given in two parts, due to software restrictions.
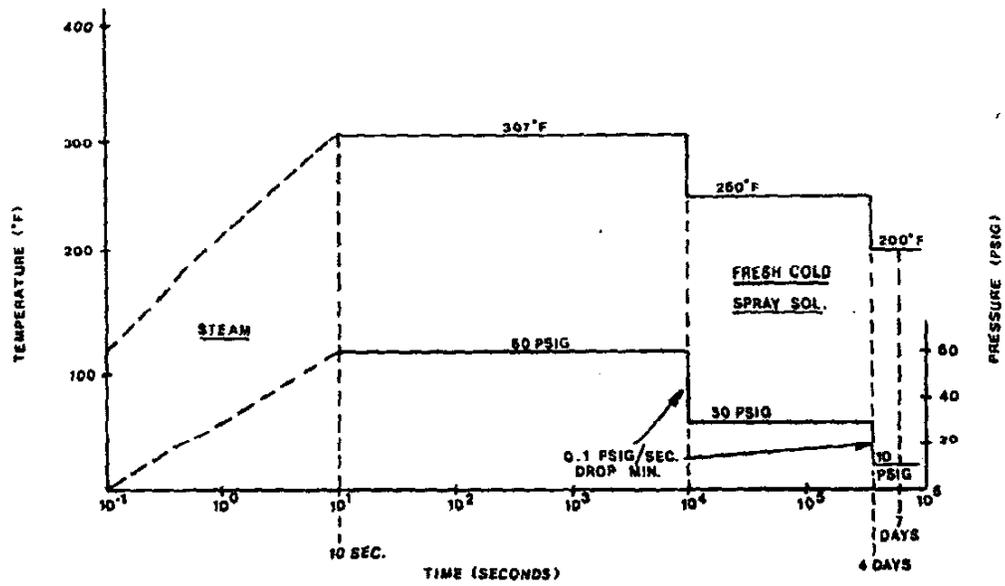
Figure 3-14. Typical Pressurized Water Reactor Design Basis Accident (DBA) Testing Parameters (from ASTM D3911-95). (Note: The ASTM figure contains an error: 30 psig should be 15 psig, which is equivalent to 30 psia).

**System 1, Full DBA - Part 1**
**8/21/00**
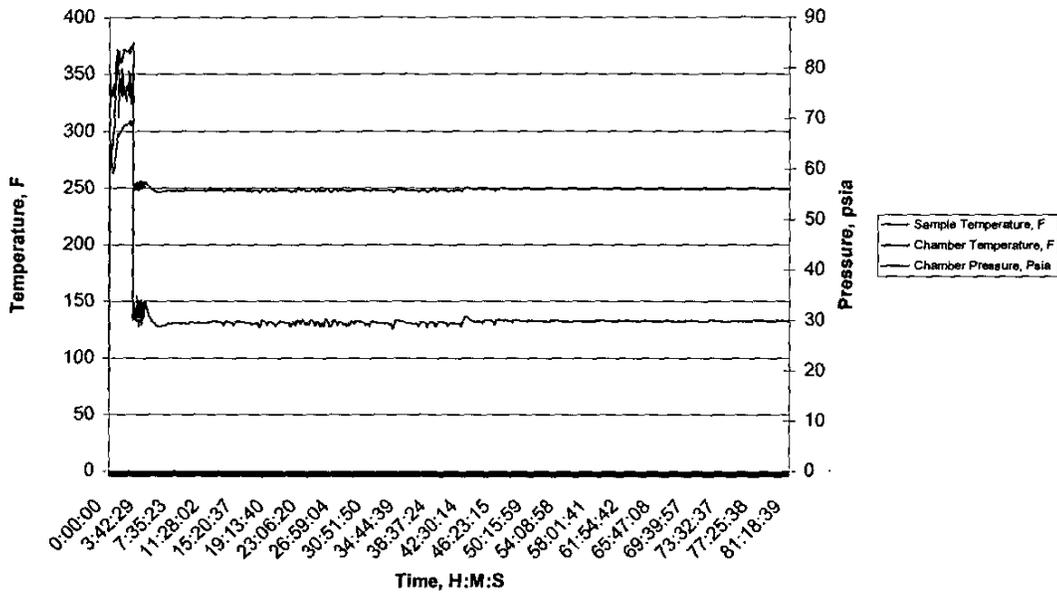


**System 1 Full DBA-Part 2**
**8/21/00**
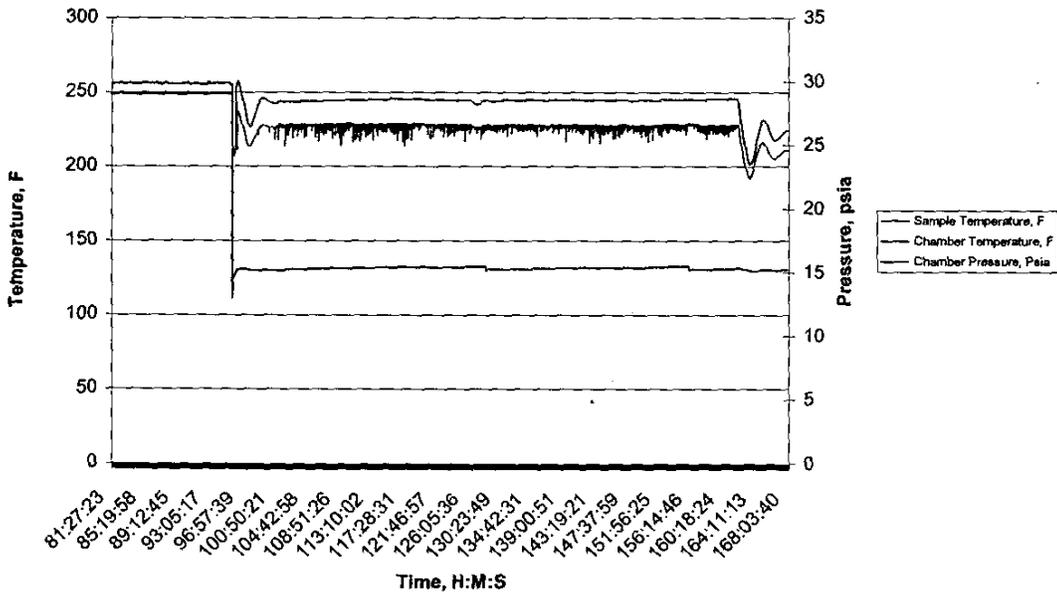


Figure 3-15. Typical Temperature-pressure Profile from SRTC System 1 D3911 DBA-LOCA Test.

Computer modeling indicated a susceptibility to failure of an epoxy coating during a rapid pulse transient, if water were present beneath the coating (see Section 3.2). A similar rapid transient has been calculated

3-10

for nuclear power plants using the MELCOR computer model. To examine System 1 coating performance in this type of plant-specific LOCA event, the SRTC coatings performance evaluation system was used to subject aged and non-aged System 1 specimens to a rapid temperature-pressure pulse (Figure 3-16).
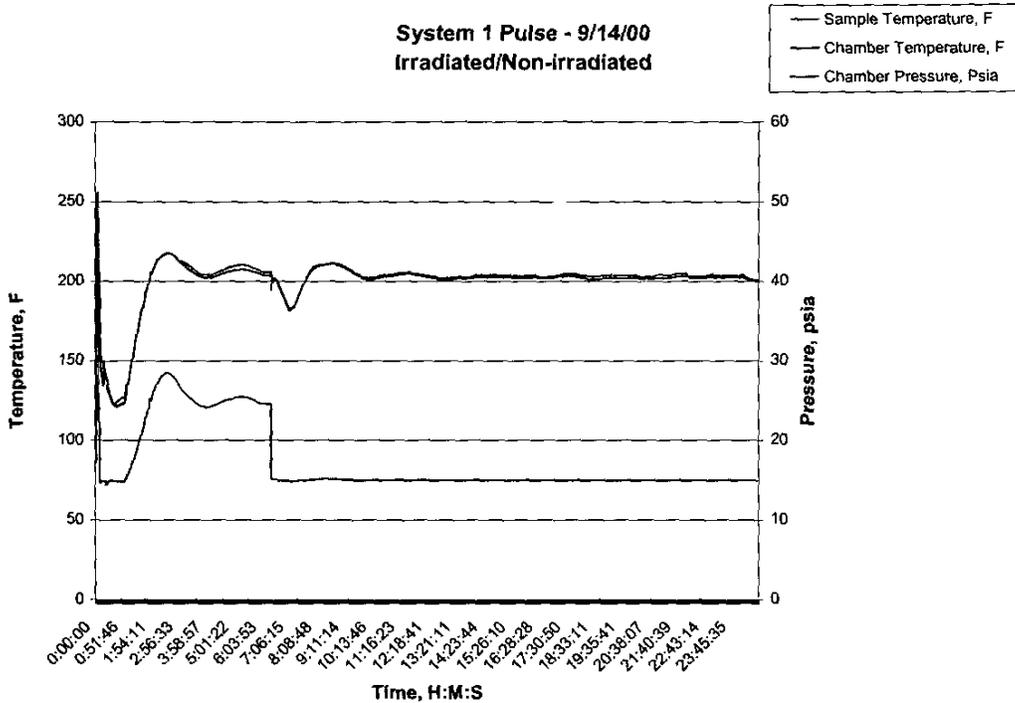


Figure 3-16. Temperature-Pressure Curves from Plant-specific LOCA Test

## 3.4 Coating Performance

Characterization of the performance of Phenoline® 305 following irradiation-aging*, DBA exposure, and irradiation plus DBA exposure was performed by a variety of standard metallurgical and analytical techniques. Chemical and compound information were obtained using SEM/EDS. Optical and SEM microscopy were used to provide details on the structure and debris source term geometric characteristics. The principal findings are 1) the resistance of the non-aged coating to any significant degradation and, 2) the development of blistering and the creation of a debris source in the aged (irradiated) coating. The debris source term forms in the top 1-2 mils of the topcoat, and is formed only under certain temperature and wetness conditions.

Significant changes appear to occur in the near-surface layer of the aged (irradiated in air) System 1 coating. A surface color change from the unirradiated material (Figure 3-21) was observed. The color change extends a few thousandths of an inch into the topcoat. This depth of color change is presumed to be related to oxygen permeation during irradiation, and does not appear when specimens are irradiated in an argon atmosphere.

System 1 specimens, which were irradiation-aged, exhibited blistering after having been exposed to elevated temperature in air or in water. Similar blistering was observed during the testing of SRTC Systems 2 and 5 coatings. For example, numerous small blisters appeared in free-film specimens, which

---

* Unless otherwise noted, irradiation-aging refers to irradiation with the SRTC cobalt-60 gamma source to $1 \times 10^9$ rads total dose at $1 \times 10^6$ rads/hour and 120° F.

had been irradiated to 1 x 10$^9$ rads, when they were heated in air to 200 °F during tensile testing (Figure 3-17). The blisters were approximately 10 mils in diameter and remained intact. Similar small, but less numerous, blisters were formed when free-film specimens were irradiated to 1.0 x 10$^8$ rads or 2.5 x 10$^8$ rads, then immersed in 200°F water (Figures 3-18 and 3-19). Much larger blisters appeared when specimens which had been irradiated to 1 x 10$^9$ rads were heated in 200°F water (Figure 3-20). In all cases, the blisters which were formed were quite thin compared to the nominal 12 mil coating thickness, and were quite fragile when dry. The thickness of the coating layer forming the blister was only about 0.001 inch (1 mil). The thickness of the blisters indicates they are formed in the darkened, ostensibly oxygen affected, outer layer of the irradiated coating. The blisters are presumed to be the result of agglomeration and/or expansion at elevated temperature of gases produced in the topcoat during irradiation.



0.020 in
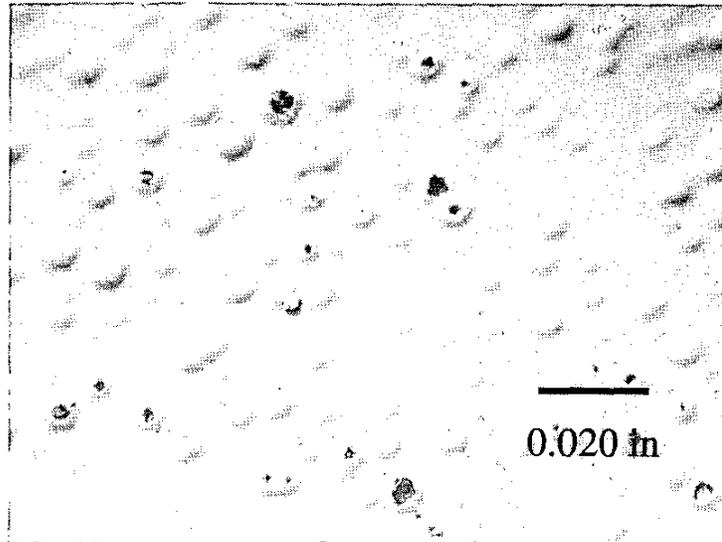
**Figure 3-17 Micrograph of blistering formed on Phenoline® 305 free-film specimen following irradiation to 1 x 10$^9$ rads and heating to 200°F, dry; original magnification approximately 20x.**
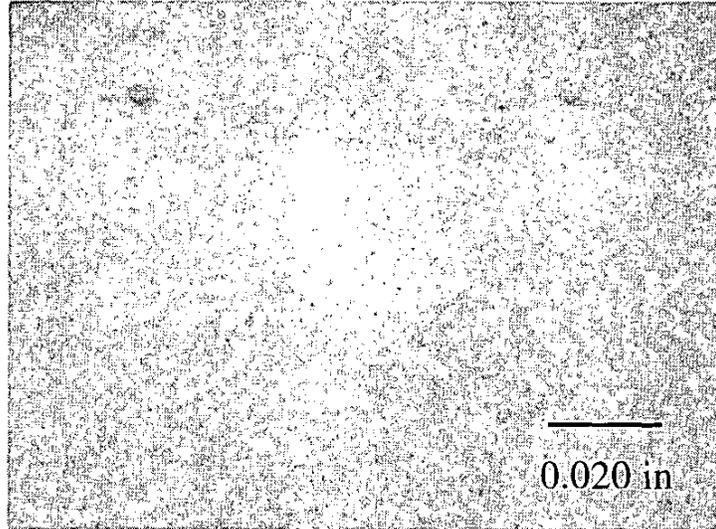
**Figure 3-18** Micrograph of blistering formed on Phenoline® 305 free-film specimen following irradiation to 1.0x $10^8$ rads and immersion in 200°F water; original magnification approximately 20x.
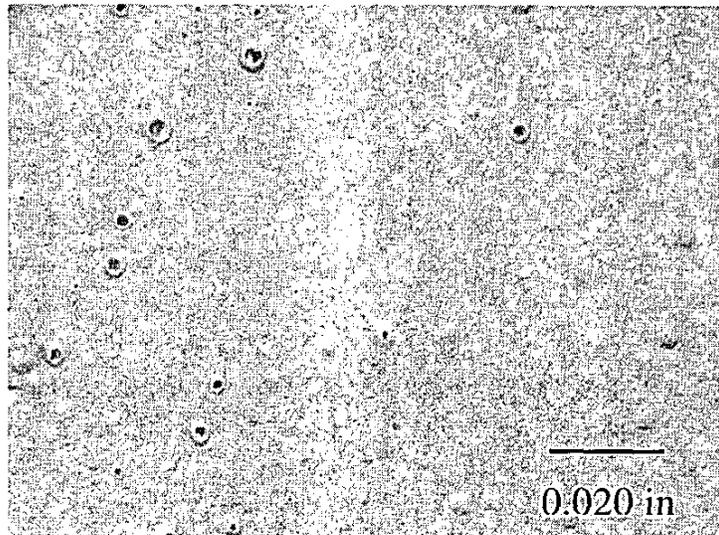


**Figure 3-19** Micrograph of blistering formed on Phenoline® 305 free-film specimen following irradiation to 2.5 x $10^8$ rads and immersion in 200°F water; original magnification approximately 20x.
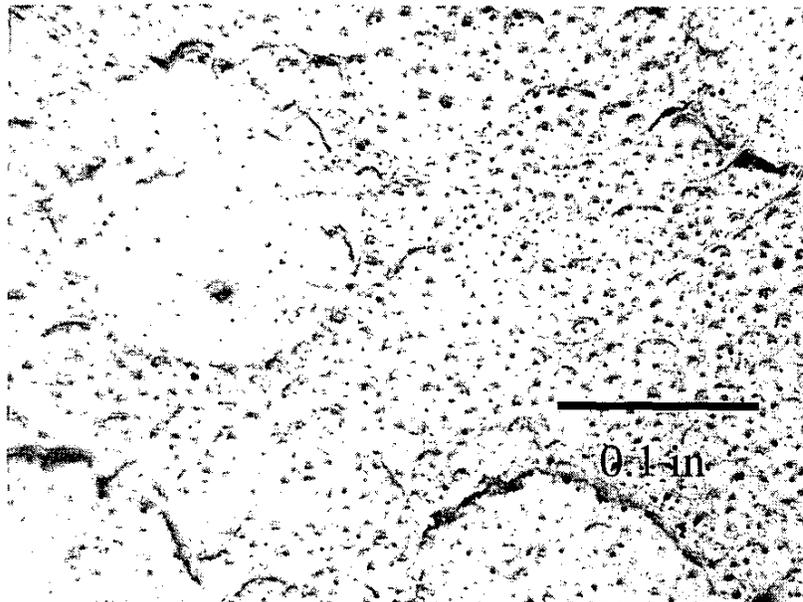
**Figure 3-20 Micrograph of blistering formed on Phenoline® 305 specimen following irradiation to 1 x 10⁹ rads and immersion in 200°F water; original magnification approximately 7x.**

As shown in Figure 3-1, the ductility of Phenoline® 305 increases significantly with increasing temperature; the effect is even more pronounced when the coating is wet as shown in Figure 3-2. Therefore, it is possible that gases which are formed within the coating agglomerate and expand with heating of the specimen, contributing to the formation of blisters.

Significant blistering was not observed in irradiated coating specimens during DBA-LOCA testing performed in accordance with ASTM D3911-95 (Figures 3-22 and 3-23). However, microscopic examination of the surface of the irradiated specimens following testing revealed evidence of coating softening and the presence of numerous pores in the coating (Figure 3-24). A cross-section of the irradiated coating made after DBA-LOCA testing (Figure 3-25) verified the pores are confined to the outermost layer of the topcoat. Therefore, it is possible any gases which formed in the topcoat during irradiation were released from the coating during the high-temperature steam exposure, which occurs during the first 2.8 hours of the DBA test cycle. During this time, the specimen is heated with 75 psia steam to 307°F. At this temperature, the coating may become so soft, and the gases so mobile, that the gas pressure is relieved through the coating without forming large blisters. It is probable, however, that small debris particles were released from the coating at this time, although this speculation has not been confirmed.
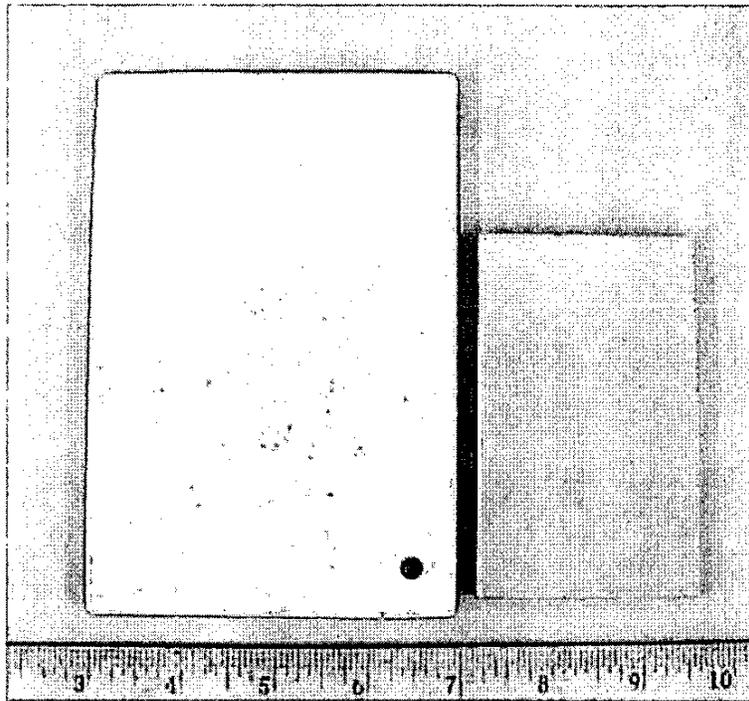
Figure 3-21.  Overall views of System 1 specimens before (left) and after irradiation-aging.
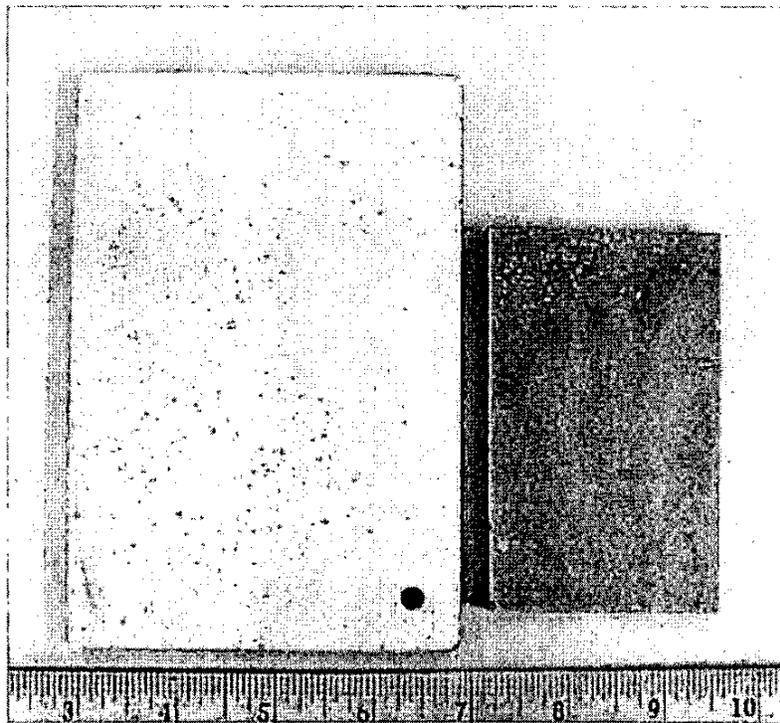


Figure 3-22. Overall views of  System 1 specimens after DBA/LOCA testing according to ASTM D3911-95.
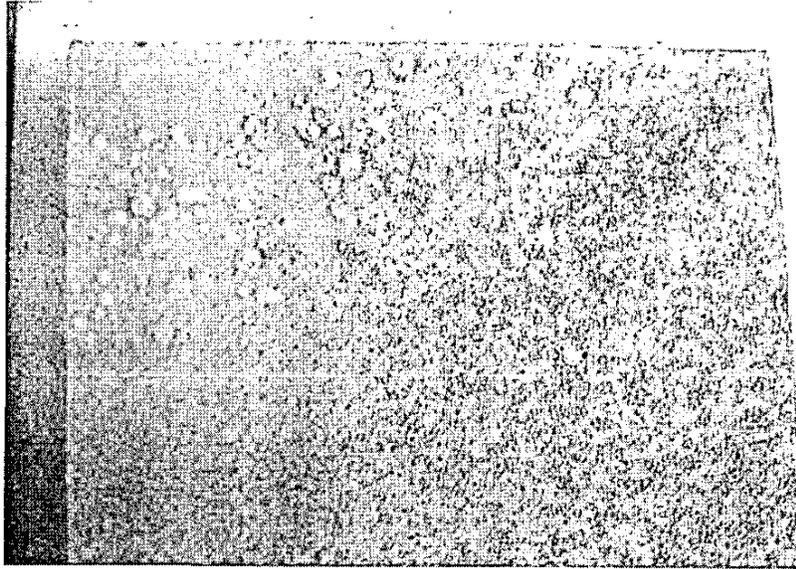
**Figure 3-23. Detail of the surface of the irradiation-aged specimen after DBA testing. Note the presence of intact blisters in the coating.**
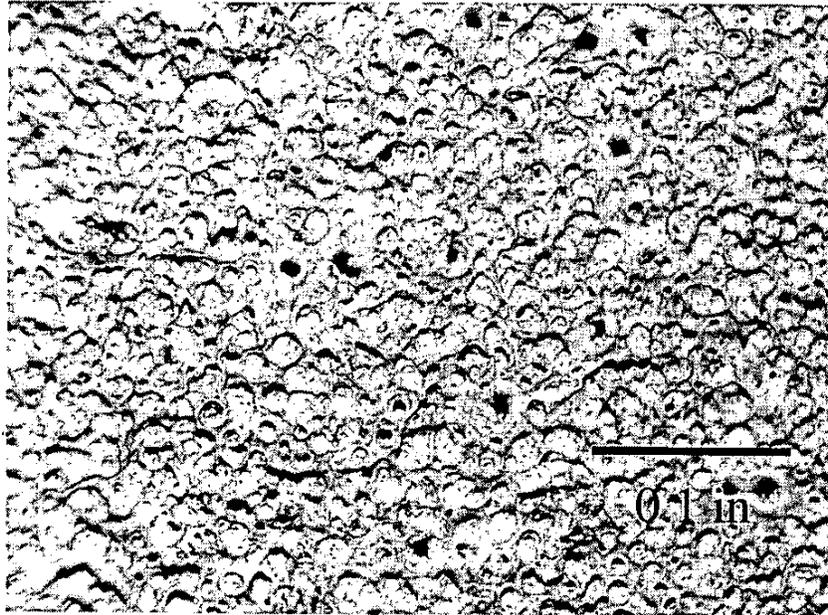


**Figure 3-24. Microscopic view of the surface of the irradiation-aged specimen after DBA testing illustrating evidence of coating softening and formation of pores. Original magnification 7x.**

Mounting Medium

Topcoat

IOZ Primer

Steel Substrate

0.01 in
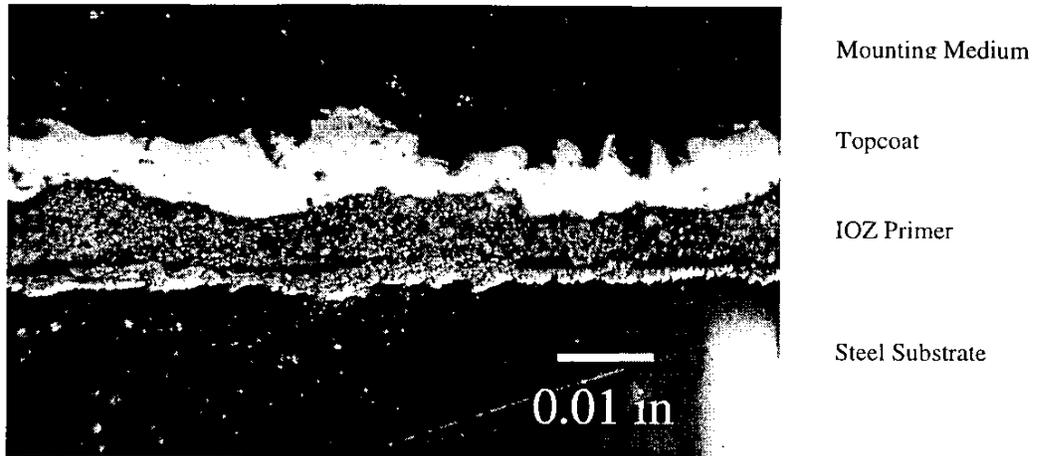
**Figure 3-25. Cross-section of the surface of the irradiation-aged specimen after DBA testing. Note the presence of pores in the coating. Original magnification 30X.**

Blistering and coating sloughing were observed in irradiation-aged specimens during plant-specific DBA/LOCA testing, where the coating was subjected to a rapid pressure/temperature pulse (Figure 3-26); no evidence of coating failure was observed in the non-aged specimens. This could indicate that any gases formed within the coating during irradiation-aging are not released through pores at high temperature (> 200°F), as is believed to occur during the full DBA/LOCA, due to the rapidity of the temperature pulse. Rather, these gases remain to form blisters during the water spray portion of the test, while the specimen is held at a temperature of approximately 200°F. Alternately, these blisters may coalesce, allowing the topmost layer of the topcoat to slip with respect to the underlying topcoat. The coating damage observed was similar to that observed in irradiated System 2 specimens. This is as expected since the topcoat was the same (Phenoline® 305) and all of the observed damage was confined to the outermost layer of the topcoat.
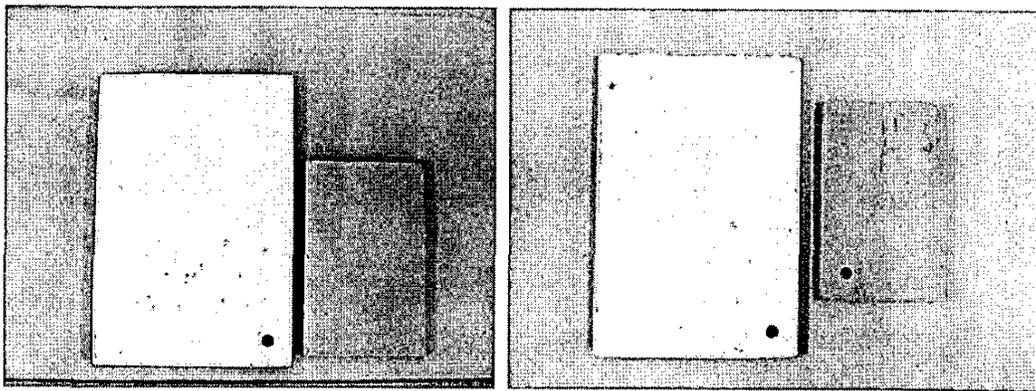


**Figure 3-26. Overall view of the non-aged (left) and irradiation-aged (right) System 1 specimens before (left photo) and after (right photo) a plant-specific DBA/LOCA test. The specimens in the left-hand photo are not the specimens used in the plant-specific test, but were identical specimens used in the full LOCA test and included here for illustration. The actual test specimens in the right-hand photo are oriented as they were during testing.**
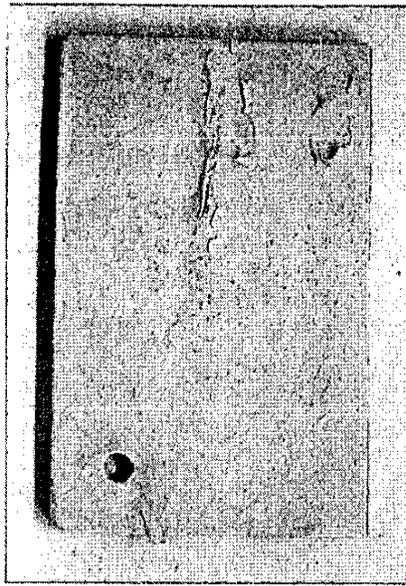
Figure 3-27. Overall view of the irradiation-aged System 1 specimen, revealing blistering and sloughing of the topmost layer of the topcoat.



Bottom Edge
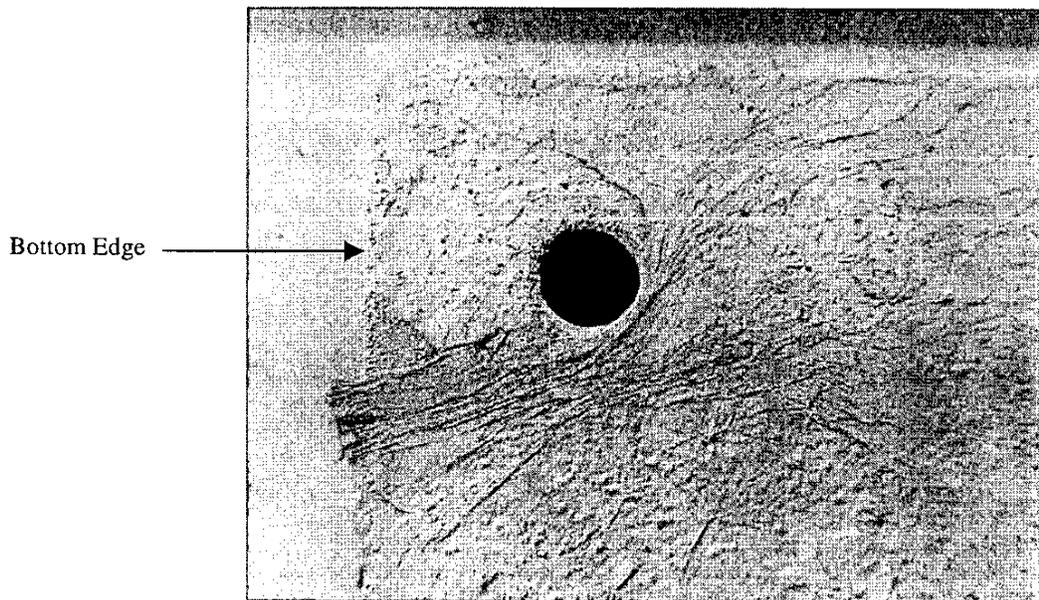
Figure 3-28. Detail view of bottom of the irradiation-aged System 1 plate illustrating the sloughing of the topmost layer of the topcoat. The left side of the specimen, in this view, was placed down during testing. Note: The outermost layer of the topcoat has slipped beyond the edge of the plate.

3-18

Mounting Medium

Topcoat

IOZ Primer

Steel Substrate

**Figure 3-29. Cross-section of the surface of the irradiation aged specimen after plant-specific DBA-LOCA testing. Note the presence of pores in the coating. Original magnification 30X**

The blisters, which form in wet, irradiated coatings, as shown above, can, in certain conditions, become a debris source term. This is illustrated by Figures 3-30 through 3-33 below, which document blister formation and coating failure in a 200° F immersion test of irradiation-aged and non-aged System 1 coating specimens.
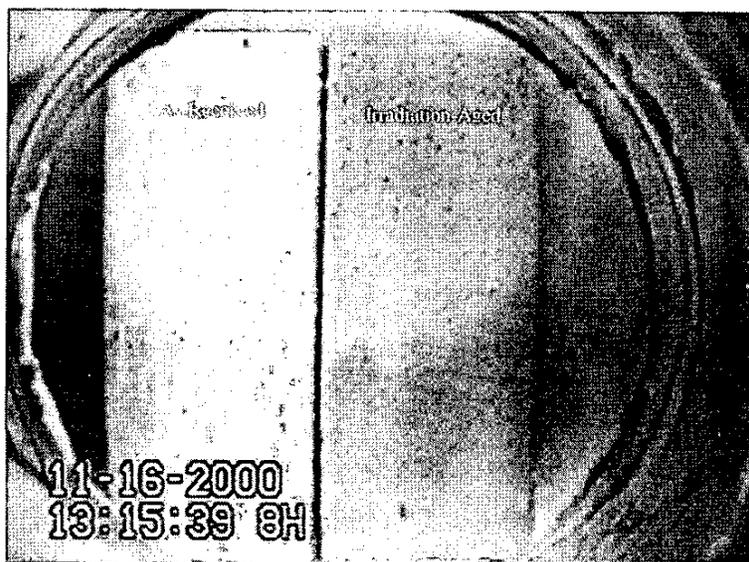


**Figure 3-30. System 1 specimens immediately after immersion in water preheated to 200° F; as-applied (left), irradiation-aged to 1x10$^9$ rads @ 1x10$^6$ rad/hour and 120° F (right).**
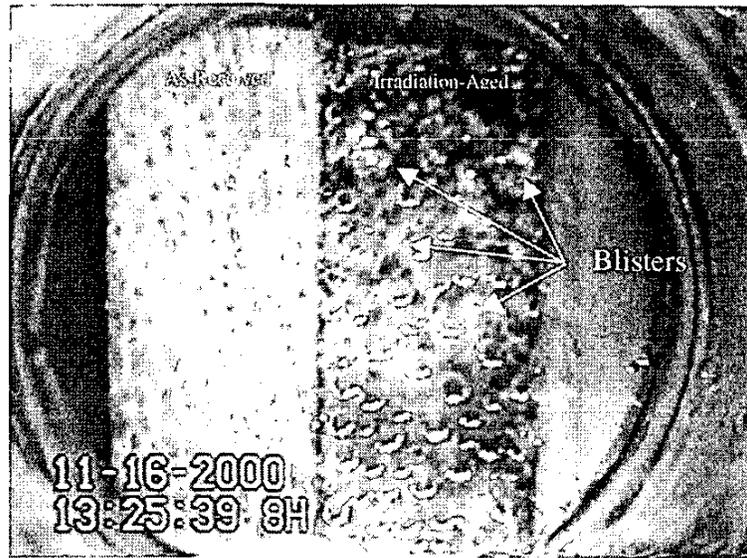
**Figure 3-31. System 1 specimens 10 minutes after immersion in water preheated to 200° F.**

The debris which is formed during immersion of the irradiation-aged coating consists of thin blisters which form in the outermost layer of the topcoat, and then break free due to the buoyancy of the gas they contain. Therefore, the surface area of these blisters is significantly larger than the surface area of the coating from which they arise, due to the ductility of the wet coating.
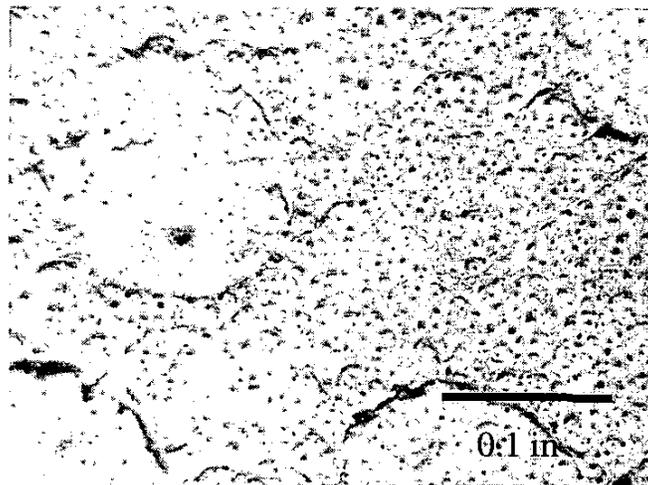


**Figure 3-32. Microscopic view of the surface of the irradiation-aged immersion test specimen illustrating the extent of blister formation and detachment. Note the presence of pores in the topcoat remnant. Original magnification 7X.**

Mounting Medium

Topcoat

IOZ Primer

0.01 in

Steel Substrate
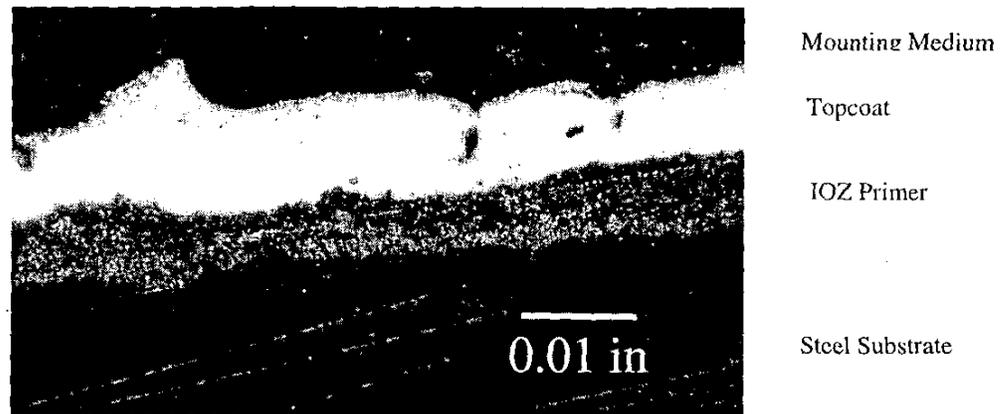
**Figure 3-33. Cross-section of the surface of the irradiation-aged immersion test specimen. Note the presence of pores in the topcoat remnant. Original magnification 45X.**

The formation of blisters has been observed during immersion testing of coated specimens of both steel and concrete, and in every case, the blistering has been confined to the outermost layer of the topcoat. During the testing of SRTC System 2, in order to determine the origin of the gases responsible for the blistering, water immersion testing was performed on free-film specimens of the topcoat, which is the same topcoat as used in SRTC System 1. Observations made during this testing confirmed that most or all of the gases, which contribute to the formation of coating blisters, originate within the topcoat.

Debris Particle Size

Analyses were performed to determine the size-distribution of particles released in immersion testing of irradiation-aged Phenoline® 305. Two different techniques were applied to two different water samples in an effort to characterize the wide range of particle sizes produced. For the relatively few larger particles, an optical image analysis technique was used to characterize coating debris generated during immersion testing of an SRTC System 2 specimen. (This debris would be expected to be equivalent to that generated by System 1, as both coating systems use Phenoline® 305 as the topcoat, and all debris generated to-date has been generated in the top few thousandths of an inch of the topcoat.) Debris was collected onto 20-micron filter paper for characterization of the larger particles. Particles smaller than approximately 0.1 mm in size were deliberately omitted in this characterization technique, due to limitations in optical imagery (see Figure 3-34). To characterize the much greater number of smaller-diameter debris particles, an electrical sensing zone technique utilizing the Coulter Principle was employed to analyze a water sample containing debris generated during an immersion test of a System 1 plate specimen. The Coulter technique determines a size distribution of particles suspended in an electrically conductive liquid by measuring a change in current, which is proportional to the volume of the particle, as the particles are passed through an aperture.

0.1 in
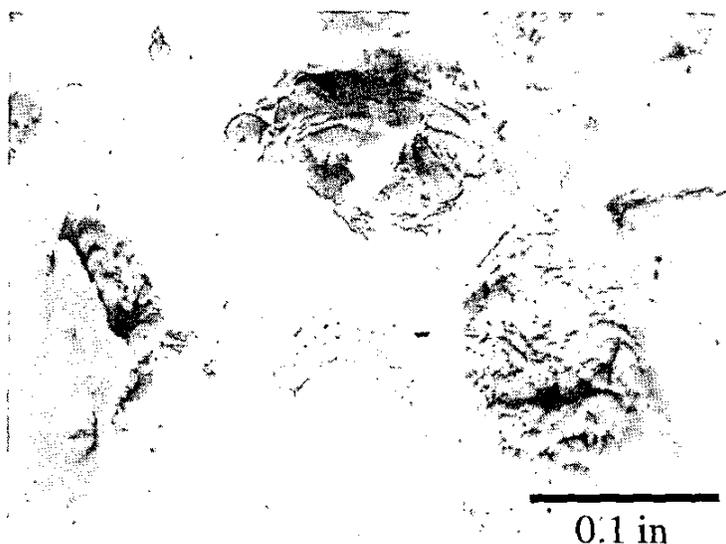
**Figure 3-34 Micrograph of typical debris particles generated from Phenoline® 305 in immersion testing. Original magnification approximately 7x.**

In the optical image analysis technique, medium magnification pictures were used to calculate the two-dimensional particle size (area) of a subjectively chosen subset of the available debris particles, with the aid of Adobe Photoshop® software. Assuming circular particles, a diameter was calculated for each particle in a sample size of approximately 250, using pixel count area. A frequency histogram of the resulting particle size diameters is shown in Figure 3-35. The mean* diameter of the particles measured optically was approximately 0.5 mm (0.021 inch); the median diameter was 0.2 mm (0.008 inch).

The Coulter technique examined over 100,000 particles between 1 and 30 micro-meters (microns), yielding a mean particle size (by volume %) of 2.6 microns (0.0001 inch), and a median diameter of 1.6 microns ($6 \times 10^{-5}$ inch), see Figure 3-36.

---

* Mean diameter is the arithmetic average of the particle sizes observed, and is greatly influenced by extreme values. The median diameter is the value at the midpoint of the frequency distribution.
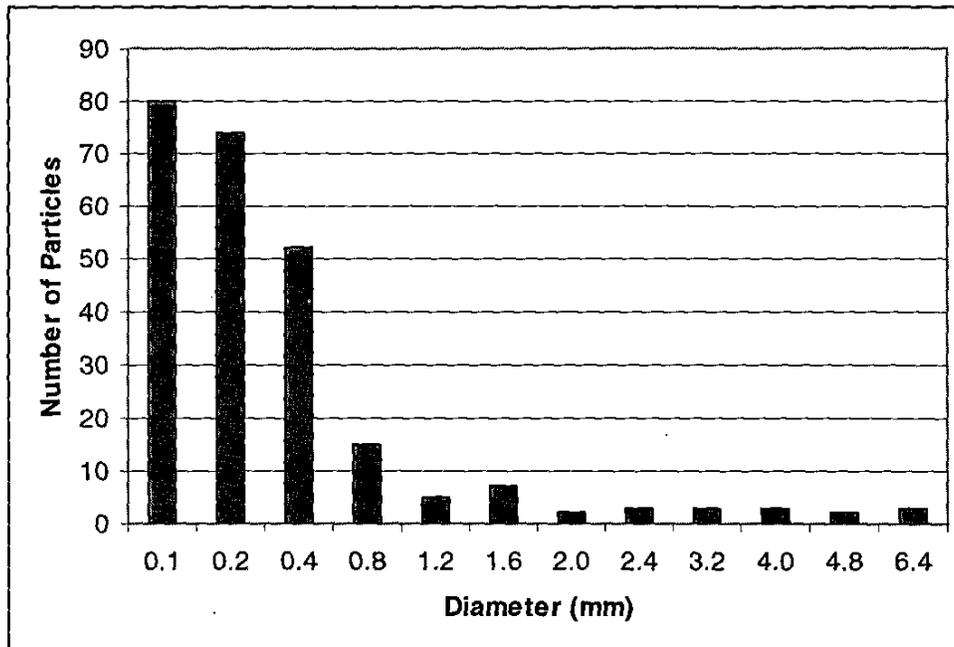
Figure 3-35  Histogram of larger debris generated in an immersion test of Phenoline® 305; debris size was measured optically.
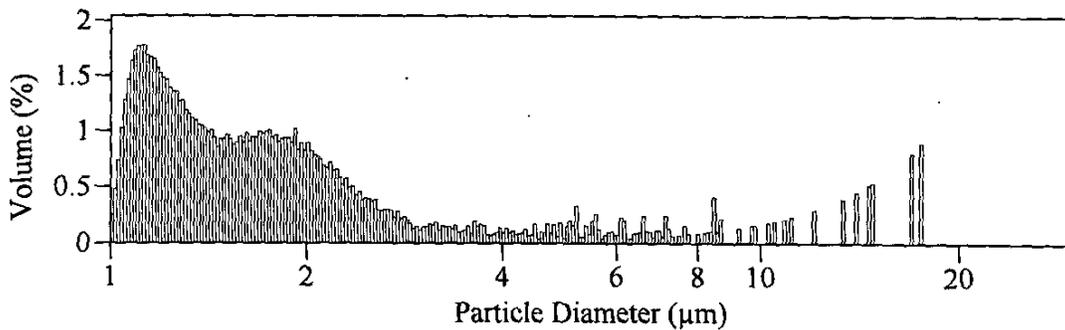


Figure 3-36  Histogram of small debris generated in an immersion test of Phenoline® 305; debris size was measured by Coulter counter.

References for Table 3-1:

1.  Handbook of Chemistry and Physics, 64$^{th}$ Ed., p. E-5, CRC Press, 1983-1984.
2.  ACI Manual of Concrete Practice, Part 3, p. 224.2R-3, ACI International, 1999.
3.  T. Baumeister, et al., (Eds.), Mark's Standard Handbook for Mechanical Engineers, 8$^{th}$ Ed., p. 4-63 (Table 3), McGraw Hill, 1978.
4.  Concrete Manual - A water resources technical publication, 8$^{th}$ Ed. (revised), p. 18, 1981.
5.  Concrete Manual - A water resources technical publication, 8$^{th}$ Ed. (revised), p. 27, 1981.
6.  Concrete Manual - A water resources technical publication, 8$^{th}$ Ed. (revised), p. 30, 1981.
7.  M. Fintel, Handbook of Concrete Engineering, 2$^{nd}$ Ed., p. 189, 1995.
8.  H. Saechtling, International Plastics Handbook, p. 387, Hanser Publisher, 1983.

# 4.0 Summary and Significant Findings

## 4.1 Coating Research Program

The SRTC program consists of three major elements, as shown in Figure 2-1 in Section 2, that are directed at determining performance of Service Level I coatings under DBA conditions. Measurements of coating mechanical and physical properties are made for input into analytical models in order to calculate coating deformations under environmental conditions. Predictions from analyses using the analytical models and the results from performance testing of coating specimens under simulated DBA conditions are used to arrive at insights into the potential for coating failure. This includes the degree of failure and the failed coating material characteristics (i.e., amount and size of coatings debris) for use in NRC's GSI-191, "PWR Sump Blockage" research program.

## 4.2 Performance of System 1 Coating

The results from the analyses and performance testing under DBA conditions of coating System 1 (Phenoline® 305 topcoat over Carbozinc® 11 primer on a carbon steel substrate), described in detail in section 3.2 and 3.3 of this report, are summarized below.

The results from the analyses and performance testing show that the performance of the System 1 coating depends upon:

- Aging Condition (Non-irradiated or irradiated)
- Defect Condition (Type, Size, Trapped Water)
- Temperature/Pressure Exposure Profile (Full DBA, Plant-Specific DBA, Water Immersion)

The performance of the System 1 coatings is discussed below using an outline format. The performance testing was laboratory tests using coated steel plate specimens, fabricated to include two conditions: non-defected; and Type 1 defect that contains an intentional delamination or embedded non-bond area. These specimens, in non-aged and irradiation-aged conditions, were exposed to DBA profiles (ASTM D3911-95 or "full DBA", and other shortened DBA tests including a "plant-specific" DBA and water immersion) to determine their expected performance under the medium- to large-break loss-of-coolant accident.

I. Non-Aged Condition

The non-aged condition represents the properly applied and cured condition of the coating that has not been exposed to an aging environment that includes temperature, irradiation, and air with humidity for long exposure times. The non-aged condition of the properly applied and cured coating is the baseline condition.

A. Non-defected

Test results from the laboratory specimens exposed to either the ASTM D3911-95 DBA or the "plant-specific" DBA profile did not reveal any evidence of coating failure. Only a slight color change due to the DBA exposure was observed. The results of the analysis using the computer model showed that tensile stresses were not sufficient to lead to major cracking of the topcoat, primer, or the steel substrate as a result of mechanical stresses introduced in the coating. In addition, the non-defected specimen was exposed to a water immersion to temperatures up to 200°F for times up to 24+ hours. Neither color change nor physical damage was observed in the water immersion testing.

Summary: No cracking or delamination was predicted by analysis or observed by testing for the non-aged coating in the non-defected condition; therefore no coating debris is likely to form in a non-aged, non-defected System 1 coating under DBA exposure conditions.

B. Defect Type 1 (Embedded Non-Bond)

1. Without Trapped Water

No significant deformation to cause failure was predicted with analytical modeling of the "full DBA" test or observed in testing.

2. With Trapped Water

The analysis results showed that a 12 mm diameter Type 1 defect would not grow by cracking during the ASTM D3911-95 DBA. This is consistent with the DBA test results of a 12 mm Type 1 defect.

Summary: A non-aged System 1 coating containing Type 1 defects ≤ 12 mm in diameter is not subject to cracking under DBA exposure conditions. Therefore, no debris source can be formed.

II. Aged Condition

An "aged" coating is defined as a coating which has been properly applied and cured, and has been exposed to an aging environment that includes temperature, irradiation, and air with humidity. The findings in this section are based on the results of specimens that have been irradiated to $10^9$ rads per ASTM D4082-95, that is, no additional thermal or simulated service aging treatment was applied to the test specimens.

The irradiation of System 1 test specimens to $10^9$ rads per ASTM D4082-95 caused a color change from the as-prepared condition. This marked color change occurred in the first 1-2 mils of the topcoat.

The findings for aged coatings are based on the measured performance tests, only.

A. Non-defected

The test results from the "plant-specific" DBA, a plant-specific rapid transient pressure/temperature exposure (with the temperature of the saturated steam approximately 200°F), and from water immersion (with the water temperature of approximately 200°F), showed the entire near-surface region (1-2 mil depth) of the topcoat will severely blister. Failure (disbondment) of the near-surface region did occur and a debris source term was formed. In the full DBA test, however, neither significant blistering nor a significant debris source was observed.

B. Defect Type 1 (Embedded Non-bond)

Disbondment of the near-surface layer of the topcoat, as described in A above, was observed

during plant-specific LOCA and immersion testing of coatings with intentional defects. However, no failures occurred as a direct result of the presence of the intentional defect. The following describes the performance of the aged coatings as a consequence of the presence of these intentional defects, only.

1. Without Trapped Water

No significant deformation to cause failure was observed during DBA-LOCA testing.

2. With Trapped Water

No DBA-LOCA testing with trapped water was performed.

## 4.3 Summary of Major Findings for System 1 Performance

1. No failure of a non-aged, non-defected System 1 coating, which would lead to the formation of a debris source term, is expected to occur under ASTM D3911-95 "full DBA" simulation.

2. The presence of a large (up to 12 mm) diameter embedded coating defect did not result in local cracking of the coating during the simulated DBA-LOCA test. Hence, no coating debris is likely to form.

3. System 1 coatings that have been aged (irradiated to $10^9$ rad per ASTM D4082-95) have shown the formation of a debris source term in both "plant-specific" DBA conditions and high-temperature water immersion conditions, at temperatures near 200°F. The debris forms as a result of blistering that tears away a near-surface region (< 2 mils) of the topcoat. Rapid heat-up and hold at temperatures near 300°F (per ASTM D3911-95) did not cause a significant debris source.

## 5.0 Understanding the Potential for Debris Formation from Aged NPP Containment Coatings Exposed to Medium-to-Large Break LOCA Conditions

### 5.1    General Conclusions

The performance testing results in this report for the System 1 coating, and the previous topical report for the System 2 coating (ref. WSRC-TR-2000-00340), clearly show that debris can form in coating systems used in NPP containment under certain conditions. Debris formation is observed in coatings that are irradiated to the present ASTM standard for irradiation of (i.e., ASTM D4082-95) and are subsequently exposed to either steam or water immersion temperature-time profiles that are relevant to medium-to-large break LOCAs. The debris is caused by disbondment of a portion of the top layer of the coating system that is degraded as a result of irradiation in air. That is, no debris formation is observed in companion specimens that have not been irradiated in air. The debris formation is dependent on both the specific irradiation treatment and the simulated LOCA exposure conditions. It is also noted that minor cracking was not observed in any System 2 specimens at the test conditions relevant to a DBA-LOCA. This is in contrast to System 1 specimens that did exhibit minor cracking including cracking in the vicinity of embedded defects. The minor cracking behavior was observed to be not significant to debris formation.

Specifically, debris formation was observed in the near-surface (approximately top 2 mils) region of an epoxy-phenolic (Phenoline® 305) on a System 1 (Phenoline® 305 topcoat over Carbozinc® 11 primer on steel) coating specimen irradiated to $1 \times 10^9$ rads at $1 \times 10^6$ rads/hour in air at 120°F. Under high temperature water immersion (at approximately 200°F) or "plant-specific" DBA-LOCA steam profiles (see Section 3 of this report), the near-surface region (approximately the top 2 mils of the topcoat) blistered and lifted off the remaining topcoat resulting in a distribution of flimsy debris. Video records show that the blistering was driven by gas evolution in the near-surface region. Similar debris formation was also observed in the System 2 (Phenoline® 305 topcoat over Starglaze® 2011S surfacer on concrete coating) which has the same topcoat as System 1 (ref. WSRC-TR-2000-00340). Phenoline® 305 is an epoxy phenolic (or phenolic-modified epoxy) coating. However, the blistering phenomenon is not presumed to be particular to the formulation nor the coating type. Blistering, although not as pronounced, was observed in a polyamide epoxy, a reference coating system used previously in the research program (ref. WSRC-TR-2000-00079).

Factors that would affect the potential for debris formation in a coating and debris characteristics that could potentially impact sump performance have been suggested following an NRC public meeting in September 2000. These have been categorized into five areas of investigation below.

### 5.2    Factors Affecting Potential for Debris Formation in NPP Containment Coating

At the present time, there is uncertainty regarding the reason the degradation has been confined to the top 2 mils of the coating, but the presumption is the degradation depth is controlled by the permeation of oxygen during irradiation. This would indicate that the damage depth would be different, if the coatings were irradiated at a different oxygen partial-pressure, and/or at a different radiation dose-rate, and/or at a different irradiation temperature.

The mechanism causing the blistering and liftoff of the near-surface layer of the irradiated topcoat material has not been fully explained. The results in the coating research program to-date suggest that the debris formation is driven by gas evolution in an oxygen-affected region of the topcoat. The mechanism appears to involve gas from the near-surface layer agglomerating and forming bubbles that load and deform the near-surface layer material. This occurs in a "temperature window" due to two basic processes. The first process is gas agglomeration with bubble development that is temperature dependent. The second process is the softening of the material that is both temperature and wetness dependent. Below approximately 150°F, the bubble formation is slow and the material is stiff. Above temperatures of approximately 200+°F, the material is softened to the extent that the gas bubbles will pop through the material leaving pores but not causing blisters. At temperatures around 200°F, the gas bubbles coalescence in the softened, oxygen-affected region of the topcoat, forming blisters, which may detach as debris.

The various factors that would affect the potential for debris formation are categorized into areas of investigation in the following sections (5.2.1-5.2.5). It is beyond the scope of the present research project to comprehensively investigate each of these factors.

It is clear that the existing ASTM standards for irradiation treatment and DBA-LOCA exposure are subject to revision to refine the ranges and controls for the treatment and exposure conditions of coating systems for nuclear service. Additional investigation of factors that are important to debris formation would be needed to support the revision of the standards. The ultimate objective of the investigation would be to predict, with confidence, the conditions under which debris would form in a given coating system and the resulting debris characteristics.

### 5.2.1    Coating Characteristics

The structure of the coating may affect its susceptibility to radiation damage and oxidation. Two general factors are in this category:

- Coating Type (e.g., epoxy, epoxy-phenolic)
- Coating Formulation (specific vendor formulation)

### 5.2.2    Combined Effects of Aging Conditions

Aging includes the effects of several degradation mechanisms, primarily radiation and oxidation, over time. These mechanisms may act synergistically to make a coating susceptible to debris formation. The factors related to these degradation mechanisms are the following:

- Irradiation Dose
- Irradiation Dose-Rate (Irradiation History)
- Irradiation Type ($\alpha$, $\beta$, $\gamma$, UV)
- Energy Spectrum
- Oxidation Conditions (e.g., Moist Air)
- Temperature History
- Age of Coating

The first four factors would affect the radiation damage of a coating. The last three factors would affect the oxidation damage of the coating. It is envisioned that radiation and oxidation damage can act synergistically to promote susceptibility to debris formation.

### 5.2.3    Combined Effects of LOCA Exposure Conditions

The development of blisters, a precursor to the formation of debris, is dependent on the evolution of gases and the softening of the coating. There appears to be a "temperature window" in which blisters form—at low temperatures, the gases do not evolve and/or the coating is too stiff; at too high temperatures, the gas escapes by pore formation in the coating. Wetness further exacerbates the softening of the coating. The following two conditions in simulated LOCA events are, therefore, factors in promoting potential debris formation:

- Steam Temperature/Pressure – Time Profile
- Water Immersion Temperature – Time Profile

### 5.2.4    Debris Formation Mechanism

The blisters from which the debris is formed are driven by gas generation. The following factors need to be investigated to characterize this gas source and blister development leading to debris generation:

- Gas Sources in Aged Coatings
- Gas Generation in Coatings Under Temperature and Wetness Conditions
- Blister Development - Kinetics of Pressurization and Blister Formation

### 5.2.5   Debris Characteristics

Debris that has left the surface of the coating is available for transport. Several factors are important to evaluate the transport of the debris:

- Total Amount of Debris per unit Initial Surface Area of Coating
- Size Distribution
- Degree of "Stickiness"
- Float Characteristics (Dependent on size, density, and shape of debris).

### 5.3   Measured Performance Testing of NPP Containment Samples

One factor that has been investigated empirically in the program is that of accelerated aging using NPP containment samples (plant samples) in comparison to the laboratory samples. The laboratory samples irradiated in this program have been irradiated per ASTM D4082-95 and several other dose and dose rate conditions. In all cases, damage due to radiation has thus far been limited to color changes and slight checking, with most of the damage being observed in the immediate surface of the coating and not completely throughout the bulk of the material. This is as expected, and is attributed primarily to the limited diffusion depth and availability of oxygen in the coating that can react with free radicals formed from the radiation-induced structural changes. This is also typical of materials irradiated at high dose rates ($1 \times 10^6$ rad/hr) in relatively short periods of time (compared to actual service life), especially for materials of relatively low oxygen permeability.

There are significant limitations of conventional accelerated-aging methodologies, particularly for radiation exposure at much higher dose-rates than anticipated in actual service. These limitations include:

- Diffusion-limited oxidation
- Dose-rate effects (chain scission vs. cross-linking)
- Synergistic effects of long-term oxidation, temperature, moisture, chemicals, etc.
- Variation in thermal transitions

Radiation exposure, DBA exposure, and characterization of recently-applied coatings, regardless of formulation, is of limited value in understanding and predicting actual long-term performance and DBA response of older, in-service coatings. For this reason, SRTC, the industry PIRT panel, and the NRC customer have worked to obtain several samples of coated substrate (primarily steel) and/or coating debris from nuclear power plants for such investigation. These samples will be characterized in both the as-received (service-aged) condition as well as following both radiation (at varying dose-rates and possibly temperatures) and DBA-LOCA exposures. The results of these studies will be reported in a letter report scheduled for issuance in March 2001.

# Appendix A

## Mechanical Testing Description

Mechanical properties are key inputs to the coatings failure model. The mechanical properties of interest in the coatings program are adhesion, adhesion G-value, tensile strength, elastic (Young's) modulus and cohesion. Adhesion is the measure of the load or strength (load divided by the load bearing area) to separate a coating from its underlying layer or substrate. The adhesion G-value is the designation given in the coating failure model for the resistance to the separation of the coating layer from an underlying layer or substrate. The adhesion G-value may be considered the fracture toughness of the interface at which separation occurs. The tensile strength is the standard material science property of the maximum load on a specimen divided by the area bearing the load. In the coatings program the tensile strength is measured in the so-called free-film coating specimen. The free film is simply the cured coating that has been removed from a very weakly adherent substrate, such as polyethlyene sheet. The elastic or Young's modulus can be measured from the load-elongation curve of the free-film specimen. It is assumed that the coating material is isotropic in these properties.

Cohesion is used here to designate the resistance to tearing of the free film. The cohesion test specimen is similar to the tensile test specimen except that it contains a notch or slit in its edge to initiate the tearing. The tests to obtain these properties were performed on an Instron universal (i.e., capable of both compression and tensile testing) testing machine (model 4507) equipped with an oven for elevated temperature testing. This appendix describes the methods developed for performing the tests.

## A.1 Adhesion and Adhesion G-value Tests

The adhesion and adhesion G-value tests were developed from two American Society for Testing and Materials standard test methods. These are D5179-98 "Standard Test Method for Measuring Adhesion of Organic Coatings to Plastic Substrates by Direct Tensile Testing" and D4541-95 "Standard Test Method for Pull-Off Strength of Coatings Using Portable Adhesion Testers." These methods use a stud or puller affixed to a coating by an adhesive that is then pulled normal to the surface by a tensile machine in the former method or a manually operated apparatus in the latter. Figure A-1 shows three pullers affixed to a test specimen. The pullers are 1.4 in. high and 12 mm (0.472 in.) in diameter; their design was adapted from that given in D5179-98. The total displacement of the puller normal to the coating surface between initial loading and separation of the puller from the specimen is of the order of a few thousandths of an inch. Such small displacements are not accurately measurable with the simple recording of the displacement of the Instron's moving crosshead. This is so because the movement in taking up slack in the linkages of the gripping system, such as in the universal couplings that ensure loading in a direction normal to the specimen, is of the same magnitude as the displacements encountered in pulling the thin coatings to failure.

In these tests the displacement of the puller was measured with a single-arm extensometer that was mounted to contact the top of the puller. The extensometer was a Materials Testing Systems model number 632-06B-20 with a full-scale range of ± 0.160 in. and capable of operating to 300°F.

The upper grip for the pullers (design adapted from ASTM D5179-98 also) was machined with a pocket to accommodate the extensometer arm (Figure A-2). The upper grip was rigidly attached to a pull rod that was connected through a universal joint to a 200-lb load cell mounted in the Instron's fixed, upper crosshead. The lower grip held the 4-in. by 6-in. by 1/4-in. blocks and was connected rigidly to the Instron's moving crosshead. Threaded couplings with backing nuts were used to make rigid the connections between the upper pull rod and the upper grip and between the lower pull rod and the lower grip (Figure A-3). Two flexible couplings remained in the load chain: the universal joint through which the upper pull rod is connected to the Instron's load cell and the connection between the upper grip and the stud. These allow necessary motion for alignment, yet they require little force (compared to the load supported by the coating) to "set" themselves. A plumb bob was used to position the puller on the load axis. These steps ensure that the puller is pulled normally to the coupon (Figure A-4). The lower grip was equipped with a rectangular metal pan that was filled with water to keep a test specimen wetted when experimental conditions demanded.
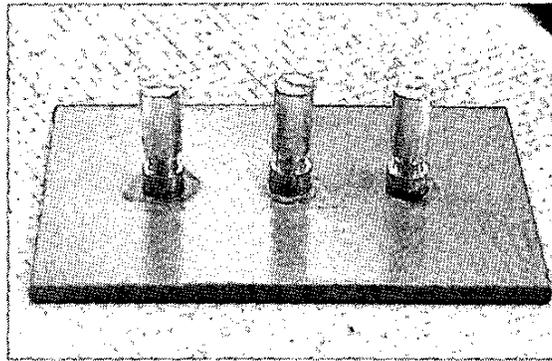
**Figure A-1. Aluminum pullers as they appear affixed to a test coupon with epoxy adhesive.**
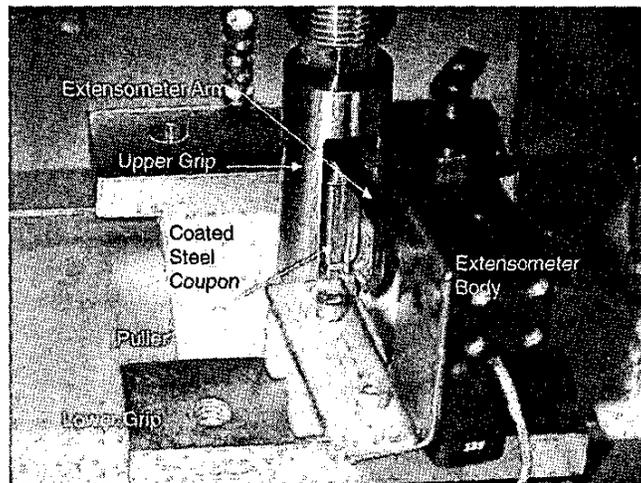


**Figure A-2. Extensometer and grip for aluminum puller.**
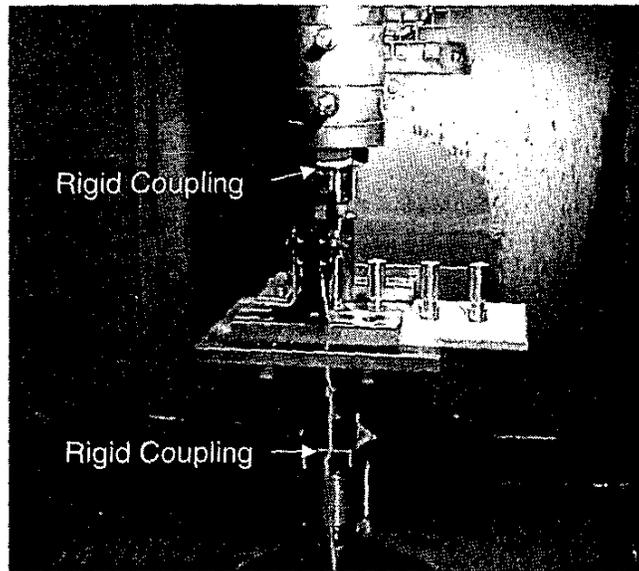
**Figure A-3. Rigid coupling of upper and lower grips to Instron.**
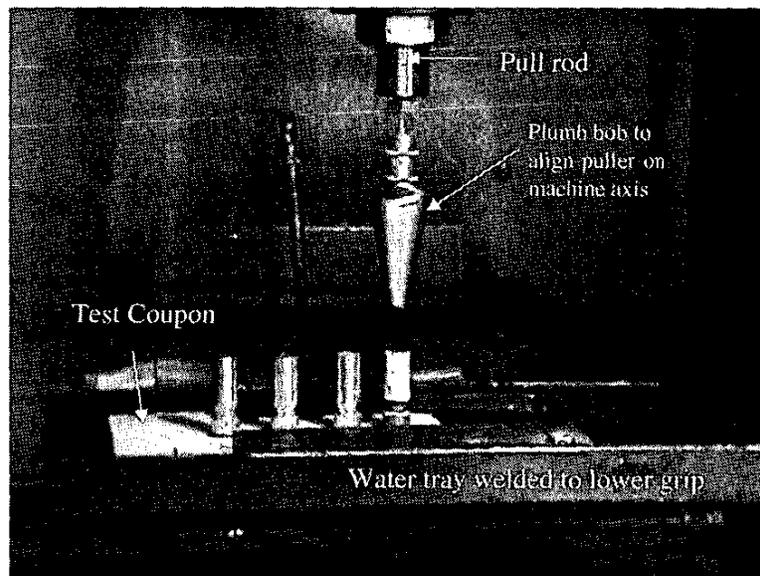


**Figure A-4. Plumb bob arrangement to locate center of puller on
Instron load axis.**

Aluminum, pullers, 12 mm in diameter, were used for both the adhesion test and the adhesion G-value test. They were affixed to the test specimens by Cotronics 4525 high-temperature (500°F) epoxy (Cotronics Corp., Brooklyn, New York). This epoxy cures at room temperature in 16 hours.

The concept of the adhesion G-value test is shown in Figure A-5. As the puller is displaced from the coupon surface the zero-adhesion (so-called type 1) defect propagates radially until failure. The zero adhesion defect is created by installing a glass disk on the substrate prior to the application of the coating(s). Twelve millimeter diameter by 0.005 inch deep holes were machined into the surface of the steel coupon to accept 12mm diameter, 0.005 inch thick (nominal) glass disks. Alternately, a magnetic mask with half-inch diameter holes is affixed to the steel plate, allowing selective application of polytetrafluoroethylene (Teflon®) spray lubricant. The prepared coupon is then coated with primer and topcoat. The same mask is used to guide the attachment of the pullers. Figures A-6 and A-7 illustrate the alternate methods of preparing the zero-adhesion defects in the test specimens.
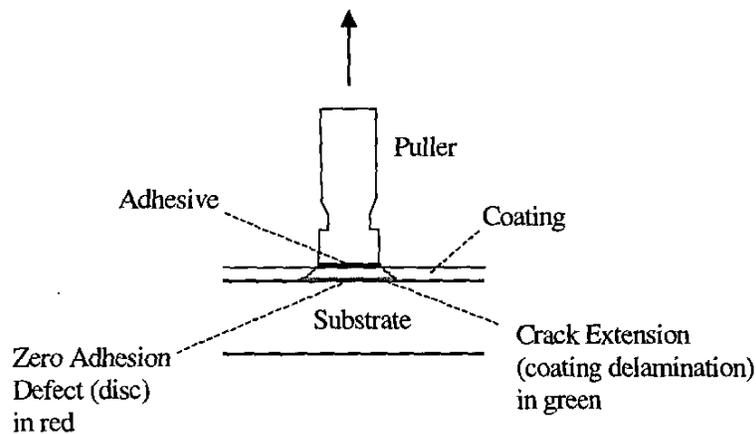


**Figure A-5. Schematic diagram of the adhesion G-value test.**
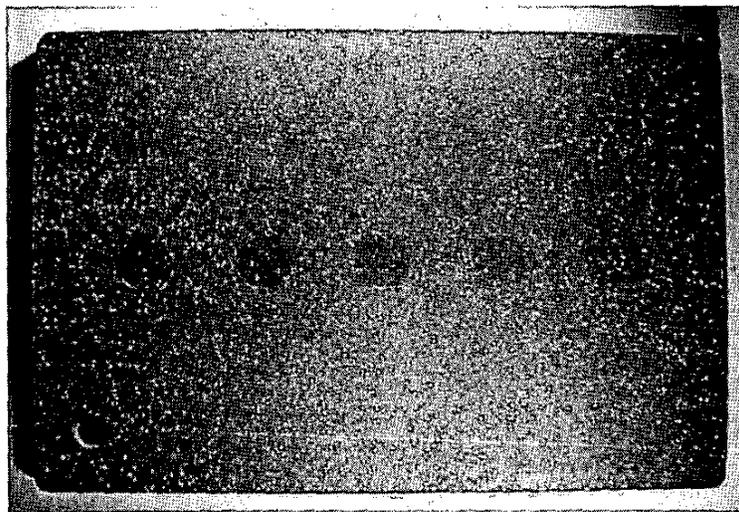


**Figure A-6. Overall view of a steel test plate illustrating placement of 12mm glass disks in machined recesses on the surface. Note: The plate has been prepared for coating by grit blasting.**

A-5
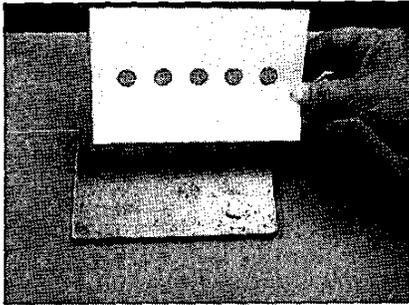
Flexible magnetic mask with 0.5 in. diam. holes
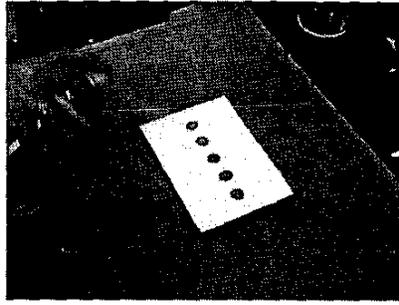


Polytetrafluoroethylene spray
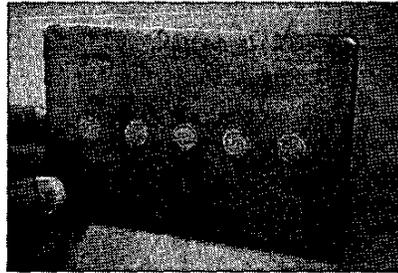


PTFE discs on steel coupon

**Figure A-7. Photographic sequence illustrating alternative method of creating Type I zero-adhesion defects by applying PTFE spray onto the surface of the steel test specimen.**

## A.2 Tensile Test

The tensile test employed so-called dogbone-shaped flat specimens that were cut from cured coating applied to a polyethylene sheet or that were molded on the sheet by spraying coating through a mask. The molded specimens were 4.5 inches in length overall with a 1.5-in.-long by 0.25-in.-wide gage section (Figure A-8). Specimens were pulled to failure at a crosshead speed of 0.02 in. per minute.
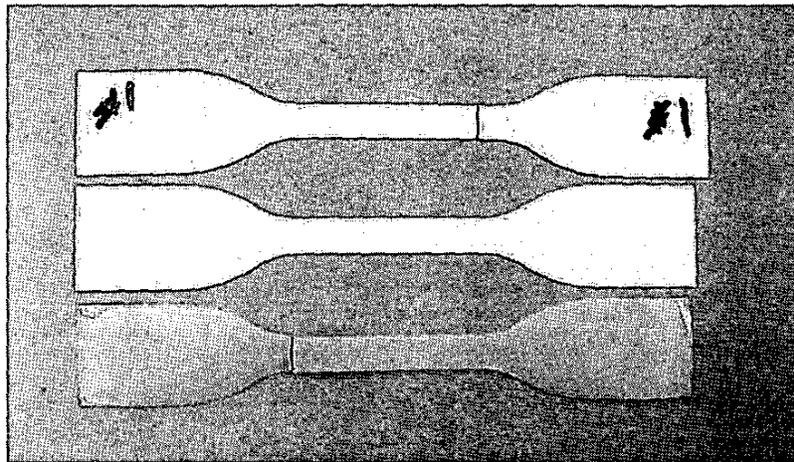
**Figure A-8. Tensile specimens of Phenoline 305®, as cured (above) and irradiated and tested to failure (below). Note minor changes in specimen length observed as a consequence of test conditions.**

The specimens were securely held in knurled grips designed for relatively soft materials (Figure A-9).
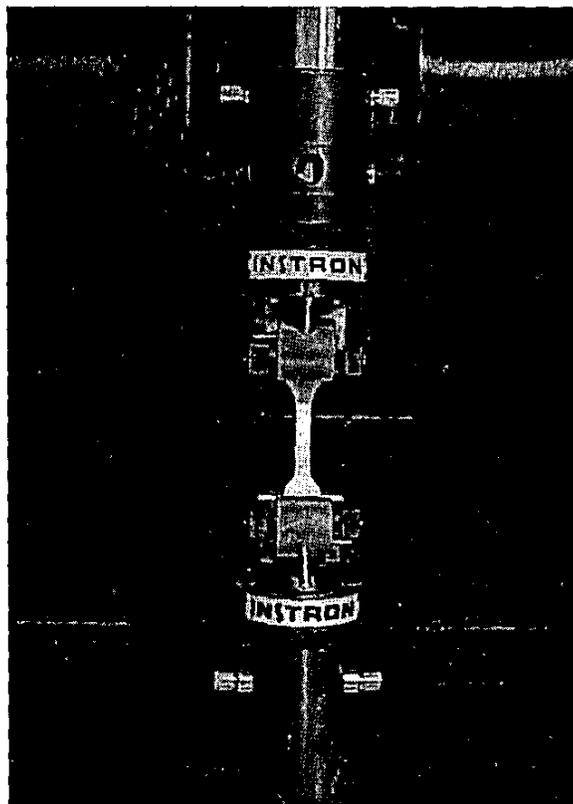


**Figure A-9. Tensile specimen fixed in knurled grips.**

# Appendix B

**Irradiation Aging of Protective Coatings**

Many protective coatings based on thermosetting, highly cross-linked resins such as epoxies, epoxy-phenolics, and polyurethanes have been shown to be quite resistant to gamma radiation to this cumulative dose level. Although thermally very stable, straight, unmodified phenolic coatings have been shown to be somewhat less resistant to gamma radiation and show evidence of degradation at levels as low as $1 \times 10^8$ Rads for some materials. For this reason as well as to improve toughness and durability, phenolic resins are typically either reinforced or modified with other resins (mostly epoxies).

Due to the range of variation in polymer processing, compound additives, specific formulations, curing agents, etc., radiation exposure testing is often necessary in order to evaluate the radiation resistance of a particular material or specific compound. In addition, it is often desirable to irradiate an intact component as would be installed in the actual application, rather than simply exposing a test sample.

Although there are limitations to the applicability of short-term, high dose-rate radiation exposure methods to predicting long-term performance, this is often the only rapid and cost-effective way to evaluate radiation effects upon critical properties. In some cases, exposure to a range of dose levels and rates can be used to develop an accelerated aging profile for a particular material to predict longer-term performance. This principle is known as superposition and has been applied to many materials qualified for long-term service in high radiation environments such as gaskets and electrical cable insulation.

The actual absorbed dose of a material depends upon its density and basic elemental composition, as well as mass absorption coefficients and other energy absorption properties. For most polymeric materials, including thermosetting polymers and protective coatings based thereon, the absorbed dose in Rads is assumed to be comparable to the energy of the radiation field applied. As the majority of polymers consist mainly of hydrogen and carbon, the mass absorption is generally comparable to that of water unless specifically measured.

There are two sources available for irradiation exposure. One is a Gammacell 220 (Figure B-1) with a current dose rate of 2.32E+04 R/hr. The second source is a J.L.Shepherd Model 109 Irradiator, with a current dose rate of 1.27E+06 R/hr. Both of these are gamma irradiators with Co-60 as the isotope. The chamber size of both sources is 6" diameter by 7.5" high. Auxiliary systems to raise or lower ambient temp and to introduce air or gas or chemicals to the system can be added.

Accelerated-aging of protective coatings has historically been performed per ASTM D4082, "Standard Test Method for Effects of Gamma Radiation on Coatings for Use in Light-Water Nuclear Power Plants". The technical basis for this test method is that the cumulative exposure dose shall be $1 \times 10^9$ Rads, and the dose rate shall be controlled at $1 \times 10^6$ R/hr or higher. The field shall be uniform to within 10% between any two locations in the sample. The $1 \times 10^9$ Rad total dose is historically based on a projected 40-year service life and includes the radiation exposure during a design basis accident (DBA). The high gamma dose was also intended to exceed plant life gamma dose to also account for possible beta exposure as well. In addition, the temperature shall not exceed 140°F (60°C) during sample irradiation due to known synergistic effects of temperature and radiation. Following exposure, samples are examined per other ASTM standards to evaluate coating performance and presence of defects such as chalking, checking, cracking, blistering, flaking, peeling, and/or delamination.
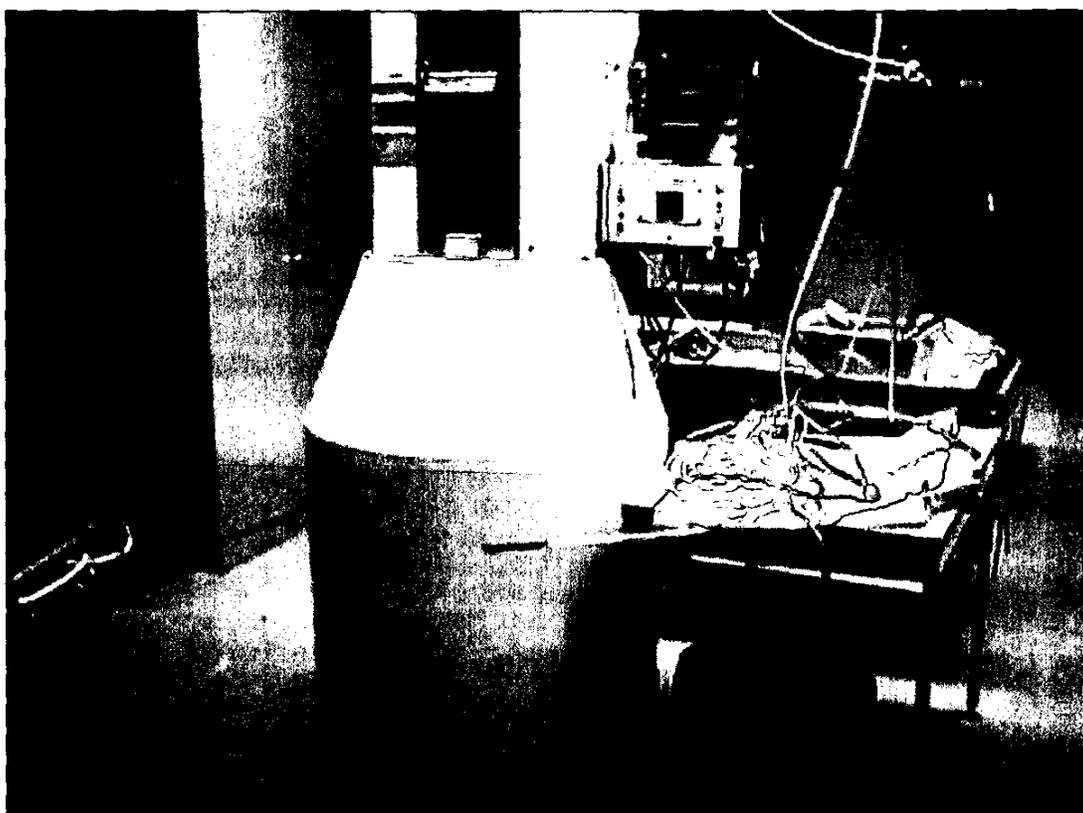
**Figure B-1.  GammaCell 220**

# Appendix C

# Application of Finite Element and Fracture Mechanics Analyses in Predicting Failure of NPP Coatings

## C.1 Overview

The NPP protective coating systems in general consist of multiple layers with various thicknesses and different properties which may be functions of environmental variables such as the temperature and wetness. The coating systems may be subjected to wide range of time-dependent loading conditions under the LOCA events. Initial defects may be postulated to exist in the coating system as a standard fracture mechanics procedure to determine the failure mechanisms.

The finite element method is considered an efficient analysis tool when many variables and scenarios are involved. There are three fundamental categories of inputs to the models:

1. Configuration – includes initial defect size, location of defect in the coating system, number of coatings and coating thickness, and type of substrate onto which coating is applied
2. Material Property – includes mechanical (modulus of elasticity or Young's modulus, adhesion energy, etc.) and physical (coefficient of thermal expansion, coefficient of thermal conductivity, etc.) properties or attributes of the coating layers and substrate materials
3. Loading – includes both direct loads (e.g., impingement of water) and environmental conditions that lead to coating stresses (e.g., thermal exposure leading to differential thermal expansion stresses)

The coating stress, strain, and the driving force leading to a defect growth will be calculated. With appropriate material failure criteria, the coating failure may be predicted and the conditions causing failure may be identified.

## C.2 Finite Element Model Description

The finite element model used for most of the calculations contains 6210 rectangular elements and 6811 user-defined nodes. Heat transfer elements were used in the thermal transient analysis and continuum elements were used for the thermal stress analysis. The continuum elements can be either plane strain or axisymmetric, depending on the geometric characteristics of the problem. Only one-half of the analysis domain is modeled because of symmetry (with respect to the centerline or center-plane of the defect).

This model is capable of analyzing an intact three-layered coating system (topcoat, primer, and substrate), a defect at the topcoat-primer interface, a defect at the primer-substrate interface defect, or an intra-primer defect. There are 10 elements through the topcoat thickness and 16 through the primer. Coarser mesh was used in the substrate region except for the area adjacent to the primer for better transition. The mesh is refined greatly for the defect driving force calculation in the region where the postulated defect edge is located. The width of the model is typically about 6 times the size of a postulated defect and is divided into 138 elements with various sizes. The ABAQUS [1] finite element program was used.

## C.3 Solution Steps

The coating system under the LOCA experiences temperature excursions. Because the different materials are used for the topcoat, primer, and the substrate, the mechanical property and thermal expansion mismatch will cause stress to develop in and between the layers. No external forces acting on the coating surface were considered throughout the present analyses. The thermal transient and stress analyses are uncoupled.

To achieve the coating failure prediction, a fracture mechanics approach was adopted. Several defect sizes were separately postulated in the coating system and modeled by the finite element method. The defect may be subject to vapor pressure loading in some cases due to the entrapped moisture at elevated temperature. This procedure allows the failure condition be established as a function of the defect size. As a result, a threshold defect size or a critical condition to cause failure may be determined.

The calculation steps are listed below:

1.  Thermal Analysis: Only conduction was considered in the current analysis. The temperature boundary condition was prescribed. Thermal transient analysis was performed based on the time-dependent ambient temperature profile, such as that given in ASTM D3911-95 DBA for PWRs. The physical properties input to the analysis are thermal conductivity, mass density, and specific heat. The properties may be temperature and radiation dependent. The temperature distribution was calculated in the finite element region.

2.  Stress Analysis: A mesh identical to that of the thermal analysis was used. Only the finite elements were changed to the continuum type. The nodal temperatures obtained in Step 1 were directly input to the stress analysis model. Linear elastic analysis was performed in this preliminary assessment. The mechanical properties required for this calculation are the Young's modulus (modulus of elasticity), Poisson's ratio, and coefficient of thermal expansion. These properties also may be temperature and radiation dependent. The nodal displacement, element stress and strain are calculated. The defect growth driving force, or the adhesion G-value, is calculated with the J-integral [2] method in the ABAQUS [1] program. The finite element mesh was designed to allow five contour integrals to be assessed near the edge of the defect. The first contour, at the tip of the defect, is normally ignored due to inaccuracy. When moisture is postulated to be trapped inside the defect, a vapor loading condition may occur when the temperature is above the boiling temperature. In this case, the moisture temperature is assumed to be the substrate temperature directly underneath the defect. The corresponding saturated vapor pressure was obtained from the thermodynamic properties of steam [3]. The pressure differential between the external environment and the vapor gives a net pressure acting on the defect. When the pressure in the external environment is greater than or equal to the vapor pressure generated inside the defect, the pressure loading is zero. This vapor pressure loading condition is also time dependent.

3.  With the changing temperature profile in the coating system and the possible vapor pressure loading within the defect, stress will develop in the coating system. In general, the coefficient of thermal expansion of the coating materials is several times higher than the substrate (e.g., coefficients of thermal expansion for the steel substrate is about $1 \times 10^{-5}$ m/m/°C and for the coating material is about $20 \times 10^{-5}$ m/m/°C). This implies that the substrate temperature must be many times higher than that in the coating in order to negate the temperature-induced strain mismatch on the interface. This condition is very difficult to achieve because the coating materials normally are good thermal insulators (e.g., thermal conductivity for the steel is 43 W/m•°C, while for the coating material is less than 1 W/m•°C), unless the coating is subject to a cool-down and the substrate remains sufficiently hot. The resulting stresses and strains will be output for assessment against the failure criteria.

4.  The G-value due to the applied load (in the present case, temperature variation and pressure loading), denoted by $G_{applied}$, will be calculated at the edge of the defect by the CONTOUR INTEGRAL option in the ABAQUS finite element code [1]. In traditional fracture mechanics, this quantity is named the energy release rate, the crack driving force, or the J-integral; in the rubber or polymeric industry, it is termed the tearing energy of the material. Physically, it is the force to extend the defect by a unit length, or the energy available per unit width to extend the defect by a unit length. The $G_{applied}$ obtained in the stress analysis is also time dependent. The value of $G_{applied}$ can be compared to $G_{material}$ (the material resistance to defect growth) obtained from testing of the coating materials, to determine if a defect grows in size.

## C.4 Defect Modes and Failure Criteria

Two failure modes may be postulated, based on observations of irradiated and DBA tested coatings. These are termed Mode 1 and Mode 2.

1.  Mode 1 Failure – Blistering followed by delamination and cracking

Figure C-1 shows an initial defect in the coating system. It can be an interfacial or intra-layer crack. Due to thermal expansion mismatch (leading to buckling) or vapor pressure loading, a blister may form. As the deformation progresses, the defect may grow in a self-similar manner, a delamination failure may occur but the blistering material remains adhered to the coating system. However, if the ultimate stress ($\sigma_{ult}$) or the failure strain ($\varepsilon_f$) is exceeded in the blistering/delaminating material, this defect will rupture, as depicted in Figure C-2. A local finite element mesh representing the deformation of a Mode 1 defect is shown in Figure C-3. Therefore, two competing failure mechanisms may exist:

1. If $G_{applied} \geq G_{material}$ is met but $\varepsilon_{applied} \leq \varepsilon_f$ and $\sigma_{applied} \leq \sigma_{ult}$, the defect delaminates to form a larger defect in a self-similar manner. The $\varepsilon_{applied}$ and $\sigma_{applied}$ represent the strain and stress due to the applied load, respectively.

2. If $\varepsilon_{applied} \geq \varepsilon_f$ or $\sigma_{applied} \geq \sigma_{ult}$, the defect should rupture at the location where the criterion is met.

When the Mode 1 defect is considered, axisymmetric finite elements are used in the calculation. Because the topcoat provides good thermal insulation, the temperature variation through the thickness of the coating system would be significant. Thermal transient analysis should be performed to obtain the temperature profile, which is then input to the subsequent stress analysis to determine the deformation and stress states of the defect.
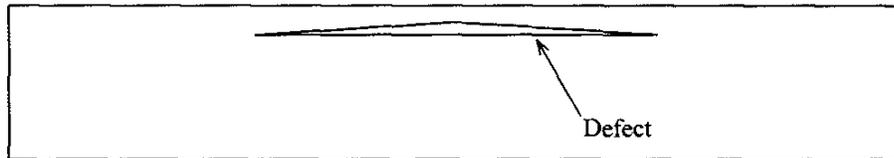


**Figure C-1. Initial Mode 1 Defect**
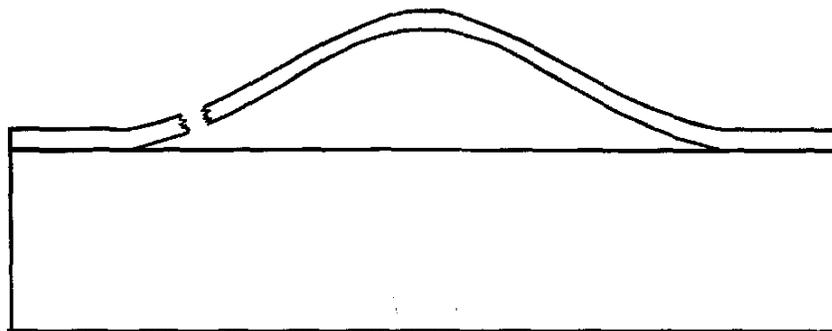


**Figure C-2. Mode 1 Coating Failure**
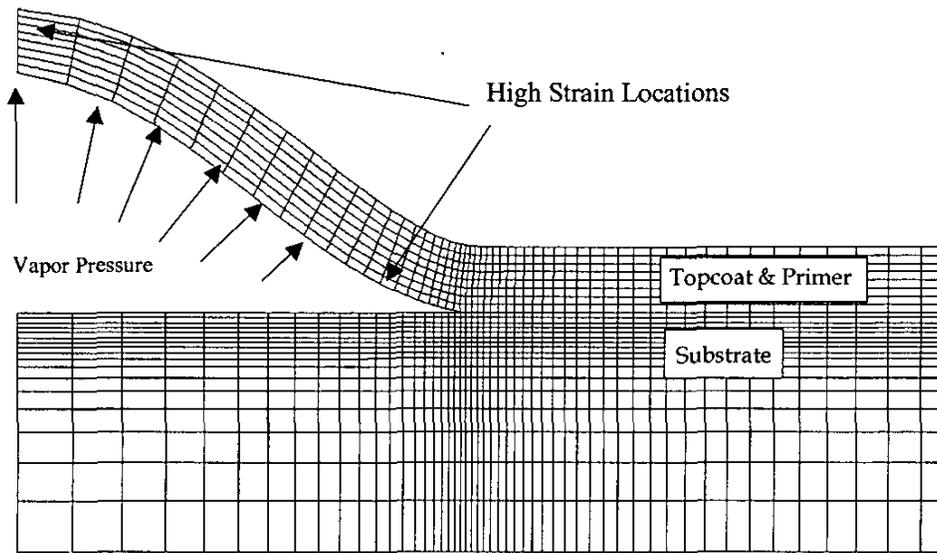
**Figure C-3. Blistering due to buckling and/or vapor pressure loading**

II. Mode 2 Failure – Cracking followed by delamination

A scratch-like crack penetrates through the topcoat to the primer or the substrate is assumed to exist. The main defect within the coating layer is perpendicular to this through-coating crack and is parallel to the coating layers (Figure C-4). Under the conditions of temperature variation and thermal expansion mismatch, this defect may peel back and the defect may grow when $G_{applied} \geq G_{material}$. Eventually it will fall off the NPP containment wall when the condition $\varepsilon_{applied} \geq \varepsilon_f$ or $\sigma_{applied} \geq \sigma_{ult}$ is met. A deformed shape near the peel-back defect calculated by the finite element method is shown in Figure C-5.
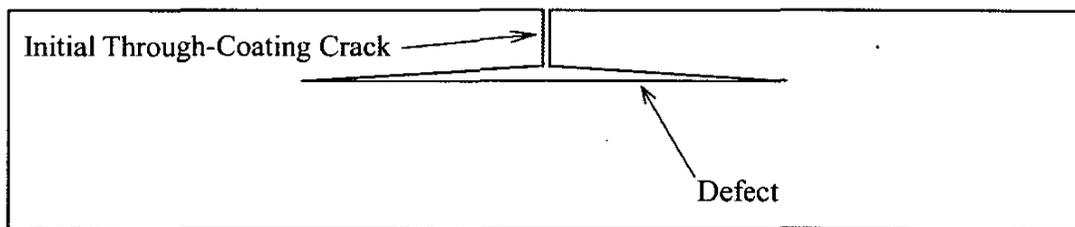


**Figure C-4. Model for Mode 2 Coating Defect Analysis**
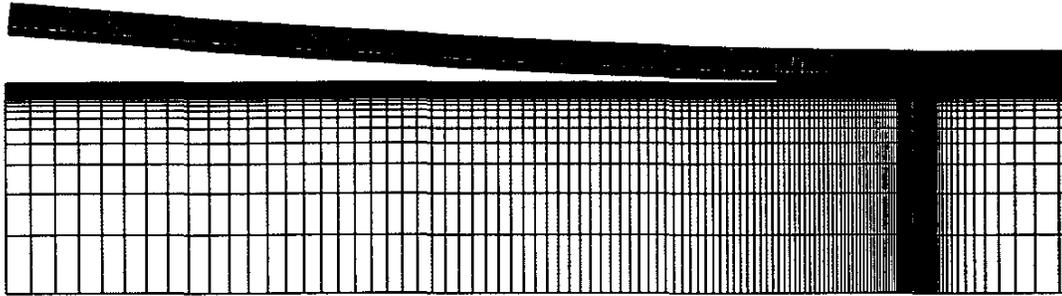
**Figure C-5 - Peel-Back due to thermal expansion mismatch ($\alpha_{topcoat} < \alpha_{primer}$)**

Because of the initial, through-coating crack, the ambient temperature is short-circuited to the sublayer(s) which may have high thermal conductivity. This phenomenon is especially pronounced in the case of IOZ primer which is a zinc-rich layer and may have even higher thermal conductivity than that of the steel substrate. Therefore, a uniform temperature is quickly reached throughout the entire coating system. As a result, thermal transient analysis is not needed to establish the temperature distribution through the coating thickness. The deformation (peel-back) and stresses are caused by the temperature differential and thermal expansion mismatch. Two-dimensional plane strain elements were used for the Mode 2 defect analysis.

### C.5 References

1.  ABAQUS/STANDARD, Version 5.8, Hibbitt, Karlsson & Sorensen, Inc., Pawtucket, Rhode Island, 1999.
2.  Rice, J. R., "A Path Independent Integral and the Approximate Analysis of Strain Concentration by Notches and Cracks," Journal of Applied Mechanics, Vol. 35, pp. 379-386, 1968.
3.  Keenan, J. H. and Keyes, F. G., THERMODYNAMIC PROPERTIES OF STEAM INCLUDING DATA FOR THE LIQUID AND SOLID PHASES, First Edition, John Wiley & Sons, New York, 1936.

# Appendix D

**Test Apparatus Descriptions**

The SRTC coatings performance evaluation system (Figures D-1, 2, and 3) is used to examine the performance of NPP coatings in conditions simulating those expected to exist in a DBA LOCA. Figure D-3 shows a test specimen being placed into the coatings performance evaluation system. It is currently being used to simulate DBA conditions specified in ASTM D3911-95 (Figure D-4)..
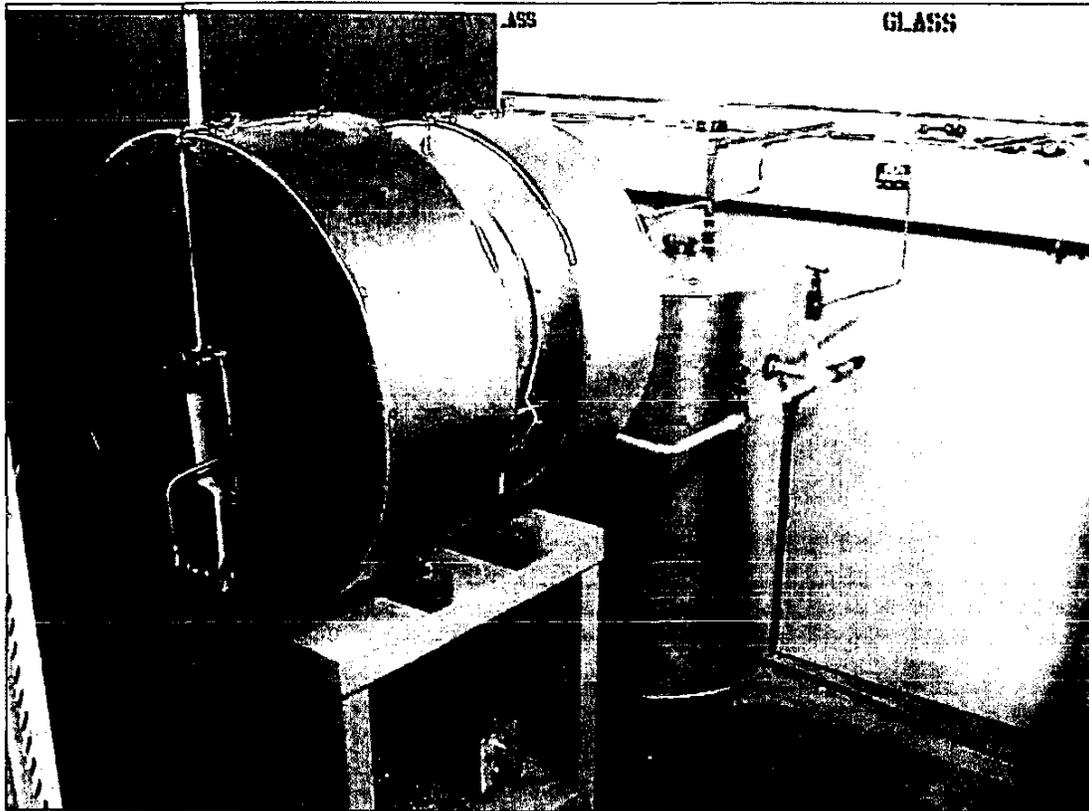


**Figure D-1. SRTC Coatings Performance Evaluation System. Insulated environmental test chamber is shown on the left, the 10 gallon steam generator is on the right.**
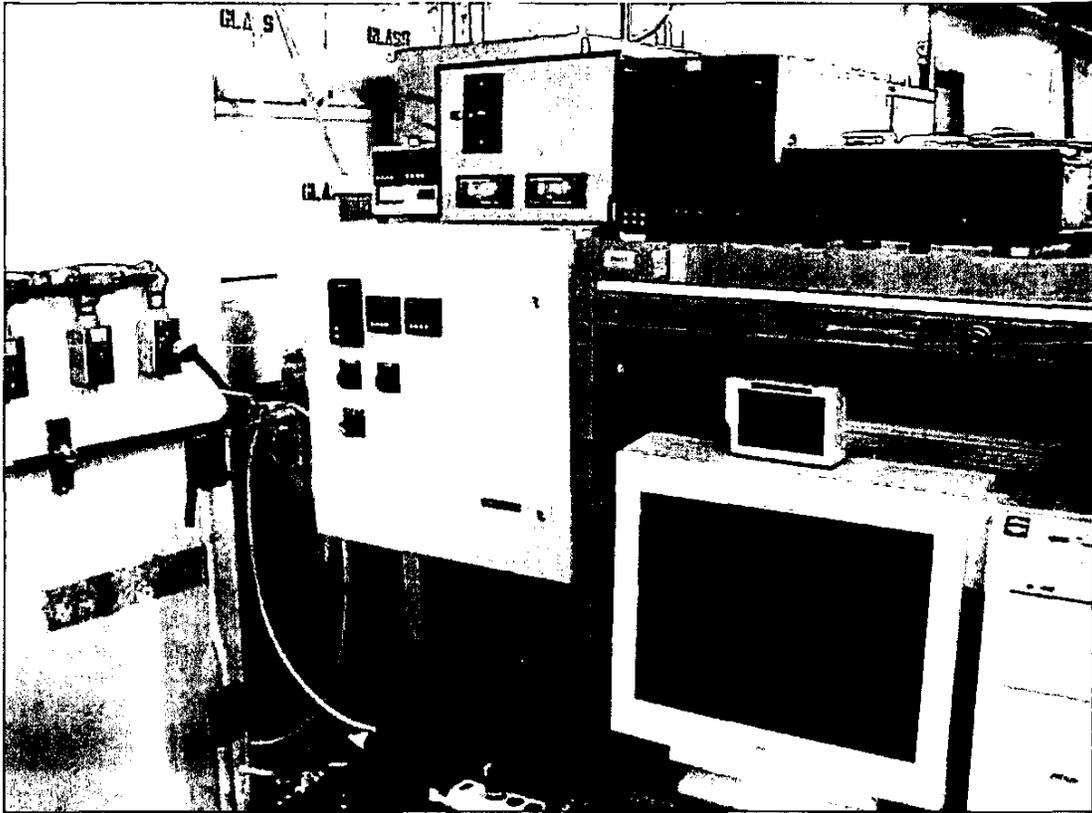
**Figure D-2. Overall view of the heater control console and the video monitoring and data acquisition systems for the SRTC Coatings Performance Evaluation System**
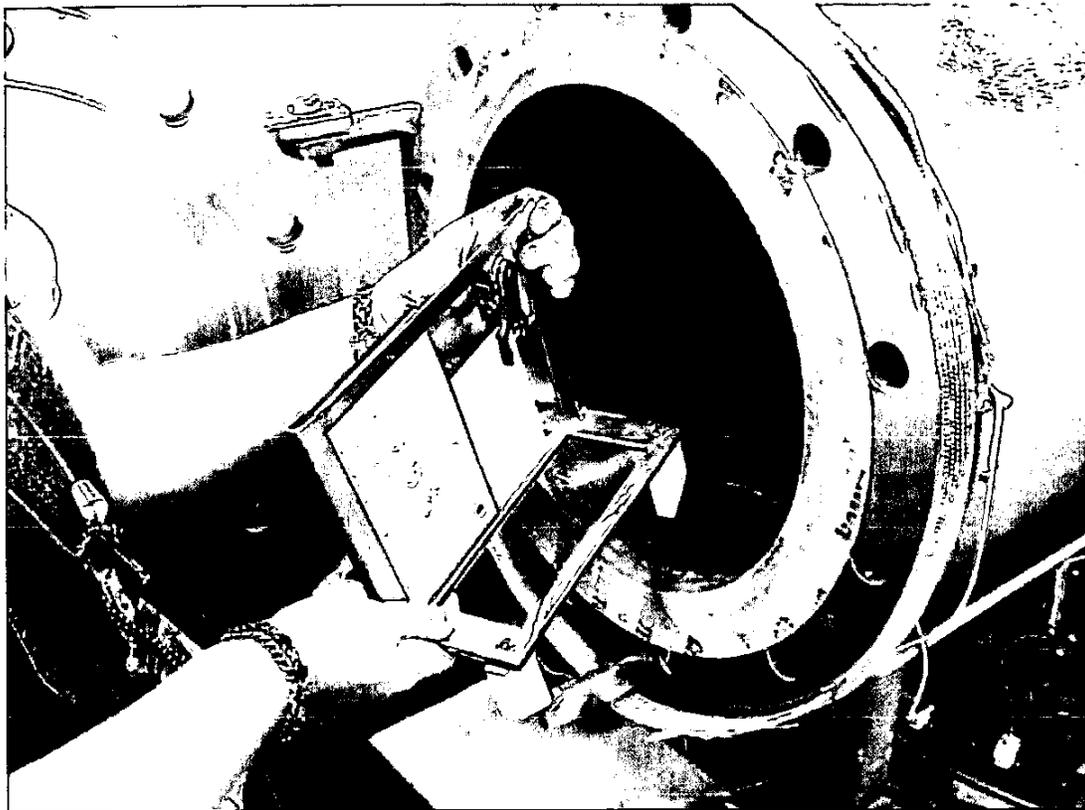
**Figure D-3. System 1 Test Specimen being placed into the Coatings Performance Evaluation System**
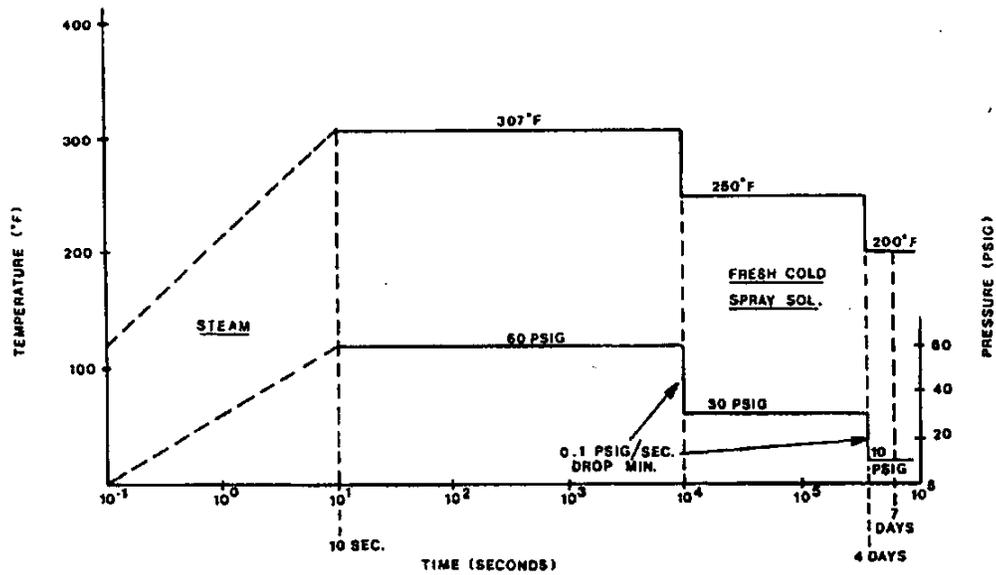


**Figure D-4. Typical Pressurized Water Reactor Design Basis Accident (DBA) Testing Parameters (from ASTM D3911-95). (Note: The ASTM figure contains an error: 30 psig should be 15 psig, which is equivalent to 30 psia).**

D-4

## System 1, Full DBA - Part 1
### 8/21/00
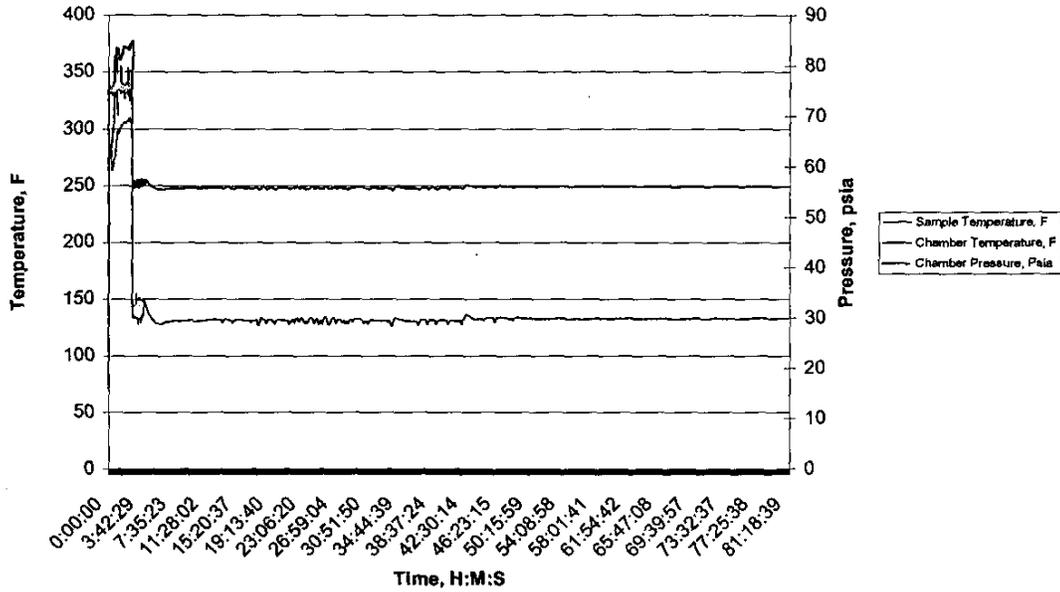


## System 1 Full DBA-Part 2
### 8/21/00
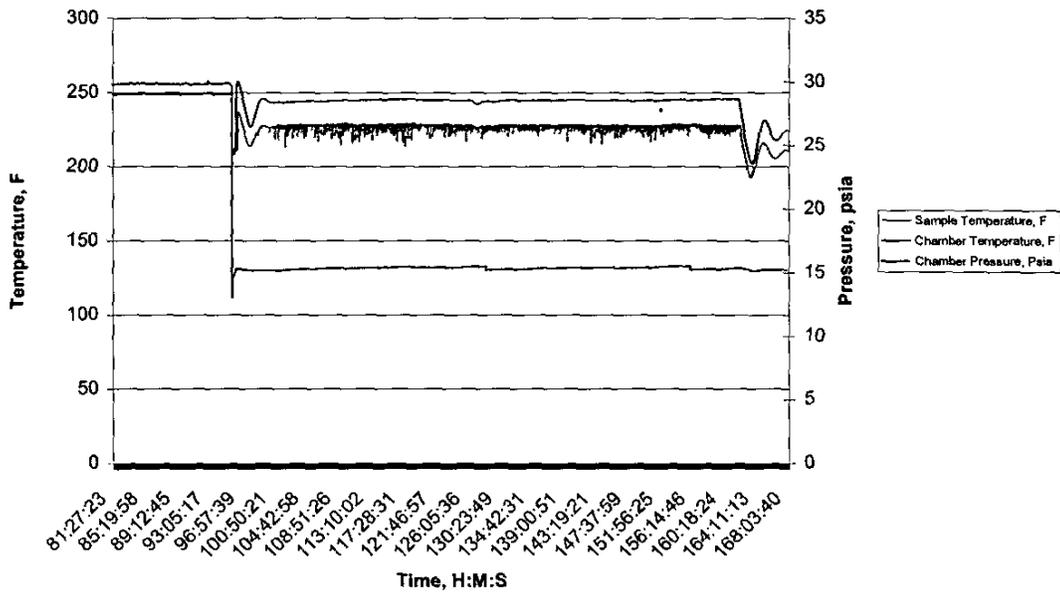


**Figure D-5. Typical SRS DBA Test Cycle.**

The SRTC coating evaluation system is based on a monitored environmental test chamber (known as the METC) which can be supplied with live steam and/or cooling water spray (Figure D-6). The environmental test chamber is an insulated 12-inch diameter by 18-inch long pressure vessel, with flanged closures at each end. It is fabricated of Type 316 stainless steel. The ASTM code-stamped pressure vessel is protected with a 150 psi pressure relief valve. Strap and tape heaters are installed for supplemental control of temperature in the chamber (not shown in the schematic).

A 10-gallon stainless steel autoclave provides steam to the test chamber. A 500-psi rupture disk is installed on the autoclave.

Pressure transducers and thermocouples are installed on the autoclave and the test chamber, and a data acquisition system using Labview® software is utilized to document specimen test conditions. A video-borescope is installed in the test chamber and connected to a videotape recorder to document specimen performance during testing. An image from the video borescope is shown in Figure D-7.

The cool-down phase of the ASTM D3911-95 DBA cycle, which simulates activation of the emergency spray cooling headers in the NPP, is facilitated by a spray system installed in the test chamber. The system consists of a 1000 psi Baldor pump, a heat exchanger to cool the spray solution that is recirculated from the bottom of the chamber, and a storage reservoir. Solution is supplied to the chamber through 0.25-inch diameter tubing. Two metering jet spray nozzles are installed in the chamber, each providing up to 0.030 gpm in a fine mist. Other spray configurations and rates are possible. All materials are Type 316 stainless steel to provide corrosion resistance to various spray solution compositions. To simulate the immersion of some NPP coatings during the early phases of emergency cooling system activation, a shallow reservoir was placed beneath some test specimens to allow the collection of spray coolant, with resultant immersion of a portion of the specimens.

The evaluation of the performance of coatings during immersion was performed in the METC, as stated above, and in an apparatus specifically designed to allow documentation at elevated temperatures, while at atmospheric pressure. This apparatus consisted of a custom-made glass container placed on a thermostatically controlled hot plate (Figure D-8). The container was designed to allow unrestricted observation of the specimens while at elevated temperature. A video camera connected to a time-lapse video recording system was used to document specimen performance (Figure D-9). An image of a specimen during testing is shown in Figure D-10.
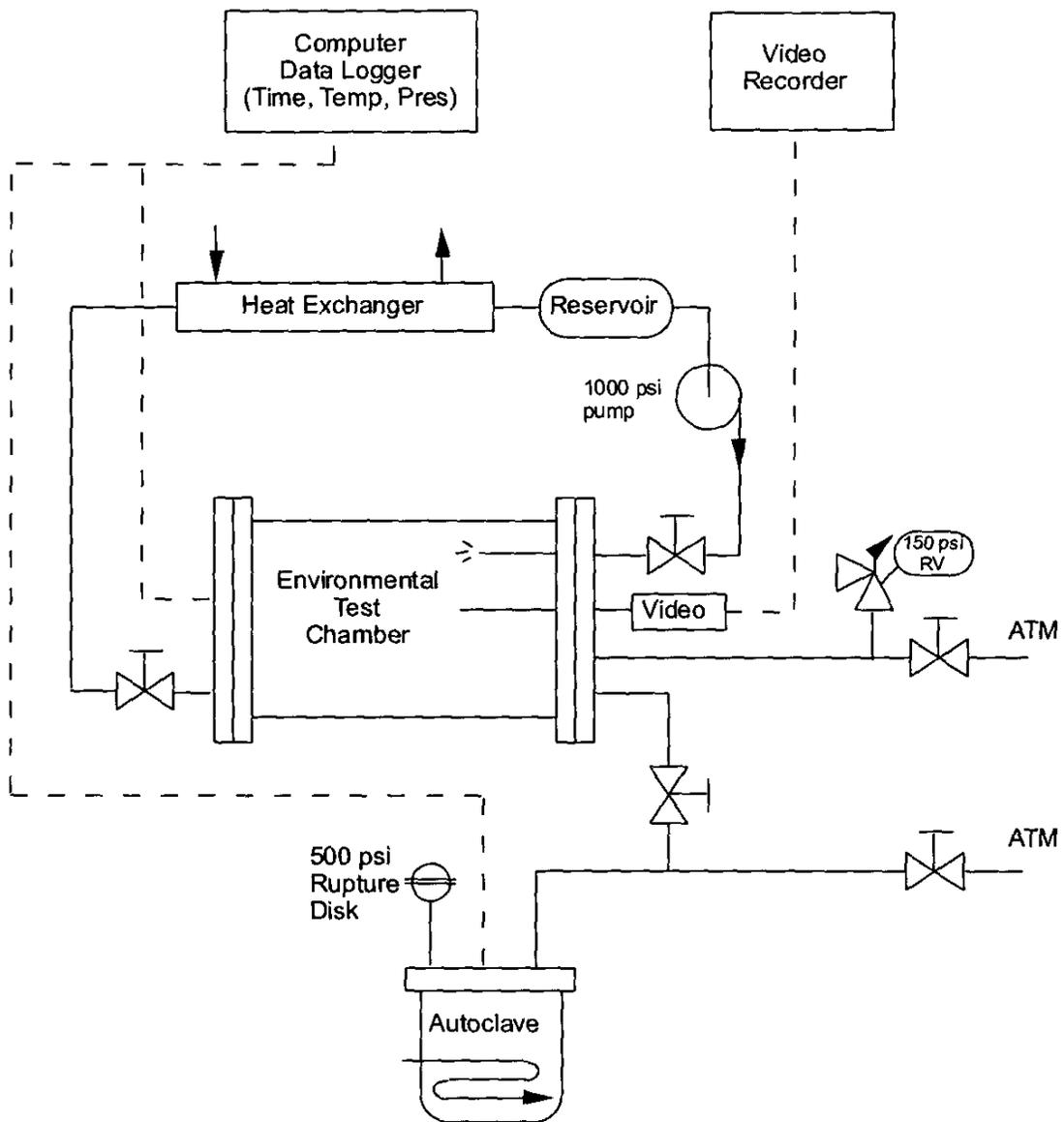
**Figure D-6. Process schematic of coatings performance evaluation system**

**Figure D-7.** Video Borescope Image of Non-Aged (left) and Aged (right) System 1 Specimens.
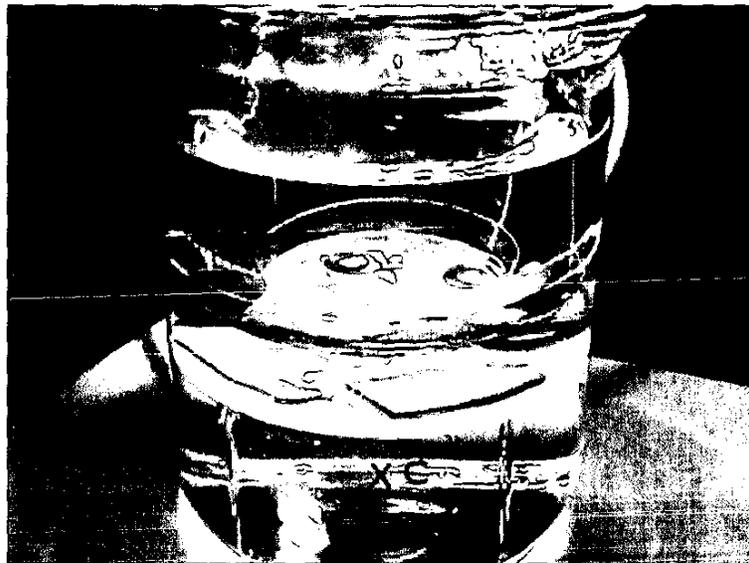


**Figure D-8.** Overall view of soak test vessel. The vessel is placed on a thermostatically controlled hotplate. Note coating specimens placed on permeable glass frit stage. A magnetic stirring bar is visible on the bottom of the vessel.
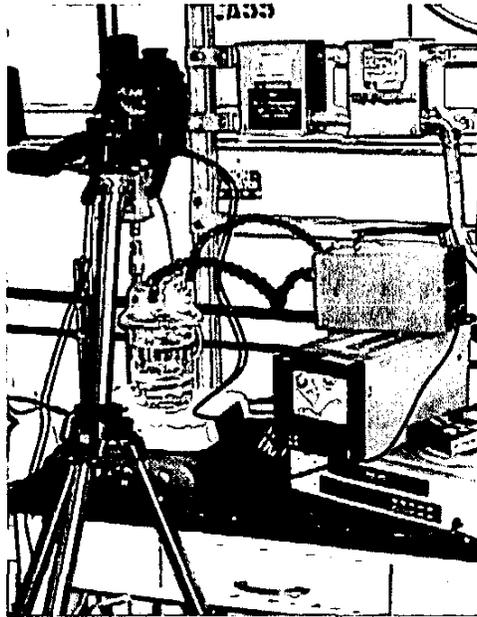
**Figure D-9.** Overall view of soak test system, illustrating video camera (on tripod), fiberoptic lighting system (orange box), time-lapse video recorder, and video monitor.
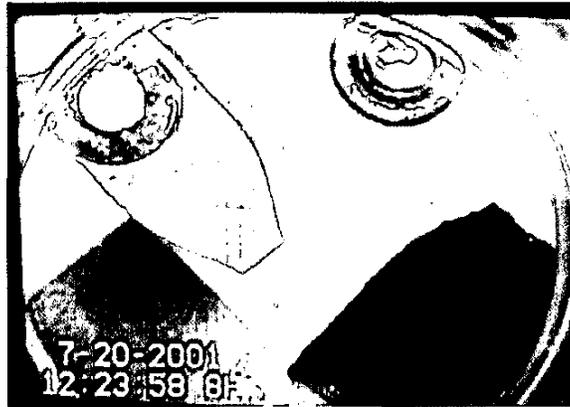


**Figure D-10.** Video image of specimens at the beginning of testing, as recorded.

# Appendix E

**PerformanceTest Descriptions**

DBA Testing

The SRTC coatings performance testing system is used to subject coating specimens to conditions simulating those which would be expected to exist in a NPP during a DBA LOCA. The system, described in Appendix D, has been used to simulate the temperature and pressure profiles found in ASTM D3911-95. A typical exposure test proceeds as follows:

1.  Place specimen into specimen holder within environmental test chamber. Affix thermocouple to face of specimen. Confirm borescope view of specimen. Seal test chamber.
2.  Prepare videotape recorder and computer data logger for collection of test data.
3.  Preheat autoclave steam generator. Preheat test chamber with external strap/tape heaters.
4.  Introduce steam into test chamber so that chamber pressure reaches 75 psia within 10 seconds. Maintain chamber pressure at 75 psia for 2.8 hours with supplemental strap/tape heaters. Judicious use of steam to maintain chamber pressure is permitted. Specimen temperature will be approximately 307°F.
5.  After 2.8 hours, activate spray cooling system. Monitor chamber pressure and vent as necessary to achieve 30 psia within 5 minutes. Maintain chamber pressure with supplemental strap/tape heaters and by control of recirculation rate of spray coolant. Specimen temperature will be approximately 250°F.
6.  After 4 days, stop application of spray coolant and vent chamber to atmospheric pressure. Reset external heaters to maintain sample temperature at approximately 200°F.
7.  After 3 days, turn off electrical heaters and allow sample to return to room temperature.
8.  Remove specimen and examine for blistering, delamination, peeling, and/or cracking of coating. Per ASTM D3911-95: Blistering is limited to intact blisters, completely surrounded by sound coating bonded to the surface. Delamination and peeling are not permitted. Cracking is not considered a failure unless accompanied by delamination or loss of adhesion.

Soak Testing

The SRTC soak test apparatus is used to subject coating specimens to immersion in water at elevated temperature. Immersion of coatings is expected to occur to some depth in NPP containment following activation of the emergency cooling spray systems. The soak test apparatus is described in Appendix D. A typical soak test would be conducted as follows:

1.  Partially fill immersion test canister with distilled water. Tap water may be substituted if desired. Allow enough free space above liquid to allow insertion of top of canister.
2.  If free-film specimens are to be tested, place glass frit stage into test canister to support free-film specimens. Use of glass frit stage will permit the use of a magnetic stirrer bar, if desired.
3.  Place test canister onto thermostatically controlled hot plate. Set controller to desired temperature. Activate temperature controller, if pre-heating of water is required.
4.  Position video camera above test canister ensuring entire test chamber is visible in video monitor.
5.  Insert blank video tape into time lapse recorder and set recorder to desired recording period (i.e., 8, 24, or 40 hours). Confirm time and date are set correctly in video recorder.
6.  Position fiber-optic light source for optimum illumination of test specimen.
7.  Place specimen(s) into test canister. Adjust lighting as necessary.
8.  Record coating performance test.

# Appendix F

**Characterization Facilities Description**

SRTC maintains state-of-the-art testing and analytical capabilities to support the wide range of research and application programs related to nuclear applications. The materials and analytical research group totals over 100 engineers, scientists and technicians. They have a broad range of experience in nuclear materials and applications and form the core of all the materials technology programs currently underway at SRTC. These range from materials applications involved in nuclear materials production, to reprocessing and waste storage and disposition.

A summary of the materials characterization facilities and available equipment and techniques is provided in Table F-1.

**Table F-1. Relevant SRTC Experimental and Analytical Capabilities**

| Sample Preparation, Testing & Failure Characterization | |
| --- | --- |
| - *Laboratory Capabilities* | Three existing autoclaves, high temperature/high pressure, computer controlled pressure/temperature profiles, data acquisition system, one system on order. Environmental Chamber for Temperature/Relative Humidity with viewing window and fiber-optic capable *for sample inspection during tests.* New environmental chamber (delivery expected: 10/97) temperature/pressure/humidity 0-275 psi/0-325°C/5-99% R.H., gas/liquid feed-throughs, fully automated and data acquisition system, stainless steel chamber, fiber optic viewing<br>One Dry Source Gamma Cell at approximately 1.79E+06 Rads/hr,<br>One Dry Source Gamma Cell at approximately 1.00E+04 Rads/hr,<br>One Wet Source Gamma Cell, 1.0 E+06 Rads/hr<br>Blasting/coupon surface preparation/coating application to be performed by certified/qualified personnel, certifications documented. (SSPC/NACE) |
| - *Analytical Capabilities* | SEM (scanning electron microscopy) substrate composition, coating debris characterization<br>FT-IR (infrared spectroscopy) polymer/coating identification<br>DSC (differential scanning calorimeter) thermal transitions, TG (glass transition temperature)<br>TGA/DTA (thermogravimetric analysis) weight loss, volatility<br>XRD (X-ray diffraction) crystallinity, radiation effects<br>NMRS (nuclear magnetic resonance) coating analysis, bond types<br>SIMS (secondary ion mass spectroscopy) surface analysis, composition<br>TEM *(transmission electron microscopy) thin film* analysis, structure<br>AE (acoustic emission) debonding/delamination<br>Image analysis particle size/morphology<br>Mechanical testing; tensile strength, elongation, elastic modulus, adhesion testing (Elcometer), bend testing, etc.<br>Laser interferometry residual stress measurements<br>Magnetic gauges; dry film thickness (DFT)<br>Electrical Impedance Spectroscopy (EIS) |

**Figure F-1.** SRTC Analytical Capabilities: Scanning Electron Microscope (top), Transmission Electron Microscope (middle), and X-ray Diffraction Unit (bottom)

**Figure F-2. FT-IR Spectrophotometry Equipment**

# Appendix G

**Phenomena Identification and Ranking Table Process**

### A.1 PIRT Process Overview

The information obtained through the Phenomena Identification and Ranking Table (PIRT) process identifies phenomena derived requirements which are then integrated into experiments and/or analytical modeling to simulate accident scenarios or conditions of safety concern. Because importance ranking is a fundamental element of the PIRT process, judgments when prioritized with respect to their contribution to the accident scenario or safety concern, provide a structured approach to research program planning based on phenomena of highest importance. Since it is neither cost effective, nor required, to assess and examine all the parameters and models for arriving at a best-estimate code (or supporting experiments) in a uniform fashion, this methodology focuses on identifying those processes and phenomena that are expected to dominate the transient behavior, with the recognition that all plausible effects are considered in development of the PIRT. This screening of plausible phenomena, to determine those which dominate the plant response, ensures that a sufficient and efficient analysis of the problem has been performed. Since PIRTs are not computer code-specific, PIRTs are applicable to the accident scenario and plant design regardless of which code may be chosen to perform the subsequent safety analysis.

A typical application of the PIRT process is conceptually illustrated in Figure G-1 and is initiated by a definition of the problem and PIRT objectives. The PIRT process focuses on phenomena/processes that are important to the particular scenario, or class of transients in the specified nuclear power plant (NPP), i.e., those that drive events. Plausible physical phenomena and processes, and their associated system components are identified. From a modeling perspective, phenomena/processes important to a plant response to an accident scenario can be grouped in two separate-categories: 1) higher level system interactions (integral) between components/subsystems, and 2) those local to (within) a component/subsystem. Although the identification of plausible phenomena is focused toward component organization, experience gained has indicated it can be most helpful to relate the phenomena to higher level integral system processes. Time can often be saved when it can be demonstrated that a higher level integral system process is of low importance during a specific time phase. A subsequent and equally important step is the partitioning o the plant into components/subsystems. This latter step is a significant aid in organizing and ranking phenomena/processes. The phenomena/processes are then ranked with respect to their influence on the primary evaluation criteria, to establish PIRTs. Primary evaluation criteria (or criterion) are normally based on regulatory safety requirements such as those related to restrictions in fuel rods (peak clad temperature, hydrogen generation, etc.) and/or containment operation (peak pressure, emergency core cooling system performance, etc.). The rank of a phenomenon or process is a measure of its relative influence on the primary criteria. The identification and ranking are justified and documented.

The relative importance of environmental conditions and phenomena present is time dependent as an accident progresses. Thus, it is convenient to partition accident scenarios into time phases in which the dominant phenomena/processes remain essentially constant, each time phase being separately investigated. The processes and phenomena associated with each component are examined, as are the inter-relations between the components. Cause and effect are differentiated. The processes and phenomena and their respective importance (rank) are judged by examination of experimental data, code simulations related to the plant and scenario, and the collective expertise and experience of the evaluation team. Independent techniques to accomplish the ranking include expert opinion, subjective decision making methods (such as the Analytical Hierarchy Process), and selected calculations. The final product of the application of the PIRT process is a set of tables (PIRTs) documenting the ranks (relative importance) of phenomena and processes, by transient phase and by system component. Supplemental products include descriptions of the ranking scales, phenomena and processes definitions, evaluation criteria, and the technical rationales for each rank. In the context of the PIRT process application to PWR containment coatings failures, the primary elements of interest are described in Section 2. The PIRTs resulting from this specific application are documented in Section G.7.

### G.2 PIRT Objectives

The industry coatings PIRT panel is comprised of the following industry identified specialists:

| | |
|---|---|
| Jon Cavallo, Chm. | Corrosion Control, Consultants and Labs, Inc. |
| Tim Andreycheck | Westinghouse Electric Corp., Pittsburgh, PA |
| Jan Bostelman | ITS Corporation |
| Dr. Brent Boyack | Los Alamos National Laboratory |

Garth Dolderer        Florida Power and Light
David Long           PP&G Keeler and Long (retired)
Yuly Korobov         Carboline Corp.

The PIRT objectives identified by the panelists were:

a.    To identify coatings systems applied to steel and concrete substrates in PWR containments to be considered for the PIRT process,

b.    To identify phenomena and processes applicable to coatings applied inside PWR containments, and,

c.    To rank those phenomena and processes with respect to their importance to coating failures.

## G.3  Generic PWR Containment Coating Systems

The generic identification of protective coating materials applied to NPPs was derived from EPRI Report TR-106160, "Coatings Handbook for Nuclear Power Plants," plant responses to GL 98-04, June 1996, nuclear industry surveys and inputs from PWR Owners groups. EPRI TR-106160 lists data collected from 29 NPP respondents and represents over 200 commercial coating products applied to over 1000 different plant-specific areas or equipment. The industry coatings PIRT panel reviewed all available information, and based on their collective coatings knowledge identified following eight generic coatings systems for consideration in SRTC's coating research program.

a.    Steel substrate, inorganic zinc primer, epoxy phenolic topcoat,
b.    Steel substrate, epoxy phenolic primer, epoxy phenolic topcoat,
c.    Steel substrate, inorganic zinc primer, epoxy topcoat,
d.    Steel substrate, epoxy primer, epoxy topcoat,   (SRTC System 5)
e.    Concrete substrate, surfacer, epoxy phenolic topcoat,
f.    Concrete substrate, surfacer, epoxy topcoat,
g.    Concrete substrate, epoxy phenolic primer, epoxy phenolic topcoat,
h.    Concrete substrate, epoxy primer, epoxy topcoat.

The PIRT for coating system (a) is reported in the Industry Coatings PIRT Report No. IC99-02, June 16, 2000, which is available through the NRC Public Document Room. PIRTs for coating systems (a), (d), (f), (h) and non-topcoated inorganic zinc on steel have been submitted to the NRC. These systems were judged to be representative of coatings that were applied in the early to middle 1970s.

A cross-referencing of coating systems identified by the PIRT panel and coatings products selected by SRTC to represent those generic systems is provided in Section 2 of this report.

## G.4  Coating System Components

To enable development of the individual PIRTs, the industry coatings PIRT panel partitioned each coating system into components as follows:

STEEL SUBSTRATE

a.    Substrate
b.    Substrate/Primer Interface.
c.    Primer
d.    Primer/Topcoat Interface
e.    Topcoat

CONCRETE SUBSTRATE

a.    Substrate
b.    Substrate/Surfacer Interface
c.    Surfacer
d.    Surfacer/Topcoat Interface
e.    Topcoat

Figure G-2 illustrates the layering of coating materials on a steel substrate and postulated coating defects that was used in the PIRT process.


## G.5  Accident Scenario

The industry coatings PIRT panel discussed a number of accident scenarios postulated for occurrence in PWR plants and their potential effects on containment systems, structures, and components (SSCs), coating systems, and the generation of coating debris which could transport to PWR containment sump(s). The following coating failure scenario was selected by the panel for use in its subsequent deliberations:

a.    Normal plant operation for 40 years (potentially longer due to plant life extension),

b.    Mechanical damage (see Figure G-1 for illustration of incipient and developed defects in coatings on concrete and steel substrates),

c.    Chemical damage (from plant process fluid leakage and over-spray/leakage of decontamination chemicals),

d.    Normal plant operation for 40 years (potentially longer due to plant life extension) followed by intermediate / large LOCA without jet impingement (note: small break LOCA was not considered because containment spray is not initiated and thus significant coating debris transport to the sump(s) is not probable).

Scenarios a, b, c, and d above may occur independently or synergistically to cause coating failure.

Jet impingement due to a LOCA was omitted from the panel's deliberations, since industry test experience indicates that none of the coating systems applied to PWR SSCs will survive direct steam impingement.


## G.6  Scenario Phases

The coating failure accident scenario divided into the following phases (or time intervals).

PHASE 1: Normal Operation Followed by LOCA, No Jet Impingement

(-) Time Coating System Installation
                    -Surface Preparation
                    -Coating Application
                    -Curing
                    - Integrated Leak Rate Testing (ILRT)
T=0            Start of Power Operations
T = 40 years    Medium or Large Break LOCA Occurs
(T could be 60 years in the case of plant life extension)

PHASE 2:     0 to 40 Seconds After Start of LOCA

PHASE 3:     40 Seconds to 30 Minutes After Start of LOCA

PHASE 4:     30 Minutes to 2 Hours After Start of LOCA

PHASE 5:     Greater Than 2 Hours After Start of LOCA

## G.6 Primary Evaluation Criterion

The primary evaluation criterion, or parameter of interest, considered by the industry coatings PIRT panel concerning coatings on PWR containment SSCs is:

"Will the coating system detach from the surface to which it is applied?" or

"Will the paint fall off?"

*The panel's focus was on the second question.*

## G.7 Phenomena Ranking Scale

PIRTs utilizing complex hierarchical, multi-leveled scenarios (see Figure G-1) and the Analytical Hierarchy Process ranking methodology applied to NPPs have been time consuming and labor intensive. The PIRT panel instead selected a simplified ranking scale that drew on the knowledge of panelists who had extensive experience in NPP coating application as well as NPP accident analysis requirements and the PIRT process.

Basis for Ranking Selection:

*High* - Phenomena has a dominant impact on the primary parameter of interest (i.e. coating failure). Phenomena will be explicitly considered in the implementation of the Savannah River Technical Center (SRTC) Research Program

*Medium* - Phenomena has a moderate influence on the primary parameter of interest.
Phenomena will also be considered in the implementation of the SRTC Research Program

*Low* - Phenomena has a small effect on the primary parameter of interest. Phenomena will be considered in the SRTC research program to the extent possible.

The PIRT ranking for System 5 is summarized in Table G-1, which shows the variation of process or phenomena ranking as a function of time. Blistering and de-lamination were judged to be a HIGH concern throughout the accident scenario for the substrate/primer and primer/topcoat interface.

Tables G-2 through G-6 detail the process & phenomena rankings for the materials and material interfaces, rankings arrived at, and the definitions applied to those processes or phenomena to arrive at those rankings. The processes and phenomena, and their rankings, are subject to revision in light of the experimental program's findings.

The integration of these PIRT panel findings with project activities is discussed in Section 2 of this report.
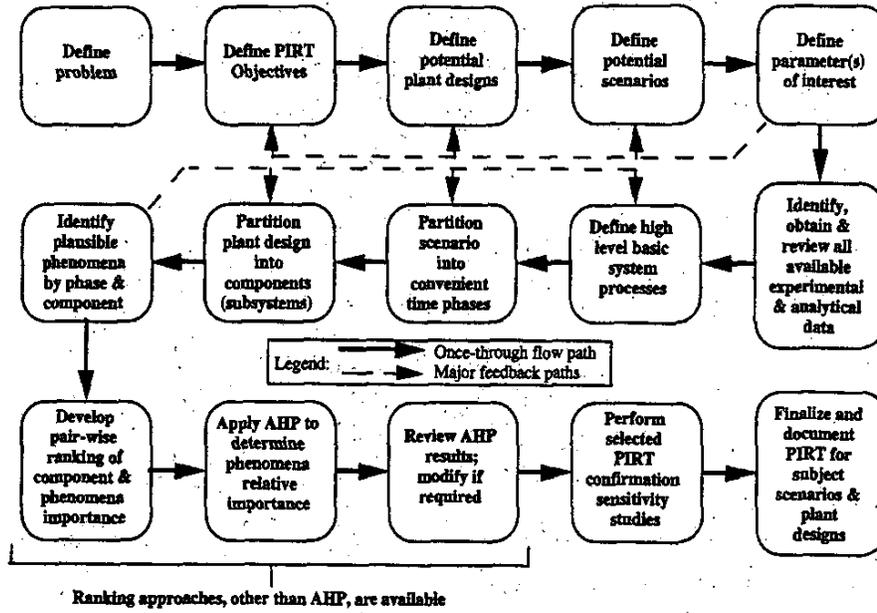
**Figure G-1. PIRT Process**
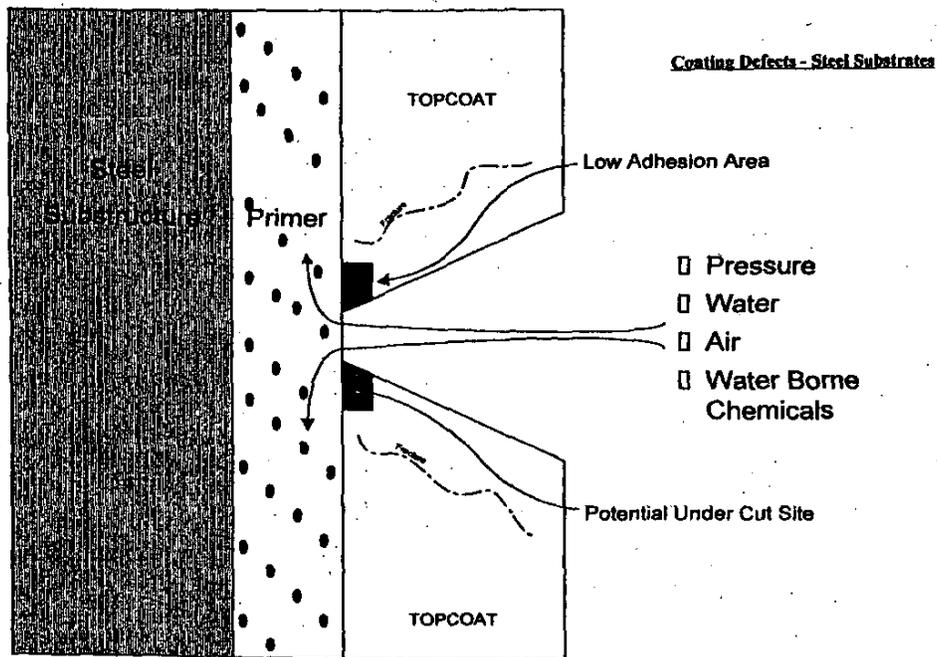


**Figure G-2. Coating Defects and Phenomena of Importance**

### Table G-1. PIRT Ranking Summary
### Steel Substrate – Inorganic Zinc Primer –Phenolic Epoxy Topcoat
### PIRT Coating System 'a', SRTC System 1

| Phases - > Process & Phenomena | | 1 | 2 | 3 | 4 | 5 |
|---|---|---|---|---|---|---|
| Substrate (Steel) | Expansion/Contraction | | | | | |
| | Temperature Gradient | | | | | |
| | Increased Radiation Exposure | | | | | |
| Substrate /Primer Interface | Differential Expansion/Contraction | | | | | |
| Primer | Differential Expansion/Contraction | | | | | |
| | Expansion/Contraction Stresses | | | | | |
| | Oxidation | | | | | |
| | Film Splitting | M | M | M | M | M |
| | Temperature Gradient | | | | | |
| | Increased Radiation Exposure | | | | | |
| | Environmental Exposure | | | | | |
| | Mechanical Damage | | | | | |
| | Minor Coating Anomalies | H | H | H | M | M |
| | Air/water & Chemical Intrusion | | | | | |
| |     Above Pool | | | | M | M |
| |     Below Pool | | | | | M |
| | Diffusion Air/Water & Chemicals | | | M | | |
| | Chemical Attack | | | | M | |
| | Moisture and Air Intrusion through Damage Sites | | | | M | |
| Primer /Topcoat Interface | Differential Expansion/Contraction | M | H | H | | |
| | Diffusion of Air/Water | | | H | H | H |
| Topcoat | Expansion/Contraction | M | | H | | |
| | Environmental Exposure | H | | | | M |
| | Mechanical Damage | M | | | | |
| | Minor Coating Anomalies | | H | H | | |
| | Diffusion of Air/Water | | | | | |
| | Immersion to Pool Surface | | | | | M |

Processes/Phenomena ranked HIGH and MEDIUM

| | |
|---|---|
| Film Splitting | Mechanical Damage |
| Expansion/Contraction | Chemical Attack |
| Environmental exposure | Air/water/chemical intrusion |
| Minor coating anomalies | Immersion to Pool Surface |

Phase 1: Normal service from time of application and through 40 years operation.
Phase 2: 0 to 40 seconds into loss-of-coolant accident (LOCA).
Phase 3: 40 seconds to 30 minutes after a LOCA.
Phase 4: 30 minutes to 2 hours after a LOCA.
Phase 5: Beyond 2 hours after a LOCA.

INDUSTRY COATING PIRT TABLE 4.1-1:     NORMAL OPERATION

COATING DESCRIPTION: Steel Substrate, Inorganic Zinc Primer, Epoxy Phenolic Topcoat

| | Component | Processes & Phenomena | Rank | Definition |
|---|---|---|---|---|
| Phase 1 Normal Operation | Substrate (Steel) | Expansion/contraction | Low | Pressure/temperature induced expansion/contraction of liner plate |
| | Substrate/Primer Interface | Differential expansion/contraction | Low | Differing rates between substrate and primer |
| | Primer (Inorganic Zinc) | Expansion/contraction | Low | Pressure/temperature induced expansion/contraction within primer |
| | | Differential expansion/contraction stresses | Low | Differing rates between filler and binder |
| | | Oxidation | Low | Semi-permeable membrane permits migration of moisture and air (oxygen) |
| | | Film splitting | Medium | Cohesive failure within the zinc film; zinc fails in shear, epoxy pulls zinc apart |
| | | Environmental exposure | Low | Heat, brittleness, breaking of bonds |
| | | Minor coating anomalies | Medium | Result from normal application process |
| | Primer/Topcoat Interface | Differential expansion/contraction | Medium | Differing rates between primer and topcoat |
| | Topcoat (Epoxy Phenolic) | Expansion/contraction | Medium | Pressure/temperature induced expansion/contraction |
| | | Environmental exposure | High | Changes in properties over time |
| | | Discoloration | Low | Polymer chemical changes |
| | | Mechanical damage | Medium | Normal wear and tear |
| | | Minor coating anomalies | Low | Result from normal application process |

INDUSTRY COATING PIRT TABLE 4.1-2:   0-40 SECONDS AFTER INITIATION OF LOCA

Coating Description:  Steel Substrate, Inorganic Zinc Primer, Epoxy Phenolic Topcoat

| Component | Processes & Phenomena | Rank | Definition |
|---|---|---|---|
| Substrate (Steel) | Expansion | Low | Temperature increases due to energy releases expansion |
| | Temperature gradient | Low | Pressure expansion is greater |
| | Increased radiation exposure | Low | Primary coolant released to containment environment |
| Substrate/primer Interface | Differential expansion/contraction | Low | Pressure/temperature induced contraction at liner plate |
| Primer (Inorganic Zinc) | Expansion/contraction | Low | Pressure/temperature induced expansion/contraction within primer |
| | Differential expansion/contraction stresses | Low | Differing rates between filler and binder |
| | Film splitting | Medium | Cohesive failure within the zinc film; zinc fails in shear, epoxy pulls zinc apart |
| | Temperature gradient | Low | Bulk thermal stresses |
| | Increased radiation exposure | Low | Primary coolant released to containment environment |
| | Diffusion rate of air/water | Low | Increases concentration of air/water |
| | Minor coating anomalies | High | Result from normal application process |
| | Environmental exposure | Low | Heat, brittleness, breaking of bonds |
| | Chemical, air, moisture intrusion | Low | Mechanical damage sites from phase 1 |
| Primer/topcoat Interface | Differential expansion/contraction | High | Differing rates between primer and topcoat |
| | Diffusion rate of air/water | Low | Increased concentration of air/water |
| Topcoat (Epoxy Phenolic) | Expansion/contraction | High | Pressure/temperature induced expansion/contraction |
| | Temperature gradient | Low | Thermal stresses |
| | Diffusion rate of air/water | Low | Increased concentration of air/water |
| | Increased radiation exposure | Low | Primary coolant adjacent to structure |
| | Condensation (cold wall) | Low | Heating the wall with condensed steam |
| | Mechanical damage | Low | DBA-generated flying debris |

Phase 2
0-40 Seconds
(Outside Zone of Influence)

# INDUSTRY COATING PIRT TABLE 4.1-3: 40 SECONDS - 30 MINUTES AFTER INITIATION OF LOCA

**Coating Description: Steel Substrate, Inorganic Zinc Primer, Epoxy Phenolic Topcoat**

| Component | Processes & Phenomena | Rank | Definition |
|---|---|---|---|
| Substrate (Steel) | Contraction | Low | Containment pressure decreasing |
| | Temperature gradient | Low | Temperature increases due to energy releases expansion |
| | Increased radiation exposure | Low | Pressure expansion is greater |
| Substrate/primer Interface | Differential contraction | Low | Pressure/temperature induced contraction at liner plate |
| Primer (Inorganic Zinc) | Contraction | Low | Pressure/temperature induced contraction within primer |
| | Differential contraction stresses | Low | Differing rates between filler and binder |
| | Film splitting | Medium | Cohesive failure within the zinc film; zinc fails in shear, epoxy pulls zinc apart |
| | Temperature gradient | Low | Bulk thermal stresses |
| | Increased radiation exposure | Low | Primary coolant released to containment environment |
| | Diffusion rate of air/water | Medium | Increases concentration of air/water |
| | Chemical attack | Low | From boric acid at locations of topcoat mechanical damage |
| | Minor coating anomalies | Medium | Result from normal application process |
| Primer/topcoat Interface | Differential contraction | High | Differing rates between primer and topcoat |
| | Diffusion rate of air/water | High | Increased concentration of air/water |
| Topcoat (Epoxy Phenolic) | Contraction | High | Pressure/temperature induced contraction at liner plate |
| | Temperature gradient | Low | Thermal stresses |
| | Diffusion rate of air/water | Low | Increased concentration of air/water |
| | Increased radiation exposure | Low | Primary coolant and noble gases adjacent to structure |
| | Condensation (cold wall) | Low | Heating the wall with condensed steam |
| | Wash down of surfaces | Low | Water films from containment spray |

Phase 3
40 Sec - 30 Min
(Outside Zone of Influence)

20

INDUSTRY COATING PIRT TABLE 4.1-4:  30 MINUTES - 2 HOURS. AFTER INITIATION OF LOCA

| COATING DESCRIPTION: Steel Substrate, Inorganic Zinc Primer, Epoxy Phenolic Topcoat | | | |
|---|---|---|---|
| Phase 4 30 min - 2 hrs (outside Zone of Influence) — Component | Processes & Phenomena | Rank | Definition |
| Substrate (Steel) | Contraction | Low | Containment pressure increase |
| | Temperature gradient | Low | Temperature increases due to energy releases expansion |
| | Increased radiation exposure | Low | |
| Substrate/Primer Interface | Differential contraction | Low | Pressure/temperature induced contraction at liner plate |
| Primer (Inorganic Zinc) | Contraction | Low | Pressure/temperature induced contraction within primer |
| | Differential contraction stresses | Low | Differing rates between filler and binder |
| | Film splitting | Medium | Cohesive failure within the zinc film; Zinc fails in shear, epoxy pulls zinc apart |
| | Temperature gradient | Low | Bulk thermal stresses |
| | Increased radiation exposure | Low | Failure due radiation exposure |
| | Diffusion rate of air/water above pool surface | Medium | Increase in pressure, humidity drives moisture into primer |
| | Chemical attack | Medium | Boric acid attack at locations of topcoat mechanical damage |
| | Minor coating anomalies | Medium | Areas of mechanical damage and/or minor coating anomalies |
| | Moisture and air intrusion through damage sites | Medium | In topcoat at areas of mechanical damage and/or minor coating anomalies |
| | Water intrusion below pool surface | Low | Water migration through topcoat at mechanical damage and minor coating anomaly sites |
| Primer/Topcoat Interface | Differential contraction | Low | Differing rates between substrate, primer and coating |
| | Diffusion rate of air/water | High | Increased concentration of air/water |

21

INDUSTRY COATING PIRT TABLE 4.1-4: 30 MINUTES - 2 HOURS. AFTER INITIATION OF LOCA

| | | | | |
|---|---|---|---|---|
| Topcoat (Epoxy Phenolic) | Contraction | Low | Pressure/temperature induced contraction at liner plate |
| | Temperature gradient | Low | Thermal stresses |
| | Diffusion of air/water | Low | Increased concentration of air/water |
| | Increased radiation exposure | Low | Primary coolant adjacent to structure |
| | Condensation (cold wall) | Low | Heating the wall with condensed steam |
| | Wash down of surfaces | Low | Water films from containment spray |
| | Immersion to pool surface | Low | Coatings submersed in coolant pool on containment floor |

## INDUSTRY COATINGS PIRT TABLE 4.1-5: >2 HOURS AFTER INITIATION OF LOCA

**COATING DESCRIPTION: Steel Substrate, Inorganic Zinc Primer, Epoxy Phenolic Topcoat**

| | Component | Processes & Phenomena | Rank | Definition |
|---|---|---|---|---|
| Phase 5 2 hrs - end (outside Zone of Influence) | Substrate (Steel) | Contraction | Low | Containment pressure decrease due to cooling of containment |
| | | Temperature gradient | Low | Temperature changes associated with containment cooling |
| | | Increased radiation exposure | Low | Radiation damage due to increased radioactivity from event |
| | Substrate/Primer Interface | Differential contraction | Low | Pressure/temperature induced contraction at liner plate |
| | Primer (Inorganic Zinc) | Contraction | Low | Pressure/temperature induced contraction in primer |
| | | Differential contraction stresses | Low | Differing rates between substrate, primer and coating |
| | | Film splitting | Medium | Cohesive failure within the zinc film; zinc fails in shear, epoxy pulls zinc apart |
| | | | Low | Bulk thermal stresses |
| | | Temperature gradient | Low | Primary coolant adjacent to structure |
| | | Increased radiation exposure | High | Increases concentration of air/water |
| | | Diffusion of air/water | Low | From boric acid at locations of topcoat mechanical damage |
| | | Chemical attack | High | Topcoat imperfections at areas of mechanical damage and/or application variations |
| | | Minor coating anomalies | High | Ingress at areas of mechanical damage and/or minor coating anomalies in topcoat |
| | | Moisture and air intrusion through damage sites | Medium | Water migration through topcoat at mechanical damage and minor coating anomaly sites |
| | | Water intrusion below pool surface | | |
| | Primer/Topcoat Interface | Differential contraction | Low | Differing rates between primer and topcoat |
| | | Diffusion of air/water | High | Increased concentration of air/water |

23

INDUSTRY COATINGS PIRT TABLE 4.1-5:    >2 HOURS AFTER INITIATION OF LOCA

| | | | |
|---|---|---|---|
| | Contraction | Low | Pressure/temperature induced contraction at liner plate |
| | Temperature gradient | Low | Thermal stresses |
| | Diffusion of air/water | Medium | Increased concentration of air/water |
| Topcoat (Epoxy Phenolic) | Increased radiation exposure | Low | Primary coolant adjacent to structure |
| | Condensation (cold wall) | Low | Heating the wall with condensed steam |
| | Chemical attack | Low | Reaction to changing pH of recirculating sump water |
| | Immersion to pool surface | Medium | Coatings submersed in coolant pool on containment floor |

24